Speed control methods for autonomous vehicles at the boundaries of the operational design domain

Thesis

Hanzhang Guo

Delft University of Technology

TU Delft

Speed control methods for autonomous vehicles at the boundaries of the operational design domain

by

Hanzhang Guo

to obtain the degree of Master of Science

at the Delft University of Technology,

to be defended publicly on Monday February 17, 2025 at 10:00 AM.

Student number: 5389690

Project duration: May 1, 2024 – February 17, 2025

Thesis committee:

Dr. ir. G. Correia,	TU Delft, supervisor (chair)
Dr. H. Caesar,	TU Delft, supervisor
Dr. ir. I. Martínez,	TU Delft, examiner

Cover: Cloudy urban scenes generated by the autonomous vehicle simulator CARLA

An electronic version of this thesis is available at `http://repository.tudelft.nl/`.

TU Delft

Contents

List of Figures

List of Tables

1 Introduction

1.1. Motivation

The rapid development of autonomous vehicles (AVs) is expected to transform transportation systems by enhancing safety, efficiency and accessibility. These vehicles utilize various sensors, such as Light Detection and Ranging (LiDAR), millimeter-wave radar and cameras, to perceive the environment. They also employ advanced decision-making and control algorithms to achieve full-process automation tasks, including acceleration and deceleration, steering, path planning and obstacle avoidance [81]. SAE J3016 defines different levels of AVs, ranging from no automation capabilities (L0) to high and full automation capabilities (L4 and 5) [65], as shown in Figure 1.1, according to Dynamic Driving Task (DDT), which defines the system's role in managing driving functions, Fall-Back, which addresses the responsibility for handling system failures, and the Operational Design Domain (ODD), which specifies the conditions and environments where the system can operate. This classification standard helps researchers and industry stakeholders clearly understand under what conditions and to what extent vehicles can independently perform driving tasks.

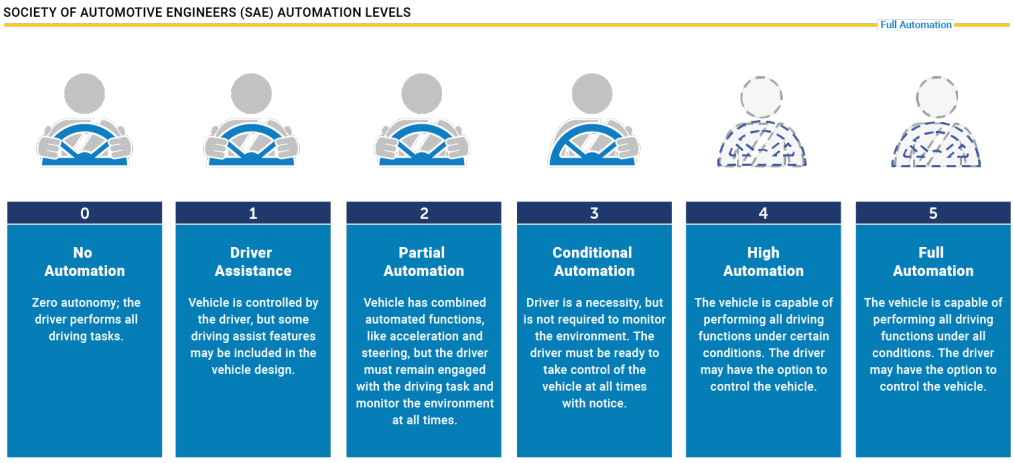

Figure 1.1: SAE levels from no automation to full automation [65]

Among the SAE standards, the ODD is introduced to distinguish L5 automation in unlimited areas from L4 automation with restrictions, such as geographic areas, road types, weather conditions, lighting (day/night), maximum speed and other limits [20, 74]. In practical applications, the most notable feature of L4 AVs is the ability to operate without human intervention under the specified ODD. This means vehicles do not require drivers to monitor driving tasks within the ODD in real-time. However, when

vehicles operate in scenarios beyond the original boundaries of their ODD, their safety and reliability are often compromised. [10].

1.1.1. Complexity at the ODD boundaries

Ideally, L4 AVs can achieve safe and efficient automation within known and controlled ODDs. However, environmental conditions and scenarios are often unpredictable in real-world traffic, which requires real-time monitoring, as shown in Figure 1.2. Weather factors (such as heavy rain, dense fog and snowfall) can significantly reduce the detection range and accuracy of sensors; road geometric features (such as sharp turns and steep slopes) and complex traffic participants (random behaviors of pedestrians, cyclists and other vehicles) also increase the difficulty for vehicles in the planning and control stages [25, 87]. When these unexpected factors occur, the vehicle may disengage from its ODD, making the original automation strategies challenging to apply, triggering safety risks and decision-making difficulty.

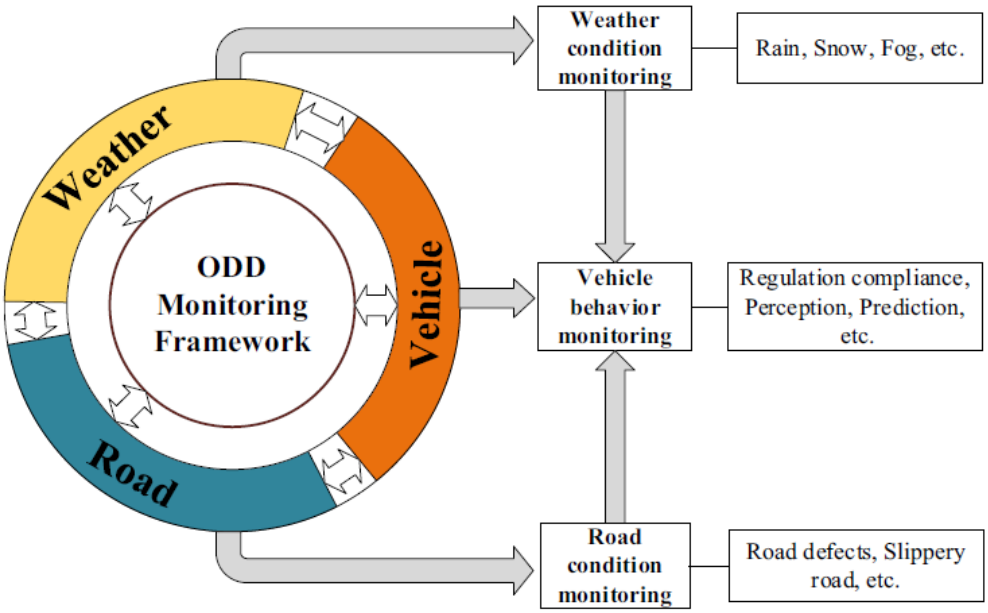

Figure 1.2: Factors affecting the ODDs and the monitor framework [87]

Studies have shown that approximately 52% of AV fall-back events can be attributed to perception-level errors, such as GPS localization deviations and misjudgments of external objects [21]. These challenges become particularly pronounced as vehicles approach or exceed their predefined ODD boundaries. Recognizing these issues emphasizes the importance of re-evaluating risks in real-time. Consequently, there is an urgent need for rapid and robust adjustments to driving strategies that can dynamically respond to the evolving operational context. These challenges not only highlight the limitations of current operational domains but also underscore the significant role environmental factors play in the performance of AV systems.

1.1.2. Environmental factors on vehicle perception and control

Environmental factors are key in determining the ability to extend ODD boundaries. For example, while sensor performance is typically optimal under clear weather conditions, LiDAR and cameras experience signal attenuation, increased noise and reduced visibility in fog, snow and rain, leading to decreased reliability in object detection and classification [10, 81]. Similarly, slippery roads, snow accumulation or icy surfaces can extend the vehicle's braking distance, increasing the risk of losing control during emergency braking or steering maneuvers. Road gradients exacerbate this issue. When driving uphill or downhill, gravity affects the vehicle's acceleration and deceleration characteristics and changes the required braking distance, impacting emergency avoidance and collision prevention capabilities.

The combination of these factors means AVs do not respond uniformly to all environmental conditions in actual operations. To achieve flexible and general-purpose AV technology, it is essential to deeply quantify the impact of various environmental factors on perception and vehicle dynamic performance, and integrate them into risk assessment and speed control strategies comprehensively. Despite the profound influence of these environmental variables on vehicle performance, current conventional responses struggle to mitigate these challenges effectively.

1.1.3. Conventional responses at ODD boundaries

When managing and handling ODD boundaries, common approaches include requiring human drivers to take over, pulling over, or decelerating and continue driving [11, 16]. However, these traditional solutions have apparent limitations:

Human takeover: This approach contradicts the concept of full automation and may diminish passengers' trust in AV technology. Additionally, passengers might lack the ability or willingness to assume control safely, and future AV designs may not feature the traditional driver seat that facilitates manual takeover.

Pulling over to the roadside: Although pulling over can mitigate immediate risks, it may introduce new safety and efficiency challenges. For instance, prolonged roadside parking can disrupt traffic flow and increase the likelihood of rear-end collisions.

Deceleration: Compared to takeover and roadside parking, deceleration aligns more closely with the principle of continuous AV operation. By gradually reducing speed, the vehicle gains additional time to process complex information and make safer decisions. However, suppose this strategy lacks sufficient quantitative analysis of environmental factors. In that case, it may result in insufficient or excessive speed adjustments, thereby upsetting traffic efficiency and vehicular safety.

Given these constraints, exploring more accurate methods that enable vehicles to make real-time decisions is imperative.

1.1.4. Risk quantification and real-time speed control

Due to the shortcomings of the strategies above, developing real-time speed control strategies has become a promising research direction. Different weather conditions should be characterized, and then the impacts on sensor capabilities and vehicle dynamics can be evaluated. These quantitative results can be integrated into the vehicle's risk assessment to provide a comprehensive basis for speed control strategies. Control strategies with real-time risk judgement capabilities enable vehicles to adjust autonomously under changing weather and road conditions, maintain operational continuity, reduce human intervention and decrease dependence on pulling over.

Although existing research has analysed environmental impact factors in specific scenarios, there is a lack of a quantitative and actionable comprehensive framework to support the integration and optimization of different factors [10, 25, 87]. This study quantifies how weather variations, road gradients, and terrain conditions affect sensor detection ranges and vehicle braking performance. It will then translate these data into an adaptive speed control strategy—moving beyond the static geofencing ODDs. To achieve this, traffic images and videos are generated under diverse conditions (e.g., different weather, lighting and traffic capacity). Based on these datasets, an object detection model is trained and evaluated to establish the maximum detection distances. Braking behaviour is then simulated to measure stopping distances under various slopes, friction and initial speeds. Finally, the detection and braking metrics are used to train an RL agent capable of dynamically adjusting speed to maintain safe driving performance, even under extreme conditions, thereby contributing to the development of dynamic ODDs.

Below are the expanded and refined sections of the report's scope, research questions and structure. The background description and research objectives will echo during the expansion process, further clarifying the research questions and report structure. These insights reveal gaps in current methodologies and underscore the need for a comprehensive framework that integrates environmental quantification with real-time risk assessment.

1.2. Research scope

This study will focus on AVs' performance optimization and safety assurance at the boundaries of their ODD. The research scope defines the relevant parameters, scenarios and strategies:

Quantification of environmental factors: This study will primarily explore the impact of weather conditions such as rain, fog, night and wet ground on the cameras' detection distance. It will also examine how road gradient changes (uphill, downhill and gradient magnitude) and weather-induced friction changes affect vehicle braking distance. This process will involve parametrising and quantitatively analyzing these impacts.

Risk quantification under ODD boundaries: The research scope includes real-time risk assessment at ODD boundaries. The risk model will integrate weather conditions, road gradients, sensor accuracy and vehicle dynamic performance to quantify the vehicle's safety margin at each moment and scenario. The risk assessment method compares the detection and braking distances in real-time. If the braking distance is shorter than the detection distance, the vehicle can fully brake when it detects an obstacle, indicating that it is operating within the ODD.

Optimization of speed control strategies: After clarifying the risks under different conditions, this study will focus on developing a data-driven speed control strategy. The research scope includes proposing dynamic decision-making strategies based on comparing detection and braking distances, enabling vehicles to decelerate when facing adverse environmental conditions beyond the defined ODD. Reinforcement learning methods will optimize speed control strategies by encouraging higher speeds under safe conditions while penalising collisions caused by excessive speeds, ensuring the vehicle's stability and safety.

It is important to note that this study does not aim to cover all scenarios within the complete ODD of AVs, nor does it focus on driver behaviour, cybersecurity risks and regulatory or ethical issues. Instead, it concentrates on the technical aspects of the vehicle, exploring how to scientifically adjust speed by quantifying external environmental impacts and internal vehicle dynamic capabilities when the vehicle approaches or exceeds original ODD boundaries.

1.3. Research questions

To guide the theoretical framework and empirical analysis of this study, the following core research questions and several sub-questions are proposed:

1.3.1. Main research question:

How can the impacts of different weather and road conditions on AVs be quantified, and how can vehicle speed control strategies at the ODD boundaries be optimized based on the comparison of detection and braking distances to ensure safety and efficiency?

The answer to this question needs to be based on the following sub-questions.

1.3.2. Sub-questions

- Which key weather and road gradient factors significantly affect the detection performance of AV detection and braking distances?
- How can these factors be quantified and applied in defining the ODD boundaries?
- How can real-time speed control strategies be designed so vehicles achieve safe and efficient driving through reasonable deceleration when facing environmental conditions beyond the original ODD?

By answering these research questions, this study will provide a clear technical pathway and reference for the safe operation of AVs under uncertain environments, laying a practical method for further developing fully automation technologies.

1.4. Report structure

This report will consist of six chapters, each connected from a macro understanding of the problem to micro-level solutions. The chapters are organized as follows:

Chapter 1-Introduction: This chapter defines the research motivation, gaps and scope, then presents the research objectives and questions. Elaborating on the research motivation and expected contributions lays the foundation for the subsequent chapters.

Chapter 2-Related works: This chapter will review existing literature and research progress on AV, ODD, environmental perception and control strategies. It will focus on identifying the limitations of current studies and seek theoretical foundations and inspirations for the risk models and speed control strategies constructed in this research.

Chapter 3-Methodology: This chapter will introduce the research methods and technical approaches, including data collection and processing methods, key parameter quantification methods, the construction logic of risk assessment models, and the design principles of speed control strategies.

Chapter 4-Experiments: This chapter will detail the experiments process and evaluation metrics, and present the quantitative results obtained through the methods above, including the variation patterns of sensor detection distances, vehicle braking distances under different weather and gradient conditions, and the performance of speed control strategies in various scenarios.

Chapter 5-Discussion: This chapter will discuss the results in depth, compare them with related studies, analyse the significance of the research findings for AV theory and practice, and discuss the implications for future technological paths. It will also point out this study's limitations and potential directions for improvement and expansion.

Chapter 6-Conclusion: This chapter summarizes the core contributions and conclusions of the entire study, and looks forward to future research directions and policy recommendations.

2

Related works

2.1. Background history

AV is not a recent innovation. Its development began in the mid-20th century with military and aerospace research into unmanned driving [33, 75]. At that time, technologies focused on conducting simple autonomous control experiments in closed or specific environments. However, due to insufficient perception capabilities and limited computational resources, these early attempts failed to achieve breakthroughs in civilian road traffic [49, 29].

The milestone event that sparked widespread attention for AV was the Grand Challenge and the subsequent Urban Challenge organized by the Defense Advanced Research Projects Agency (DARPA) in the United States in 2004, 2005 and 2007. These competitions not only showcased the potential of AV to avoid obstacles and complete navigation tasks in wilderness and urban street environments but also concentrated on the requirement of key technologies such as visual perception, path planning and sensor fusion [78, 43], as shown in Figure 2.1. Subsequently, the involvement of companies like Google (now Waymo), General Motors (Cruise) and numerous startups propelled AV into unprecedented limelight.

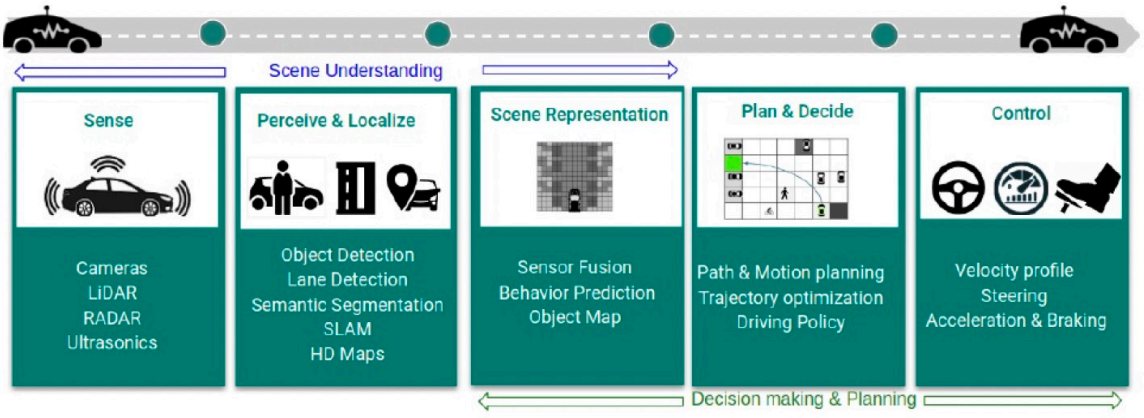

Figure 2.1: Tasks of autonomous vehicles [42]

With the advancements in Artificial Intelligence (AI) and sensor technologies (such as LiDAR, radar and cameras), AV research entered a phase of rapid expansion in the early 21st century [73, 17]. Early research and prototypes focused more on the robustness of internal vehicle perception-control loops, such as reliable control of braking and steering systems, and simple decoupling of vehicle dynamics models [47, 92]. As AV technology further developed, industry and academia gradually recognized the

need to define the operational environment of vehicles during the functional design phase, known as the ODD.

Initially, the concept of ODD was not systematically proposed but was instead limited through regional or closed-site approaches to restrict the levels of vehicle automation. For example, testing specific automation levels (L3/L4) on certain highway segments or within campuses helped reduce the complexity and potential risks associated with perception and decision-making [49, 29, 63, 80]. During this phase, different countries or cities' varying infrastructure and traffic flow characteristics can rapidly implement localized automation deployments through geofencing methods [35, 16].

The formal introduction of the ODD concept was primarily due to discussions in SAE International's AV classification (SAE J3016). When the level of automation progresses from L2 (partial automation) to L3 (conditional automation) and above, the system's responsibility for perceiving and making decisions about the external environment increases, as shown in Table 2.1. This necessitates clearly defining the environments or conditions under which the system can operate [65]. Thus, the introduction of ODD is, in a sense, driven by the need for safety and responsibility. It requires developers to clearly define the operational environments of the vehicle during the functional design phase, including road types (highways or urban streets), weather conditions (sunny, rainy or snowy) and traffic conditions (high traffic volume, low traffic volume or mixed traffic), thereby preventing the system from unthinkingly operating in unsuitable environments and causing safety issues [65, 43].

Table 2.1: SAE levels of driving automation [65]

Level	Name	Sustained Lateral & Longitudinal Vehicle Motion Control	Object and Event Detection and Response	Fallback	ODD
L0	No Driving Automation	Driver	Driver	Driver	N/A
L1	Driver Assistance	Driver and System	Driver	Driver	Limited
L2	Partial Driving Automation	System	Driver	Driver	Limited
L3	Conditional Driving Automation	System	System	Driver	Limited
L4	High Driving Automation	System	System	System	Limited
L5	Full Driving Automation	System	System	System	Unlimited

In early industry practices, the methods for delineating the ODD primarily focused on two typical scenarios: closed urban testing and highway restrictions. The first approach involves conducting road tests in specific small cities or urban areas. In contrast, the second entails achieving preliminary AV on highway sections through specialized facilities, such as Variable Speed Limits (VSL) and communication base stations [27, 90, 29]. These efforts laid the technical and practical foundation for the subsequent refinement of the ODD concept and led the industry to gradually recognize that defining ODD solely based on geography or road type is insufficient to address the diverse variables present in the real world (such as weather conditions, temporary construction and insufficient nighttime lighting) [49, 5]. Subsequently, the International Organization for Standardization (ISO) and research groups (such as SAE) progressively incorporated more environmental factors into ODD descriptions, resulting in a more systematic definition of ODD [49, 35, 64], as shown in Figure 2.2.

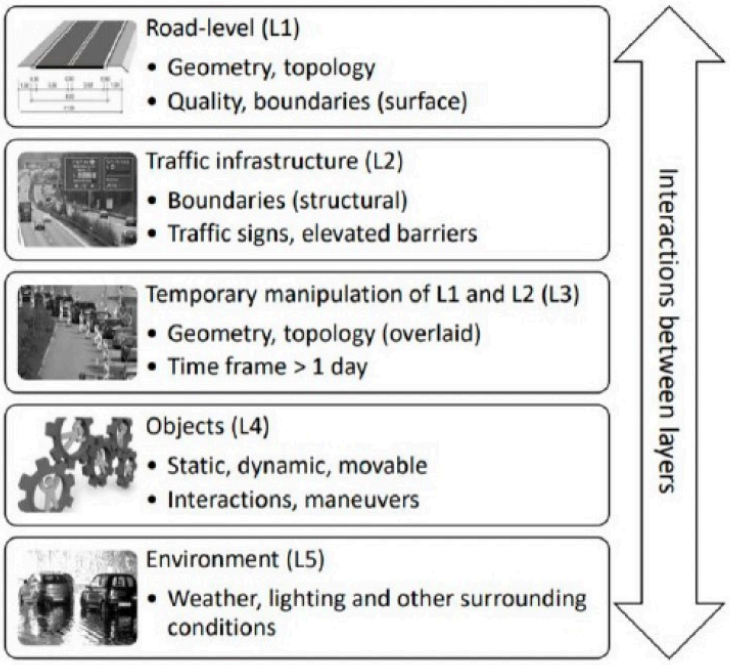

Figure 2.2: Different layers of the ODD [71]

From both academic and application perspectives, geofencing ODD lacks appropriate descriptions when facing dynamic environments with multiple traffic flows, pedestrian flows and sudden failures, making it difficult for vehicles to revert to safe mode when encountering boundary scenarios promptly [47, 24]. Therefore, over the past decade, more fine-grained ODD research has continuously emerged, with many studies focusing on how to incorporate additional environmental dimensions such as weather, terrain and traffic rules into ODD [44, 40, 49], and leveraging advanced Vehicle-to-Everything (V2X) technologies to enhance the interaction between vehicles and infrastructure [4, 6], as shown in Figure 2.3.

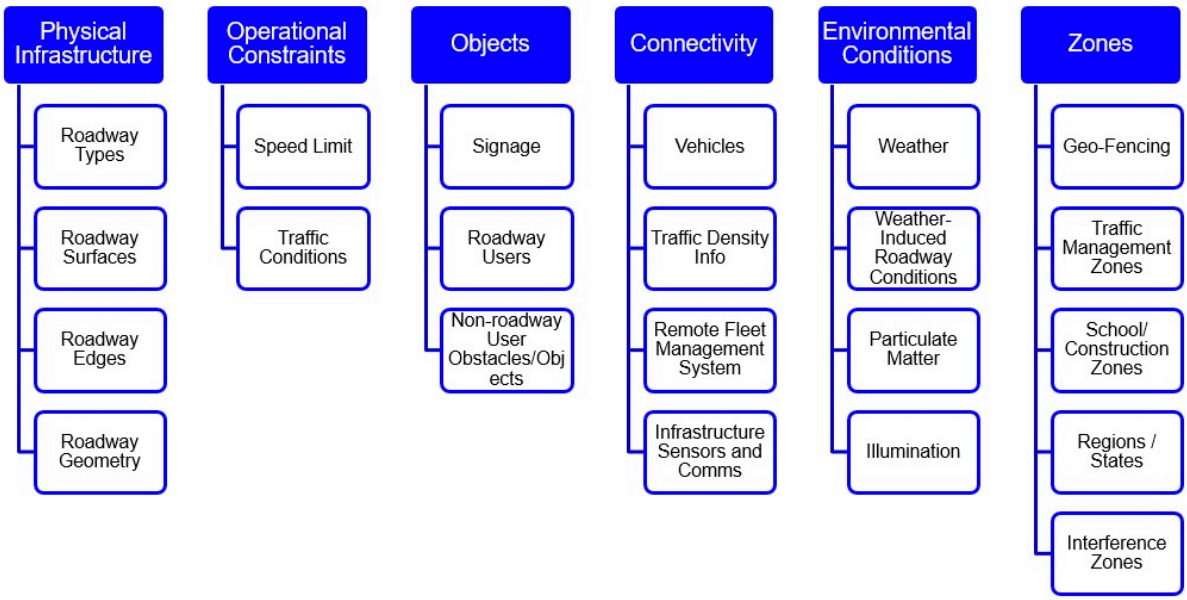

Figure 2.3: Different factors of the ODD [78]

In current practices, the industry predominantly concentrates AV tests and demonstrations on the following two types of scenarios [14, 1]:

Highways or simple expressways often provide controlled environments conducive to deploying L2–4 automation applications, such as platooning and highway pilot assistance. These scenarios benefit from more spartan road conditions and fewer pedestrian interferences, which can reduce the complexity of perception and decision-making [14, 27]. However, due to high-speed operation requiring rapid responses and more stringent demands on vehicle emergency braking distances, perception accuracy and system reliability, enhancements such as VSL [90, 86], Automatic Emergency Braking (AEB) [92], and other functionalities become necessary.

Urban restricted roads serve as designated operational zones where Robotaxi services are deployed with pre-marked information, providing a controlled environment for AVs. In these settings, urban authorities mitigate regulatory risks by confining operations to specific areas via measures such as geofencing combined with special permits [77, 66, 37, 57, 56]. While this controlled approach facilitates operational predictability, it inherently struggles to cope with unplanned challenges—such as adverse weather conditions, traffic accidents or temporary construction—that may arise within urban environments. Consequently, these limitations hinder the comprehensive assurance of driving safety under all circumstances [44, 49, 5, 57].

Additionally, in environments characterized by low speed and closed routes such as campuses, parks and ports, high-level AV applications can be implemented earlier by restricting vehicle routes and speeds, and allowing immediate stops in emergencies [29]. In these settings, the boundaries of ODD are relatively straightforward, and risks are controllable, but they present significant limitations for large-scale commercialization [56].

As commercial deployment expands, ODD research gradually shifts from closed routes or small-scale urban pilots to fine-grained management of complex scenarios. When vehicles need to navigate complex pedestrian and vehicular traffic in city centers, handle changes in road gradients in mountainous areas, or cope with sudden weather changes (such as rain, fog or heavy snowfall), traditional geography-based ODD boundaries often fail to meet safety requirements [59, 70, 75]. Some researchers have begun proposing dedicated ODD strategies for specific scenarios like extreme weather [39, 52, 67] and ultra-complex urban intersections [54, 76]. These strategies include using multi-sensor fusion [22, 36] and reinforcement learning for decision-making [12, 45] to enhance robustness.

However, most companies currently tend to downplay the limitations of ODD in their marketing, excessively emphasizing that vehicles are capable of handling complex urban areas or supporting adverse weather conditions without providing precise data or boundary conditions [65, 43]. This risks causing public misunderstandings about AV safety and creating confusion for regulatory bodies. Without unified, transparent and enforceable ODD standards, it is challenging to assess ”How safe is safe enough”. Therefore, both at the technical level and within policy and regulatory frameworks, deeper discussions on defining, expanding and validating ODD are urgently needed for the entire AV industry [49, 48, 35, 18].

In summary, although relying on geofencing or specific highways or urban areas, models currently help to initially reduce deployment difficulties. As the levels of AV advance and higher demands for safety and commercialization emerge, the industry increasingly requires more dynamic and comprehensive ODD definition methods [49, 48, 35]. Only by incorporating multi-modal factors such as weather, terrain, traffic flow and unexpected events into a real-time monitoring and dynamic adjustment ODD framework, can the safety and feasibility of AV be ensured in broader and more realistic traffic environments [2, 26, 18].

2.2. Key challenges

After reviewing ODD’s development and current status for AV, this section will focus on the main challenges and issues faced by the current ODD framework. The early concept of ODD primarily evolved from geofencing or closed route testing, aiming to delineate a clear safety boundary for AVs. For example, specific city pilots allow vehicles to operate only within fixed blocks or highway sections, publicly declaring that vehicles can achieve a high level of automation [83, 14]. This geographical approach

initially offered the advantages of rapid deployment and regulatory controllability, so it provided quick solutions for safety and compliance in the early stages. However, as AV functions become increasingly complex and their application scope gradually expands, the limitations of this approach have become more apparent.

A key challenge is the disconnection from real traffic environments. In the real world, factors affecting driving safety are intricate and diverse: weather and lighting conditions, road gradients and friction coefficients, and dynamic disturbances such as pedestrians and non-motorized vehicles, all of which cannot be fully encapsulated by a single administrative boundary or road zoning [59, 70]. While geofencing can help projects to be rapidly deployed using long-term weather data, it easily overlooks dynamic environmental changes such as sudden heavy rain, as shown in Figure 2.4, approximately 20% of crashes are weather-related. Once the vehicle moves beyond the initially defined area or encounters unforeseen scenarios, it may only be able to disengage automation mode or become incapacitated abruptly [32, 75].

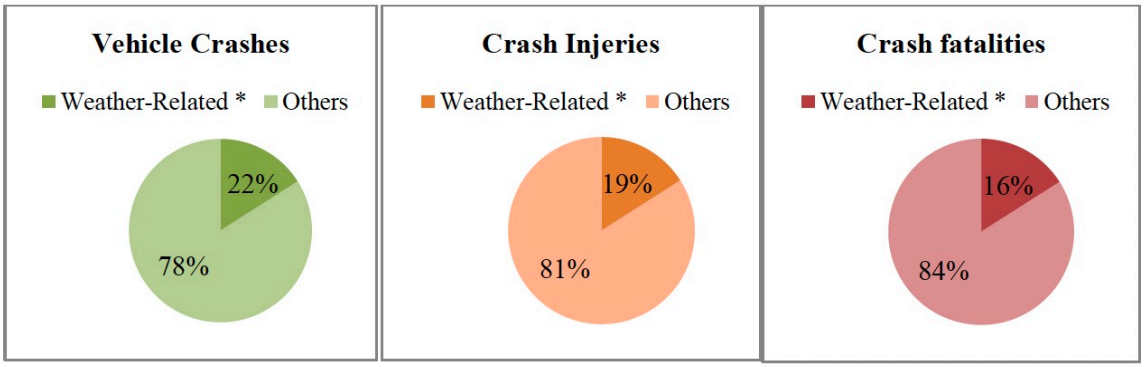

Figure 2.4: Approximately 20% of crashes are weather-related [44]

Another significant issue is the lack of consideration for degradation modes. Geofencing ODD often present a binary classification of "either operational or not operational"; once the external environment deviates from the ODD boundaries, the system either continues to operate forcibly (posing significant risks) or immediately disengage the automation, requiring the driver to take over [14, 66]. Consequently, both academia and industry are increasingly emphasizing that AV should possess multi-level progressive operational modes—from regular operation to degradation, and then to the Minimal Risk Maneuver (MRM)—to mitigate the risks associated with sudden disengagement [26, 84]. And in ISO standards, this process ends with a stable stop [30]. Under geofencing ODD classifications, such more nuanced safety strategies have not been adequately reflected.

A further complication arises from the neglect of Human-Machine Interaction (HMI). ODD frameworks centerd around geographical restrictions often assume that vehicles can achieve high levels of automation within closed or designated scenarios. Yet, they overlook whether human drivers can perceive and take over promptly under critical or boundary conditions [2, 14]. Without robust takeover mechanisms and HMI designs, if the system suddenly prompts the driver to take over when outside the ODD, the driver may fail to respond promptly due to distraction or insufficient reaction time, potentially leading to accidents or legal disputes [32, 43]. Additionally, ethical and liability issues arise: if the system fails to identify ODD boundaries or the driver does not respond to takeover prompts in time, resulting in an accident, questions of responsibility become particularly challenging [14, 43].

Furthermore, there is an ineffectiveness in managing complex traffic participants. In complex urban traffic environments where there is a mix of pedestrian flow, non-motorized vehicles, and various new types of mobility tools, relying solely on geographical boundaries cannot precisely determine when stricter perception and obstacle avoidance strategies are necessary [49, 24]. When a vehicle exits or approaches the preset geofencing area, it should theoretically perform a functional downgrade or require manual takeover [63, 14]. However, temporary switching can easily create conflict risks if this occurs at high speeds or in congested areas, and overly frequent switching can degrade user experience [5, 8].

Finally, a significant hurdle is the difficulty in balancing flexibility and safety. The long-term goal of AV is to operate across cities, regions and even countries. However, different areas have varying road infrastructures, traffic regulations and climatic conditions. Relying solely on geofencing to restrict the ODD means that each cross-regional deployment requires extensive testing and certification, severely limiting technological and industrial expansion [49, 57, 5, 16].

Therefore, the industry is beginning to incorporate multi-modal factors such as weather, road conditions, traffic flow and sensor status, allowing vehicles to update and adjust safety strategies in real-time during operation, and thereby gradually moving away from the simplistic geofencing model [35, 29].

2.3. Attempted solutions

To address the challenges above, researchers have proposed various solutions, and this section will elaborate on the existing improvement ideas and technical implementation pathways.

2.3.1. Overview of existing countermeasures

In response to the shortcomings of geofencing ODD management models based on geofencing or closed roads, academia and industry have proposed multiple improvement strategies. The main strategies can be summarized as follows:

Geofencing + enhanced operational restrictions have been fundamental in early approaches to AV deployment. Initially, AVs were confined to a fixed geographic area, where they could safely engage higher levels of automation [49, 29, 16]. Building on this foundation, several pilot projects have introduced additional operational constraints—such as limitations on vehicle speed, weather conditions, and traffic flow—to further enhance safety and system performance [14, 1], as shown in Figure 2.5. However, relying solely on passive geofencing is insufficient for addressing the dynamic nature of real-world driving conditions; sudden changes in road conditions, construction activities, or adverse weather can surpass preset parameters, potentially forcing the system to execute an emergency disengagement.

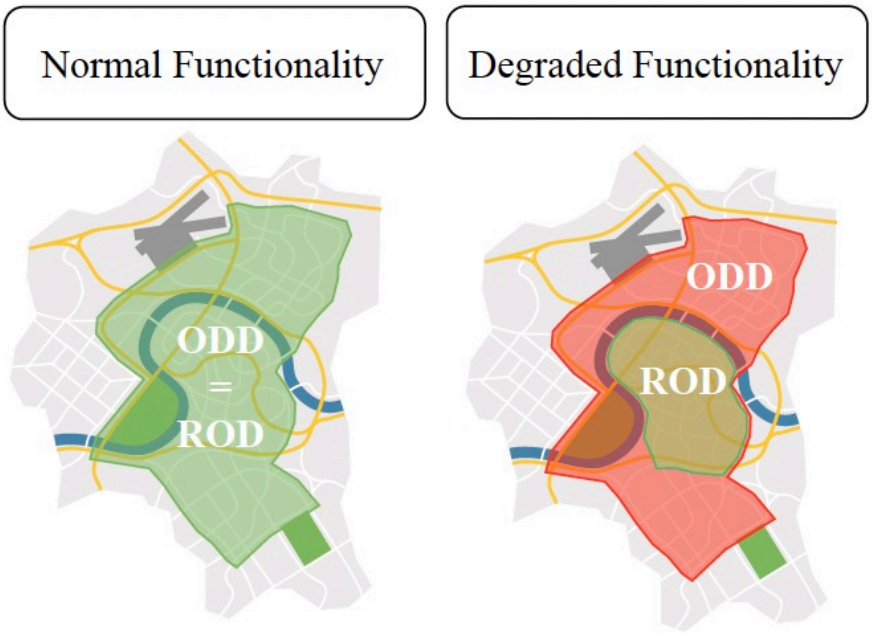

Figure 2.5: Geographic partition and change restrictions under different conditions [14]

A refined approach to ODD has emerged by moving beyond the traditional binary classification of ”operational” versus ”non-operational.” In this new framework, ODD is divided into nuanced modes—namely ”Normal”, ”Degraded” and ”MRM”—that allow AVs to adapt more flexibly to varying environmental con-

ditions [32, 14, 66], as shown in Figure 2.6. When conditions deviate from the ideal yet remain manageable, vehicles transition into a degraded mode by, for example, reducing speed or disabling specific functionalities like overtaking or lane changing to maintain control. Only when safety can no longer be assured does the system execute an MRM. This approach necessitates rigorous research to determine appropriate trigger thresholds, establish operational limits within degraded conditions, and effectively manage interactions with surrounding vehicles and pedestrians.

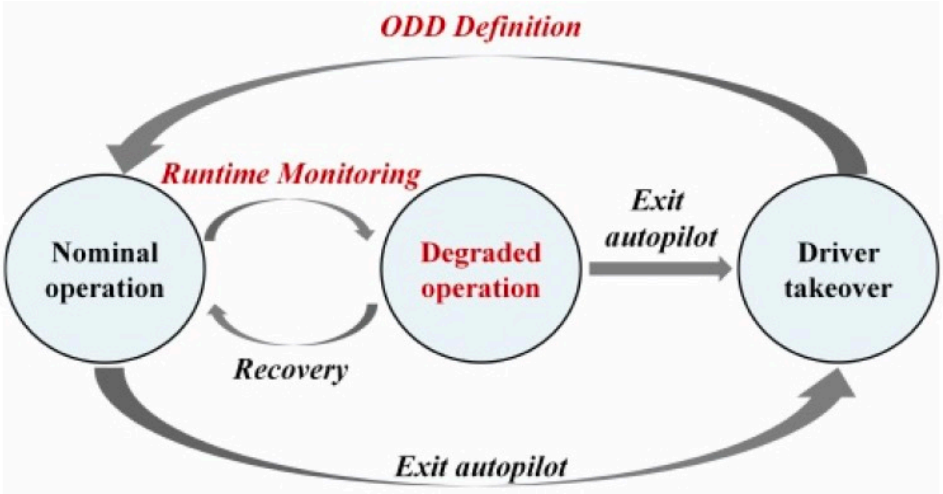

Figure 2.6: Monitoring the ODD to degrade or exit autopilot when condition changes [34]

VSL has been explored in recent studies that extend traditional implementations by prescribing a lower, more conservative speed range specifically for AVs to mitigate collision risks [27, 90, 24, 86]. Typically, these implementations are deployed on fixed road segments or within closed urban environments, which limits their flexibility. As a result, they often lack the dynamic adjustment capabilities required to respond effectively to extreme weather conditions or fluctuating real-time traffic flows, thereby hindering their adaptability to evolving driving conditions.

Driver takeover is initiated when the operational environment exceeds the defined ODD—for instance, during sudden weather changes, sensor perception degradation, or when the vehicle ventures into non-designated areas [63, 35]. In such scenarios, the system promptly issues a takeover request to the driver. However, if this request occurs while the vehicle is navigating high-speed or complex road segments, any delay in the driver's response can introduce additional safety hazards, potentially compounding the risks associated with the transition from autonomous to manual control.

The safe stop is a critical AV response when a vehicle determines that it has exceeded its operational boundaries or can no longer sustain automation. In such cases, the system initiates an MRM by either pulling over or exiting the main lane [63, 80]. While this strategy is effective in low-speed or campus environments, executing an abrupt stop on highways or high traffic capacity areas can lead to secondary accidents or severe congestion.

Multi-modal perception and real-time ODD monitoring leverage external sensors and communication systems, including LiDAR, cameras, radar and V2X communications, to perform a high-frequency fused perception of the surrounding environment [22, 36, 4, 6]. It promptly initiates real-time ODD verification when the system detects significant environmental deterioration, such as widespread radar signal loss or camera obstruction due to rain or snow. This verification process informs the system's decision to either adaptively degrade its operation or disengage automation, as highlighted in [32, 70, 69, 12, 45, 68]. However, implementing this approach demands substantial hardware and computational resources alongside meticulously designed thresholds to prevent frequent and unintended degradations.

Scenario or risk-based testing and coverage redefines the characterization of the ODD by extending beyond dedicated areas to encompass a multi-dimensional framework that includes various weather conditions, terrains and traffic densities. This is achieved through scenario simulation and large-scale

data-driven, or called AI, methods [78, 89, 84]. Effective implementation of this approach necessitates precisely identifying the vehicle's current scenario, yet challenges persist. Notably, there is still a significant gap between simulation and reality, and the generalization capabilities of many AI models remain unproven.

Infrastructure-supported ODD capitalizes on the integration of roadside sensors, high-precision maps and V2X information—exemplified by the Infrastructure Support for Automated Driving (ISAD) architecture [19]—to augment a vehicle's capacity to foresee conditions such as construction activities and adverse weather [77, 1]. However, this approach faces considerable challenges, including the high costs associated with upgrading infrastructure in large cities or along highways, the absence of unified cross-regional standards, and the difficulties inherent in achieving widespread adoption in the short term.

2.3.2. Attempt at dynamic ODD

To effectively apply those above "Dynamic ODD" thought—defined as "the set of environment and roadway conditions that require on-board sensing to detect state changes relative to vehicle position at a second-to-minute rate" [72, 13]—to AV, it is necessary to integrate multiple technical elements such as perception, decision-making, HMI, simulation and testing, and engineering into a comprehensive implementation pathway. A critical starting point is dynamic environment modeling, which involves real-time detection of weather, road surface conditions and the behaviors of traffic participants through multi-sensor fusion and AI algorithms [59, 32, 70]. Coupled with V2X communication technology, this modeling allows the system to obtain prior information on critical road sections, forming the foundation for managing the ODD by ensuring accurate real-time identification of environmental states and determining the appropriate degradation strategy.

Another essential aspect is the rapid real-time evaluation and decision logic. Once environmental changes are detected, the system must quickly assess whether it has exceeded the safety boundaries of the ODD and select suitable degradation or disengagement strategies [14, 26]. Standard methods such as Bayesian networks, fuzzy logic or temporal logic reasoning can be employed to set safety thresholds and avoid excessive disengagements—thereby preventing "cry wolf" scenarios that reduce passenger comfort. Equally important is implementing multi-level operational modes alongside effective HMI. When the environment deteriorates, the system should enter a degraded mode by automatically limiting speed and issuing clear warnings via the HMI. Suppose the driver does not take over promptly, or the situation worsens, the vehicle must be prepared to execute an MRM [32, 14, 43]. This capability is crucial for L3 scenarios where timely and precise takeover requests are vital.

Scenario testing and validation also play a vital role in verifying the integrity of the ODD. Large-scale simulations using scenario-based approaches—alongside closed-course testing with tools such as Scenic and ASAM OpenScenario—can help the system perform reliably under extreme conditions [78, 89, 84]. When new extreme scenarios are identified, it becomes necessary to iteratively update the ODD definitions and real-time monitoring strategies, with subsequent validation through Vehicle-in-the-Loop or road tests [75, 66]. Finally, engineering considerations and cross-regional deployment are crucial. When AVs are deployed in different countries or cities, they must adapt to local infrastructure and regulations to reduce the costs associated with repetitive certification and testing [29, 57, 56]. As infrastructure becomes increasingly digitized—providing enhanced external perception data (e.g., via ISAD)—the management of vehicle ODD is expected to evolve into a more dynamic and refined process. Integrating these elements creates a pathway that enhances AV's safety and reliability, and enables their scalable and efficient deployment across varied environments.

A unified approach to ODD has not yet emerged despite multiple attempts at standardization at the international level. SAE J3016 categorizes AV from L0 to L5. While it does not provide a complete structural definition of ODD, it emphasizes the importance of functional boundaries for safety by specifying varying requirements for environmental recognition and decision-making responsibilities at each level [49, 5, 65]. Meanwhile, ISO 26262 primarily focuses on functional safety with relatively limited attention to external environments [29, 35], and ISO/PAS 21448 (SOTIF) introduces the concept of "Safety of the Intended Functionality" to address risks both inside and outside the ODD [29, 8]. Additionally, ISO 34503 proposes a structured description method for ODD by defining it across multiple dimensions such as roads, weather, traffic participants and time [49, 35]. The UNECE WP.29 working group has

also discussed regulations for L3/L4 AV, proposing principled requirements regarding automation disengagement and human takeover [49, 57]. However, significant differences between countries regarding standards and testing processes for weather, terrain, and traffic conditions continue to pose practical implementation challenges [29].

Real-world experiences offer valuable insights into ODD implementation. Companies such as Waymo and Cruise typically employ city-level geofencing to provide Robotaxi services, while automation disengages during heavy rain or severe nighttime disturbances [29, 80]. Pilot programs such as truck platooning on highways are limited to specific mileage and weather conditions [27, 16]. Within campuses, low-speed autonomous shuttles operate only under ”daytime + good weather” conditions and switch back to manual driving during periods of high pedestrian flow [63, 64]. These examples indicate that many regions currently adopt a ”geographical restriction plus simple environmental assumptions” approach to managing ODD. However, a lack of unified and detailed regulations and testing standards remains a barrier to large-scale, cross-regional commercialization [49, 5, 35].

However, these attempts did not go entirely smoothly. One of the challenges in implementing dynamic ODD is overcoming sensor and computational bottlenecks. High-frequency monitoring necessitates substantial sensor redundancy and powerful processing capabilities, yet sensor false alarms, adverse weather obstructions, or processing delays can lead to system misdegradation [59, 66, 75]. Another critical challenge is bridging the scene recognition and semantic gap. Although scene-based testing can simulate extreme conditions, the myriad long-tail scenarios present in the real world mean that the generalization and robustness of AI models require extensive, long-term validation [78, 84]. The digital transformation of infrastructure and deploying numerous onboard sensors come with significant financial and logistical challenges. Successful implementation demands coordinated efforts and substantial investment from governments, automakers and road managers alike [77, 1]. Lastly, there are notable disparities between countries or regions in ODD’s definition and verification methods, with evolving standards such as those from ISO. These inconsistencies pose challenges for cross-regional applications, necessitating efforts to harmonize regulations to ensure reliable and scalable AV solutions [55, 2, 65].

Despite these challenges, the collective exploration of dynamic ODD has laid an essential foundation for the next development phase. Higher levels of AV can initially be implemented safely in local or specific environments, while the practical experiences gained will inform future cross-city and cross-national operations. It is foreseeable that future ODD will increasingly rely on onboard perception, roadside facilities, cloud big data, and the coordinated evolution of regulations and insurance systems to establish genuinely scalable and reliable safety domains for AV.

2.4. Experience failures

Systems must maintain stability and safety in highly diverse and dynamic environments to achieve more practical and wide-ranging AV. Compared to the factors neglected by traditional geofencing ODD, the following three aspects of complexity pose higher challenges to automation performance.

Heavy rain, heavy snow, fog, sandstorms and other weather conditions can significantly reduce the observation range of cameras and LiDAR, even causing complete failure [59, 70]; if the system lacks redundant sensors or perception degradation strategies, it can quickly lose control in sudden situations [18, 75]. Insufficient lighting at night, tunnel environments or direct intense light can impact the robustness of visual sensors. Snow or water accumulation can also decrease the visibility of lane markings, increasing noise in perception algorithms [44].

Steep slopes, curves, pothole-ridden roads, temporary construction, landslides and other factors place higher demands on longitudinal acceleration and deceleration, lateral stability and tire friction estimation [31, 41]. In reality, secondary roads, ramps, roundabouts or multi-lane expressways often differ significantly from the traditional binary classification of ”urban/highway”. If the ODD does not include a detailed description of these diverse road conditions, it can easily result in overlooked speed control or decision-making blind spots [49, 5, 58].

City centers often have dense pedestrian flows, non-motorized vehicles crossing randomly, and frequent instances of traffic participants not following rules [83, 55, 78]. A static ODD, where AVs work

at a fixed location or all the situations can be predicted [13], alone cannot handle unexpected events, such as pedestrians suddenly appearing or cyclists changing lanes. On highways or in congested urban areas, high vehicle density means that vehicles can suddenly change lanes or cut in at any time [27, 90]; if the ODD does not incorporate real-time monitoring and response strategies for traffic flow changes, following and lane-changing algorithms will fail [12, 76]. The diversification of mixed vehicles (traditional fuel vehicles, intelligent connected vehicles, electric scooters) and the fact that some traffic participants are not connected to V2X make global information perception more difficult, significantly increasing system prediction and planning uncertainties [24, 80, 53]. Under the impact of these environmental variables, if AV relies solely on a single geofencing or road type classification, it will be difficult to promptly identify and respond to dynamic changes in weather, terrain, or traffic conditions, often resulting in insufficient risk prediction, missing degradation modes and failure of complex interactions [77, 26]. Therefore, the industry has been attempting to dynamically expand or contract the ODD through multi-modal perception and real-time risk assessment. However, in the absence of algorithm real-time performance, hardware costs and incomplete regulatory standards, large-scale deployment still faces numerous challenges [49, 5, 8, 29, 57, 56].

In addition to technical aspects, applying ODD to practical management and legal regulations also faces numerous difficulties. Although SAE J3016 requires L 3-5 AVs to declare their ODD, it does not provide unified metrics or verification processes [65]; standards like ISO 34503 attempt to provide classification frameworks, but they are still relatively broad and challenging to implement at the city management or testing and certification levels [2, 26]. Countries or states vary significantly in their approaches to AV testing permits (e.g., some US states allow only night-time on certain roads, some European countries pilot on multi-lane highways), lacking a universal protocol to assess scenario coverage and safety redundancy [77, 55, 66]. Some companies emphasise automation's ability on a broader road network in their promotions, but the specific limitations of ODD are often vaguely stated, usually only noted in small print within legal documents or test reports [43, 75]. Regulatory bodies face information asymmetry that under different weather, terrain and traffic loads, it is difficult to assess the system's actual performance, and the public may form over-expectations or doubts due to company promotions, thereby affecting the acceptance of AV [14, 43].

2.5. ODD quantification based on real-world variables

Compared to traditional methods of defining ODD based on urban/highway areas, the new generation of solutions emphasises defining the ODD as a function of real-world variables—such as road slope, road surface friction coefficient, traffic flow, weather visibility and lighting conditions—rather than being limited to a particular city or road segment [59, 70, 18]. Dynamic environmental assessment indicators can be established so that vehicles determine in real-time, via onboard sensors or external data sources like meteorological radar and road sensors, whether they remain within the safe operational envelope [26, 69]. When environmental indicators (such as rainfall, snowfall or visibility) exceed predefined thresholds, the system can automatically trigger operational degradation or prompt the driver to take over [44, 52]. In addition, for mountainous areas or long downhill sections, dynamically assessing the vehicle's limits by integrating high-precision maps with real-time slope measurements from the Inertial Measurement Unit (IMU) is essential [18, 41, 91].

A key element in this approach is real-time perception and data fusion. In adverse weather conditions, integrating data from LiDAR, cameras, radar and V2X-based meteorological sources (like road temperature data from city traffic management centers) can yield more precise indicators. For instance, when rainfall intensity exceeds 50 mm/h and visibility drops below 100 meters, the system can trigger degradation automatically [32, 70, 75]. Moreover, by combining inputs from vehicle IMUs, wheel speed sensors and high-precision maps, the system can estimate slope, grade length, and turn radius in real-time to verify if these parameters meet current dynamic limits [18, 41, 48, 44]. Real-time estimation of the friction coefficient—using data such as wheel speed differences, brake pressure and acceleration—further aids in adjusting speed or extending braking distances under slippery or icy conditions [51, 91]. Although this multi-modal, attribute-based approach better captures the variability of weather and terrain, it also increases the demands on sensor perception, computation capability and data communication, and sensor or network failures under extreme conditions remain a risk [59, 70, 66]. Additionally, setting dynamic segmentation thresholds that accurately reflect actual safety risks

still calls for extensive empirical validation [26, 28].

Another significant innovation is the use of multi-modal fusion and redundant perception. Instead of relying primarily on cameras or LiDAR, both academia and industry are shifting towards systems that integrate cameras, radar, LiDAR and vehicle networking data [59, 70, 69]. This multi-modal approach compensates for the limitations of individual sensors, especially under conditions such as rain, fog or sudden lighting changes, like entering or leaving tunnels, where detection quality can degrade [75]. However, deploying multiple redundant sensors increases equipment and maintenance costs and places higher demands on onboard computing resources [66, 43]. In highly dynamic scenarios, the timely processing of sensor data may also be hampered by communication bandwidth limitations or high latency, particularly if external infrastructure (providing alerts like construction or visibility warnings) is not sufficiently integrated [77, 1]. So practical assessments for commercialization and large-scale application further add to the complexity of this approach [43, 55].

Equally important is a hierarchical degradation strategy that includes an MRM mode. In this framework, there are three operational states[32, 14, 26]:

- Normal ODD: The vehicle can operate with designed automation capabilities;
- Degraded ODD: When the environment deteriorates but remains manageable, the vehicle reduces speed, increases following distance or limits lane-changing frequency;
- Extreme ODD (MRM): When the environment is completely beyond limits and automation cannot be maintained, the vehicle executes an MRM (emergency braking or moving to the shoulder).

This model emphasises stepwise degradation, allowing drivers time and sufficient information to take over or assist in decision-making, thereby avoiding premature ”hard exits” while controllability still exists [66, 43]. However, hierarchical degradation can reduce safety hazards caused by blurred boundaries. Still, if thresholds are improperly designed or vehicle environment perception is inaccurate, it may lead to frequent switching, causing driver annoyance or distraction. During the hierarchical degradation process, the HMI is crucial. When the vehicle detects the need to switch to the degraded ODD, it should provide understandable warnings or visual explanations [14, 66]. If the driver does not respond promptly or lacks attention, the system can further enter the MRM to safely park or move to the roadside [32, 70, 43]. However, tests show that takeover timing and driver characteristics (gender, age and driving experience) significantly affect safety [9, 3]. In low-visibility environments, human drivers may also struggle to discern lane markings and lose control [62]. Therefore, relying solely on the ”disengagement ODD for manual takeover” approach still carries additional risks. If substantial real-time computation is required within the degraded ODD (such as VSL or curve control), insufficient computational power or algorithmic misjudgments can introduce new risks. How HMI can effectively switch in high-speed or busy traffic conditions still requires in-depth human factors research and field validation.

Finally, scenario simulation and data-driven ODD tuning are vital for continuously refining automation. The scenario-based testing approach involves decomposing factors such as weather, road types, traffic flow and interactions with pedestrians or bicycles into multiple dimensions, which are then recombined to form critical scenarios that challenge the vehicle’s systems [78, 89, 84]. By incorporating real-world failure cases (such as sudden construction, mixed ice and snow road surfaces) into the scenario library, systems can identify and adjust ODD boundaries early during the simulation phase [26, 18]. With large-scale fleet operations, the perception data and event logs collected by each vehicle can continuously refine the ODD [32, 66, 84]. Statistical analysis of extensive operational data on rainy and snowy road sections may reveal that the feasible speed is much lower than initially set, allowing for dynamic ODD adjustments. Relying solely on a one-time compiled ODD document without continuously updating it based on large-scale operational data makes it difficult to cover more long-tail scenarios [70, 69]. Although scenario simulation can cover numerous theoretical combinations, if the simulation of weather, terrain or human-vehicle interactions is not sufficiently realistic, there remains a gap between simulation results and reality [78, 84, 75]. Data-driven approaches also require robust backend platforms and fleet management support. Still, due to privacy considerations and commercial competition, data sharing between companies is challenging, limiting unified industry-wide ODD improvements [55, 43].

2.6. Significance

2.6.1. Promotion of safe operations

Dynamic ODD offers several significant safety benefits. Reducing the probability of accidents and emergency takeovers is key. Compared to traditional geofencing ODD, the dynamic ODD that integrates multi-modal factors such as weather, terrain and traffic flow can more promptly detect sudden risks like blizzards, sharp curves or traffic congestion, triggering warnings or hierarchical degradation. In complex urban road conditions or extreme weather, vehicles can decide when to reduce speed, increase safety distance or automatically change lanes through high-frequency monitoring (e.g., rainfall intensity, visibility and road slope), thereby avoiding perception failures and drivers being caught off guard [59, 26, 70]. Relying solely on multi-sensor fusion does not guarantee ”zero accidents”, and it still requires HMI and social management strategies. If a vehicle suddenly disengages automation on a highway, the takeover process may still lead to secondary accidents or traffic blockages. Therefore, through real-time environmental monitoring and degradation mechanisms, multi-modal ODD is expected to further reduce the risk of emergency takeovers in sudden situations and enhance the safety boundaries of AV.

Enhancing coverage and response capability for long-tail scenarios is another benefit of this approach. By employing scenario-driven methods that exhaustively cover rare combinations—such as icy roads, sharp curves and low nighttime visibility—the system can evaluate and build in safety redundancies during development and iterative improvement stages [78, 84]. Furthermore, vehicles can continuously learn from extreme real-world situations by collecting and updating ODD data based on both routine operations and unexpected events. This continuous learning enhances adaptability to long-tail scenarios, although progress may be hindered if extreme scenario and accident data are not effectively shared across companies or regions.

Preventing vehicles from unconsciously operating in uncontrollable environments is also critical. By proactively anticipating when adverse conditions—such as severe weather, significant road defects or non-standard traffic disturbances—are likely to push risks beyond safe limits, the ODD mechanism can prompt the vehicle to reduce speed, change lanes or alert the driver to take control [14, 66, 75]. However, care must be taken to manage this proactive response to avoid chain reactions (like sudden deceleration or emergency stopping) that could lead to secondary accidents.

2.6.2. Impact on future large-scale commercialization

In the past, testing in new cities or highways required extensive manual boundary definitions; the dynamic ODD, which is primarily based on environmental attributes, can determine feasibility more efficiently, allowing for quicker cross-regional deployment [26, 69, 50, 66].

In addition, the dynamic ODD supports a unified evaluation framework for cross-province or cross-national operational scenarios—such as Robotaxi and truck platooning—by offering a relatively consistent safety assessment [77, 66]. Nevertheless, cross-regional deployments still contend with differences in regulations, infrastructure and cultural environments. While dynamic ODD addresses technical flexibility, institutional and infrastructural advancements must progress in parallel.

Moreover, as the industry increasingly adopts multi-modal ODD, efforts to refine evaluation metrics are gaining momentum. Relevant international standards, such as ISO 34503 and UNECE WP.29, are gradually incorporating factors like weather, terrain, and dynamic traffic participants into certification processes [79, 2, 65, 37]. This evolution helps mitigate the gray areas of operations beyond ODD by mandating that vehicles possess real-time monitoring and degradation strategies—thereby compelling the industry to fundamentally enhance safety redundancies [55, 78]. However, because implementing these standards requires multi-party negotiations, some companies may choose to simplify ODD in order to accelerate commercial progress, potentially introducing hidden risks.

Furthermore, enhancing intelligent infrastructure is also critical to extending the coverage of the dynamic ODD in more extreme scenarios. Achieving this goal requires the integration of roadside sensing units and vehicle-road collaborative systems that provide real-time information on construction activities and weather warnings [77, 1]. Yet, constructing large-scale intelligent roads demands substantial financial investment and cross-departmental collaboration—efforts that may initially be confined to a few demonstration areas. In regions where infrastructure is less developed, fully realizing the advantages of dynamic ODD remains a significant challenge.

2.7. Remaining problems

According to the literature review, several critical challenges remain in accurately defining and managing the ODD for AVs. In particular, the following four issues must be addressed:

A fundamental challenge is the lack of comprehensive datasets capturing extreme conditions. Although many studies recognize that severe weather (e.g., heavy rain, snow, fog or sandstorms) can significantly degrade sensor performance. However, most available data cover only moderate conditions. Extreme-case data are critical for validating models under worst-case scenarios. Relying solely on standard datasets may overlook rare but impactful events that could lead to unexpected failures. Collecting and analyzing extreme data enables more robust safety margins and better calibration of simulation models.

While the literature consistently notes that adverse weather increases sensor noise and reduces detection range, most studies offer only qualitative insights into this relationship. There is a pressing need to quantitatively assess how weather conditions—ranging from drizzle to downpours—affect sensor detection distances. Accurate quantification would enable a more precise determination of when AV operates safely within its ODD.

Braking distance is influenced by numerous factors—including road friction, slope and weather—which interact in complex ways that a simple formula may not adequately capture. Instead of relying solely on analytical formulas, braking simulations can incorporate these complexities using detailed models that reflect real-world dynamics. A simulation-based table of braking distances under various combinations of weather and road slopes provides a comprehensive and practical reference for system safety thresholds. This approach offers flexibility and precision, capturing the compound effects (such as slippery surfaces on steep slopes) that are difficult to model with closed-form equations.

Traditional control methods such as Proportion-Integration-Differentiation (PID) or Model Predictive Control (MPC) rely on fixed mathematical models and require precise system identification, which may not adequately handle the dynamic nature of real-world driving conditions. In contrast, an RL approach can learn optimal control policies from real-time data without explicit system models. This is especially beneficial for adjusting vehicle speed when sensor detection ranges and braking distances vary continuously. RL offers the flexibility to adapt to unforeseen changes in the operational environment and can improve decision-making at the boundaries of the ODD. However, detection and braking distance still need to be integrated.

Addressing these four challenges—expanding extreme-case datasets, quantifying sensor detection under diverse weather conditions, creating comprehensive braking distance simulation tables, and developing an RL-based speed control framework integrating the detection and braking distance—is essential for advancing AV safety and scalability in increasingly complex real-world environments.

3

Methodology

3.1. Introduction

AVs still face significant safety risks in extreme weather and complex terrain environments. This research will focus on two key aspects: the limited perception range and the mismatched braking performance. Accordingly, it defines the detection distance as the maximum distance an AV could potentially detect a car—typically limited by factors such as GPU memory and sensor range—rather than the distance at which detection is sufficiently reliable for safe operation within the ODD, which is geo-featured. To address these challenges, this study proposes a comprehensive approach encompassing extreme weather dataset generation, detection distance testing, braking distance simulation and RL-based speed control. The method simulates various traffic and weather conditions in a virtual environment, quantifying the influence of weather and slope on detection and braking distances. By comparing whether the braking distance is less than the detection distance, the approach determines if the vehicle can brake in time when an obstacle is detected and, in this study, regarded as a criterion if the vehicle is within the ODD. Based on these quantified conditions, an RL-based speed control is employed to ensure safety and improve efficiency.

The following work is divided into four detailed steps:

- Extreme weather data generation: Use AV simulator CARLA and traffic flow simulator SUMO to generate images and videos under various weather conditions and traffic flow capacities. Automated annotation tools are employed to obtain vehicle position labels.
- Detection distance testing: Based on the dataset above, train and evaluate an object detection model to determine the maximum detection distance under different weather conditions and analyze the average detection distances, variance and false positive ratio among different maps.
- Braking distance simulation: Simulate vehicle braking performance in physics engine PyChrono, recording braking distances under various slopes, road frictions and vehicle speeds.
- RL-based speed control: Introduce the detection and braking distances above into CARLA. Use the Soft Actor-Critic (SAC) algorithm to train throttle and brake control. The reward function is determined by speed, acceleration, collision avoidance and the relationship between the estimated braking distance and the detection distance, enabling vehicles to ensure safety and improve speed under various weather and slope conditions.

3.1.1. Methodology logic and data flow

Extreme weather dataset generation (Step 1) generates numerous labeled multi-weather images and videos, providing training data for detection model training. The dataset addresses the limitation of insufficient data samples under extreme weather conditions.

Detection distance testing (Step 2) is primarily based on scenario simulation, which outputs the maximum detection distance of each weather, lighting, map and model combination. This step quantifies the impact of different weather on detection distances, forming the foundation for safe speed calculations.

Braking distance simulation (Step 3) focuses on vehicle dynamics, producing a braking distance table that varies with slope, friction and speed. It addresses the lack of data under extreme weather and slope conditions, providing high-accuracy data.

RL speed control (Step 4) incorporates key metrics detection and braking distances as the reward with other factors like speed, acceleration, collision avoidance and smooth driving. By dynamically adjusting speed in response to variations in detection and braking distances under different weather and slopes, the system ensures that the braking distance remains closely aligned with the detection distance. This alignment encourages the vehicle to stop safely upon detecting an obstacle to enhance safety while optimizing efficiency.

Ultimately, these four components form a complete experimental and research pipeline: evaluating the perception system, simulating vehicle dynamics and finally, using RL as the core to achieve adaptive vehicle speed control based on safe distances.

To visually present the methodological logic of this study, Figure 3.1 summarizes each step's inputs, outputs and data flow processes, while a more detailed flowchart is shown in the appendix Figure A.1. The following sections, 3.2 to 3.5, will detail each step's technical implementations.

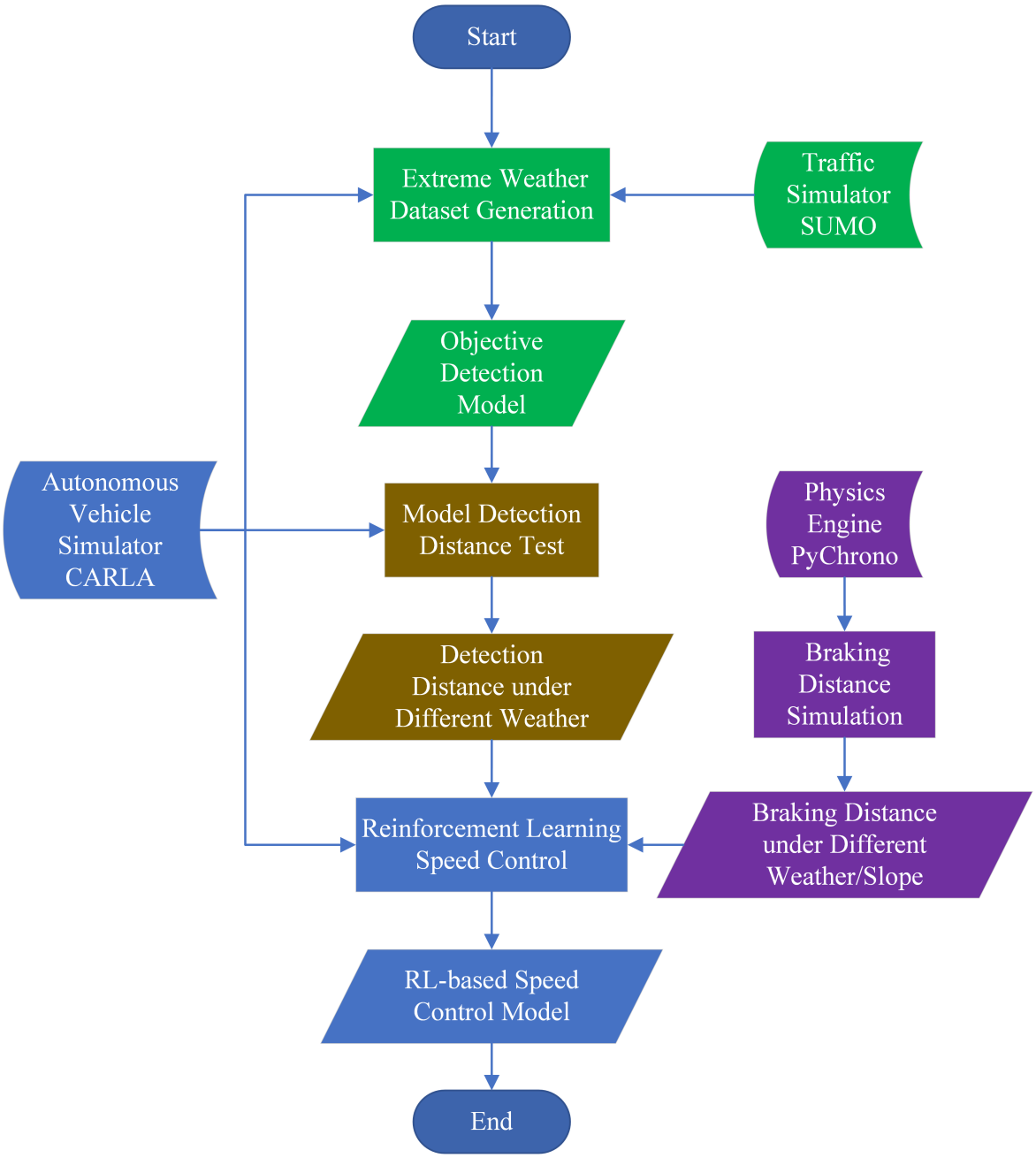

Figure 3.1: Research methods and data flow chart

3.2. Extreme weather dataset generation

In AV perception systems research, sufficient and diverse training data is crucial for model performance. However, extreme weather conditions are unpredictable, and collecting sensor data in the real world is both time-consuming and challenging, which makes it difficult to gather sufficient extreme weather scenarios. In addition, it is difficult to objectively quantify the ”intensity” of different weather events in the real world, which makes subsequent data analysis and model comparison difficult. For this reason, this study prioritizes using a simulator to generate and collect a large amount of annotated data as a basis for the subsequent vehicle detection model and detection distance testing.

Since this study aims to explore the detection performance of vehicle sensors under various weather and traffic scenarios, CARLA was ultimately selected as the core simulation platform. It is important

to emphasize that although CARLA can provide realistic rendering for extreme conditions such as rain, fog and night, snow simulation still requires further improvement. Additionally, while simulators can provide reliable data, the depiction of real-world sensor noise, lens distortion, and other factors may be limited. Therefore, subsequent experiments must maintain necessary error estimation and method adaptation accordingly.

As a macroscopic traffic flow simulator, SUMO models and controls vehicle flow (including vehicle types and speed settings) and can achieve stable global flow simulation at a lower computational cost. On the other hand, CARLA performs high-precision rendering and physical simulation of scenes at the microscopic level. By inputting vehicle trajectories provided by SUMO into CARLA, the latter can generate corresponding video data scenes with high fidelity, as shown in Figure 3.2. This co-simulation approach enables high-precision video data generation for traffic scenarios while ensuring simulation stability and improving efficiency.

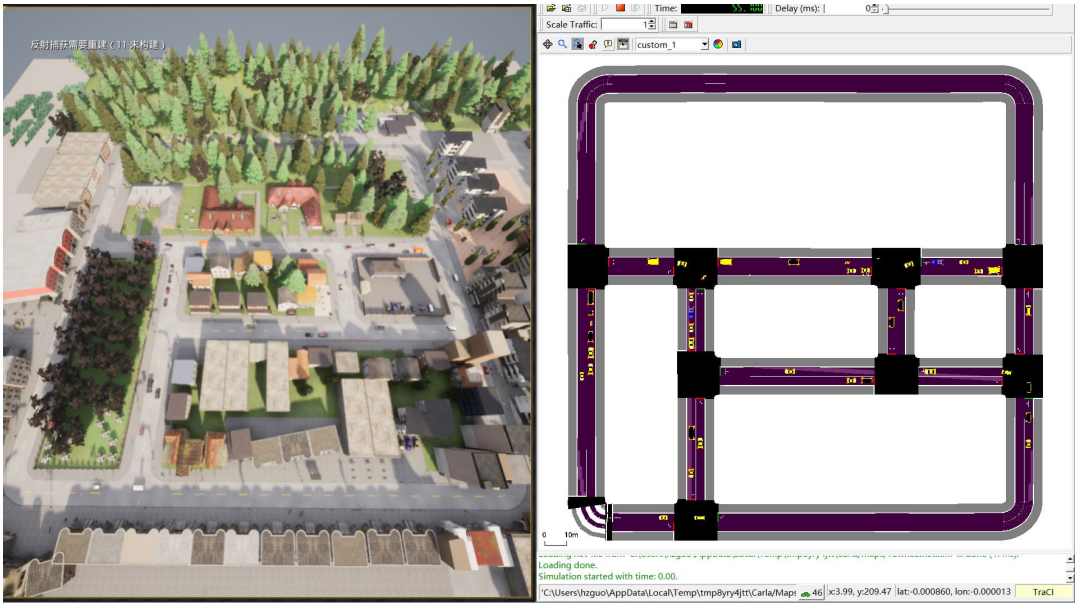

Figure 3.2: Co-simulation between CARLA and SUMO

This study has obtained a diverse and controllable dataset of images and videos featuring multiple weather conditions, maps and vehicle types through the methods above. These data encompass static vehicle scenes and dynamic traffic flow, providing the necessary materials and sufficient sample diversity for subsequent vehicle detection model training and detection distance testing. Although simulations cannot fully replicate extreme weather and real-world noisy environments, the dataset generated based on CARLA and SUMO can effectively perform quantitative evaluations of AV perception systems under various weather and traffic load conditions. The following section will conduct the detection distance testing and a comparative analysis of the vehicle detection model based on these generated images and videos.

3.3. Detection distance testing

In complex and variable road environments, the maximum detection distance of vehicle sensors and detection models is a key indicator for measuring AV's safety boundaries. If the effective detection distance of a vehicle is insufficient under certain meteorological or lighting conditions, the risk of collisions or the inability to brake in time will increase significantly. This section introduces how to utilize the CARLA simulation environment to systematically test the detection distances of vehicles under various combinations of lighting and weather conditions. Additionally, based on different map training scenarios, it evaluates the performance differences of sensors and detection models between trained and untrained regions.

This study compares two vehicle detection models: the COCO YOLO and the Extreme Weather Model.

- **COCO YOLO Model**: Pre-trained general computer vision model based on the public COCO dataset and directly applied to testing.
- **Extreme Weather Model**: Trained on the generated and annotated images and videos mentioned in section 3.2, the dataset is tailored to meet the specific requirements of extreme weather conditions.

Based on the aforementioned map types, they are categorized into fixed-city maps and inter-city maps. The dataset for the Extreme Weather Model uses the dataset from fixed-city maps, while data from inter-city maps will be utilized for domain adaptation testing. To better describe the scenarios, the Specialization Model and Generalization Model are named to represent the two scenarios respectively. The COCO YOLO Model, as a pre-trained model, does not use either scenario as a training set and, therefore, does not differentiate between the scenarios. The details are shown in Table 3.1. To reduce false positives (misclassifying the background as a vehicle) and missed detections (vehicles not being detected), this study conducts tests at detection confidence thresholds of 25% and 50%.

Table 3.1: Details of the tested models

	Specialization Model	**Generalization Model**	**COCO Model**
Model	Extreme Weather Model	Extreme Weather Model	COCO YOLO Model
Test Map	Fixed-city Maps	Inter-city Maps	Fixed-city Maps

Algorithm 3 illustrates the process of detecting the image dataset and recording the "maximum detection distance". The detection results are sequentially checked for each combination (map, lighting, weather, intensity and threshold) from 5 m to 120 m. If the target is consistently detected at a distance d and below but fails to detect at $d + 5$ m, then d is recorded as the maximum detection distance for that combination.

3.3.1. Data analysis methods

The study evaluates sensor performance and detection models by distance, variance and false positive probability. After collecting a complete dataset and training the model, different models' average detection distance and variance are determined across multiple test locations and weathers. Concurrently, false positive probability is assessed using bar charts comparing detection models and confidence thresholds. Statistics are also gathered separately for the Specialization Model (Town 01 to Town 06) and the Generalization Model (Town 07, Town 10 and Town 13) to compare detection distances under the source and target domains. Finally, line charts illustrate how detection distance and variance change under varying conditions—such as increased intensity, different weather (fog, rain and wet) and different lighting (daytime, nighttime and cloud)—providing insights into the stability and robustness of the models.

In the next section, this study will evaluate the braking distances obtained through PyChrono and compare them with these maximum detection distances. If particular weather and speed conditions result in "braking distance > detection distance," the operating condition has exceeded the vehicle's ODD for safe driving. Additionally, these results will be utilized in the RL speed control module to adjust the vehicle's driving speed dynamically.

3.3.2. Research significance and summary

Through the above two-phase data collection and model testing process, this study systematically quantified the changes in vehicle detection distance under different lighting (daytime, nighttime and cloudy) and weather conditions (rain, wetness and fog). It also compared the generalization and specialization models to verify the detection models' domain adaption performance.

These detection distance data will be matched with braking distances obtained from vehicle dynamics simulations to identify potential safety risk scenarios. Additionally, they will provide real-time references for speed decision strategies in RL, encouraging AVs to maintain controllable and efficient driving speeds in extreme environments.

3.4. Braking distance simulation

When defining the ODD, this study emphasizes that vehicles should be able to complete braking within the sensor detection distance. Therefore, in addition to the detection distance of the perception system, the other key metric is the vehicle's braking distance under different road surfaces and slope conditions. If the braking distance exceeds the detection distance, the vehicle poses a potential safety risk in that environment and may be considered disengaged from its ODD. This section will introduce how to utilize the PyChrono physics engine to systematically measure vehicle braking distances under various weather, slope and speed conditions.

3.4.1. Motivation for braking distance simulation

Traditional methods calculate braking distance using simplified formulas (such as uniform acceleration formulas $v = v_0 + at$ or expirical model $d = \frac{v^2}{2\mu g}$). However, in real driving scenarios, vehicle speed does not undergo a uniform deceleration as factors like tire-road interactions, slope effects, air resistance and brake system characteristics cause dynamic changes. To reflect these complex factors more realistically, this study selects PyChrono—a high-fidelity dynamics simulation software for complex mechanical systems.

The simulation framework evaluates braking performance across three axes of variability:

- **Friction**: Road friction coefficients model weather impacts, from dry asphalt to icy surfaces. These coefficients modulate tire-road adhesion forces, directly affecting deceleration rates.
- **Slope**: Slope angles (both uphill and downhill) introduce gravitational components that either oppose or assist braking. For instance, downhill slopes amplify braking distances, creating high-risk scenarios.
- **Initial speed**: Initial velocities span urban (low-speed) to highway (high-speed) regimes, reflecting real-world driving contexts.

A sedan model serves as the baseline vehicle due to its widespread use and balanced dynamic properties. During simulations, the vehicle is stabilized at a target speed, after which full braking force is applied. Braking distances are measured as the vehicle decelerates to a near-stop threshold, accounting for transient effects like weight transfer and ABS-like dynamics. Each scenario is repeated to mitigate stochastic noise, with results averaged to ensure robustness.

3.4.2. Detection distance comparison and risk assessment

This study compares the braking distance results against the maximum detection distances obtained in the detection distance testing section. To enhance the understanding of system behaviour under various weather conditions, typical detection distance values for foggy and rainy conditions at low, medium and high intensities are selected with specific values detailed in section 4.4.3. The study also compares the Specialization Model with the Generalization Model. Under different detection models and weathers, line charts with the slope as the X-axis and the expected speed as the Y-axis are created to intuitively demonstrate the relationship between detection and braking distance. The expected speed means that the speed of the detection distance is the same as the braking distance. When the braking distance exceeds the detection distance or the speed is higher than the expected speed, it indicates that the vehicle cannot come to a complete stop after detecting an obstacle, categorizing it as a risk scenario disengaging the ODD. These charts distinguish different weather intensities using unique colors to enhance clarity.

By jointly analyzing detection and braking distances, it is determined whether the vehicle can complete braking under each combination of weather, slope and speed. This analysis directly informs the RL speed control module, allowing real-time adjustment of the vehicle's speed strategies in different environments.

- In scenarios where the braking distance exceeds the detection distance, the RL agent must proactively reduce the maximum driving speed or adopt more conservative operational strategies to ensure safety.
- In conditions with higher friction coefficients on the road surface (dry conditions) or longer detection distances, the agent can increase the vehicle speed to optimize traffic efficiency moderately,

as supported by quantitative analysis.

By coupling the perception system with dynamic control, this study can comprehensively and quantitatively delineate the ODD boundary of AVs under various road and weather conditions. The outcomes provide a more precise technical reference for deploying AVs in complex environments, thereby enhancing their safety and reliability.

3.5. Reinforcement learning speed control

In the preceding sections, this study explored the detection distances of vehicles under different model weather and lighting conditions, and the braking distances under varying slopes, friction and speeds. To enable AVs to adaptively adjust their speed in dynamic environments, thereby consistently maintaining the objective of "braking distance not exceeding detection distance", this study employs SAC, an RL method, within the CARLA simulator to enable adaptive vehicle control to perform real-time control of the vehicle's throttle and brake.

3.5.1. Motivation of reinforcement learning

Despite the widespread application of PID control and MPC in vehicle control, they exhibit apparent shortcomings under dynamic and uncertain conditions such as extreme weather and complex road conditions. PID control is sensitive to linear systems, however, based on the above research results, both speed and slope have a quadratic effect on braking distance. While MPC relies on accurate modeling and requires solving complex optimization problems at each control horizon. When the slope decreases, the braking distance will suddenly increase and without an appropriate method to predict changes in the slope, MPC could lead to speeds exceeding safety limits. In contrast, RL, by continuously interacting with the environment, does not depend on precise models and can flexibly adapt to system nonlinearity and environmental uncertainties, and offers a more efficient and adaptive solution for handling complex, dynamic driving environments.

3.5.2. Reinforcement learning structure

The specific approach involves incorporating the current weather's detection distance by referencing a pre-established lookup table and the simulated braking distance which is determined through sensor-derived inputs for slope θ, friction μ and current speed v that are then used to query a lookup table for braking distance. These elements are integrated into the RL training to develop an adaptive speed control strategy. To verify the effectiveness of this approach, a baseline method is compared, which does not consider braking distance and only uses (μ, θ, v) as the input without designing additional safety constraints.

The detection distance (d_{detect}) is based on the results in section 3.3. The maximum detectable distance and variance, under different models, weather and lighting, have been statistically summarized offline and are assumed to follow a Gaussian distribution. During the RL training, each episode begins with a random selection of (weather, lighting and intensity) to simulate weather environments. The corresponding detection distance d_{detect} for the current scene is obtained by referencing the table. This study incorporates perturbation on the detection distance to introduce randomness. The magnitude of the perturbation is set according to the variance of detection distance obtained in the tests above. This enables the agent to adapt to various detection distances and develop strategies suitable for perturbed detection scenarios. To simplify the learning process, the system assumes that the detection distance depends solely on weather conditions, thereby ensuring reliable recognition within that range. So the system incorporates a parameter d_{front} to represent the distance to the vehicle ahead. When the preceding vehicle is outside the detection distance, d_{front} is set equal to d_{detect}; meanwhile, if the vehicle is within the detection distance, d_{front} is updated with the actual distance measured by the simulator.

While the braking distance (d_{brake}) is based on the three-dimensional braking distance table obtained using PyChrono in section 3.4, denoted as $d_{brake}(\mu, \theta, v)$, where

- μ represents the road surface friction coefficient (simulating weather conditions),
- θ represents the slope,
- v represents the current vehicle speed.

At the start of each episode, the road surface friction μ is set based on the weather, corresponding to dry, rainy and snow scenarios. The experiments found that the controlled speed under ice conditions did not exhibit significant differences from the baseline scenario, leading to the removal of this condition. The vehicle's real-time sensors obtain the current speed v and slope θ. The corresponding braking distance is queried from a three-dimensional table, where the friction coefficient is set to the actual value based on the weather and the interpolation is performed over the slope and speed dimensions.

3.5.3. Reinforcement learning environment setup

RL is a method for learning optimal decision-making strategies through interaction with the environment, as the simulator CARLA. The core elements of an RL task include the following three components:

- **State (s)**: The state represents the agent's observation of the environment at the step and is the foundation for the agent's decisions. In this study, the state includes vehicle speed, slope, friction, detection distance, braking distance and the distance between two vehicles.
- **Action (a)**: Actions define the agent's behaviors, directly influencing environmental changes. This study's actions reflect the degree of vehicle acceleration and braking, corresponding to throttle and brake controls.
- **Reward (r)**: The reward is a feedback signal resulting from the agent's actions, guiding the agent to learn in a direction that maximises cumulative rewards. The design of the reward function needs to balance driving safety and efficiency, encouraging the maintenance of reasonable speeds avoiding collisions and minimizing sudden acceleration or braking.

According to the above objectives and parameter settings of reinforcement learning, the entire process of reinforcement learning, data sources, and objectives are shown in Figure 3.3.

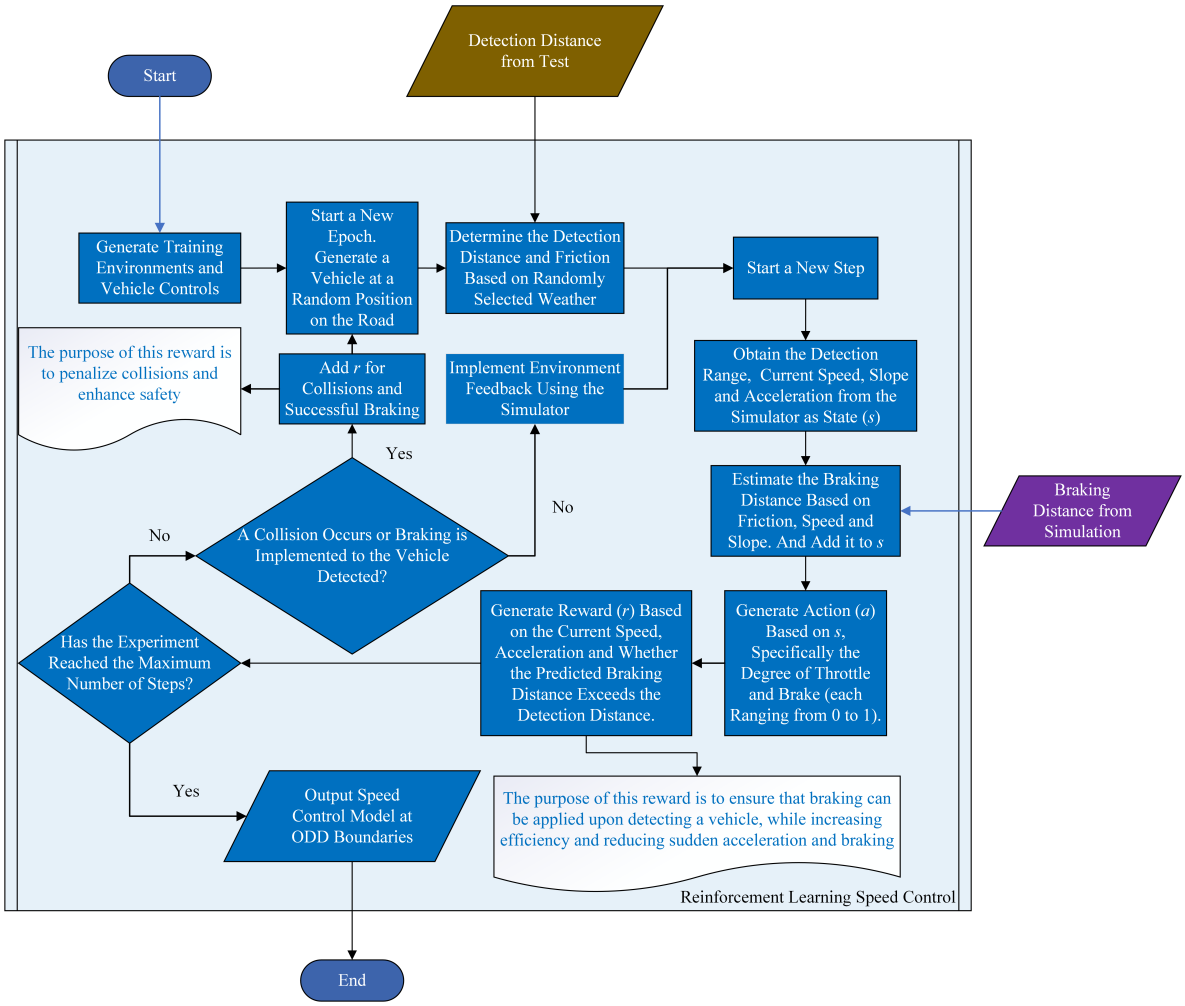

Figure 3.3: Flowchart of reinforcement learning

3.6. Conclusion

In summary, this chapter outlined the integrated methodology. First, extreme weather data is generated using CARLA and SUMO to create annotated datasets for detection testing. Next, the maximum detection distances from model testing are compared with braking distances simulated via PyChrono to assess potential risks. Finally, these distances are integrated into the RL reward function to guide adaptive speed control. Detailed implementations and experimental results will be presented in the next chapter.

4

Experiments

4.1. Introduction

Compared to the previous chapter on Methodology, this chapter focuses on the experimental details and results. It comprehensively describes the experiments conducted to evaluate the AV system under extreme weather conditions. The experiments include the generation of an extreme weather dataset using the CARLA simulator, the assessment of detection distances under various weather and lighting conditions, the simulation of braking distances across different speeds, slopes and road friction coefficients, and the development of an RL–based speed control strategy. The experimental results offer valuable insights into the impact of adverse weather on vehicle perception and dynamics, along with practical guidance for enhancing safety in challenging driving scenarios.

4.2. Extreme weather dataset generation

This section describes the process of generating a comprehensive dataset under extreme weather conditions. By leveraging CARLA's advanced weather simulation capabilities and integrating traffic scenarios from SUMO, diverse and realistic environments are created. This study first compares different simulators and justifies the selection of CARLA, then details the map settings, weather parameters and traffic flow configurations used to capture a wide range of conditions. Finally, an automated annotation process is described to explain how this research avoids human error.

4.2.1. Simulator comparison and selection

Researchers compared common AV simulators regarding different weather simulations [46], as shown in Table 4.1.

Table 4.1: Different weather conditions in various simulators [46]

Simulator	Night	Cloudy	Rainy	Foggy	Snowy
AirSim	-	-	-	-	-
SVL	✓	-	✓	✓	-
Vista	✓	-	✓	-	-
CARLA	✓	✓	✓	✓	-

Although simulating snowy scenes remains technically challenging in existing simulators, CARLA possesses the following advantages:

- Supports the simulation of various weather conditions (such as rain, fog and night) and the control of lighting conditions, including streetlights and vehicle headlights;
- Provides high-fidelity simulations of vehicle dynamics and sensor fields of view;

- Can be integrated with macroscopic traffic simulators (such as SUMO) to facilitate generating various traffic flows on specific maps.

4.2.2. Map and weather scenario settings

This study selected six maps from CARLA to comprehensively cover different road environments, ranging from Town 01 to Town 06, including urban streets, rural roads and highways. In terms of weather parameters, to simulate multiple intensities of clear, rainy, foggy and nighttime conditions, five indicators were randomly controlled: cloudiness, precipitation, precipitation deposits, fog density and the sun azimuth angle.

- **Parameter distribution**: Each parameter's value follows a uniform distribution in the $[0, 100]$ range, aiming to fully sample the entire range of weather intensities to avoid model bias due to insufficient data under specific weather conditions.
- **Day-night setting**: By randomly setting the solar altitude angle, scenes are set to be daytime or nighttime with a probability ratio of $3 : 1$, thereby obtaining data under different lighting conditions.
- **Traffic flow complexity**: On each map, between 25 to 100, vehicles of different types (such as sedans, motors, SUVs and trucks) and colors are randomly generated to simulate various traffic conditions from low to high density.

Dataset generation employs two methods: images and videos. In the image portion, CARLA's generation points randomly place stationary vehicles captured by RGB cameras positioned at car height. The camera parameters are shown in the Table 4.2. For each map scenario, $7,500$ images are generated, totaling $45,000$. The video dataset is obtained by co-simulation of CARLA and SUMO. The method for generating videos involves using SUMO to maintain traffic flow, randomly selecting five locations on each map, and placing RGB cameras at car height at these locations. Each location records a 2-minute video, resulting in 60 minutes of video data.

Table 4.2: Camera parameters

Parameter	**Width**	**Height**	**FOV**
Value	1920	1080	90

Regarding annotation, the bounding box tool provided by CARLA is used. Compared to manual annotation, bounding boxes are marked using the simulator's positional information, avoiding omissions and errors caused by repetitive manual work and significantly improving recognition accuracy under extreme weather conditions. Although the segment camera is also an automatic annotation method, it is over-detailed for vehicle recognition. When multiple vehicles are nearby, the segment camera can easily misclassify multiple cars as a single car. However, bounding box annotations may label obscured objects (vehicles behind buildings or signs) by directly reading distances, resulting in errors when the target is occluded. The experiment includes determining whether obstacles between the target vehicle and the camera are along a straight line while the obscured parts are still wholly labeled as long as a vehicle is more than half visible.

As shown in Algorithm 1, this study encapsulates the process above into an automated script. The script cameras are arranged and simulation conditions are generated by randomly selecting the map, weather parameters and traffic flow capacities. Traffic flow is first set in SUMO then the macroscopic trajectories are loaded into CARLA for rendering and recording. Upon completion, annotation and data storage are performed. Once the script has finished running, a comprehensive dataset containing multi-weather images and videos is obtained.

4.3. Detection distance testing

This section evaluates the maximum detection distance of vehicle sensors in simulated scenarios. By varying lighting, weather and map environments, the performance of different detection models under diverse conditions is assessed. These tests—using the Specialized Model and the Generalized

model—provide insights into model robustness and help determine whether vehicles can reliably detect obstacles, which is essential for defining the ODD.

4.3.1. Test environment and parameters

To better mimic real-world scenarios, the lighting condition is categorized into three types: Daytime, Nighttime and Cloudy, as shown in Table 4.3. Street lights and vehicle high beams are activated during night tests to simulate realistic lighting conditions. Under cloudy conditions, cloudiness is increased to reproduce low-light but not utterly dark weather.

Table 4.3: Cloudiness and sun altitude angle at different lighting conditions

Lighting	Cloudiness	Sun Altitude Angle
Cloud	✓	$45°$
Daytime	-	$45°$
Night	-	$-45°$

According to the adjustable weather parameters in CARLA, this study classifies the weather into three categories: Foggy, Rainy and Wet, as shown in Table 4.4. The parameters in the table represent those adjusted in the CARLA simulator, with annotations indicating their application in subsequent weather conditions and marked in parentheses. Rainy includes rainfall (precipitation) and road water (precipitation deposits and wetness); Wet no longer adds real-time rainfall but still retains road water; Foggy focuses on low and high variations in the fog concentration (fog density). For each weather type, the intensity, adjusted using CARLA's built-in parameter, is increased from 5 to 100 in 5 steps, simulating a wide range of possibilities from mild to extreme conditions.

Table 4.4: Parameters for different weather conditions

Weather	Precipitation	Precipitation Deposits	Wetness	Fog Density
Foggy	-	-	-	✓
Rainy	✓	✓	✓	-
Wet	-	✓	✓	-

To differentiate the detection capabilities of models in specialization and generalization environments, this study categorizes maps into two groups to simulate two AV strategies:

- **Fixed-city Maps**: Town 01 to Town 06, used in the data generation and model training processes described above. These maps simulate AVs operating within specialized cities, such as "Apollo Go", primarily within the region and relying on thorough learning and optimization of the local environment.
- **Inter-city Maps**: Town 07, Town 10 and Town 13, representing scenarios where the AV operates in generalized regions. These maps reflect cross-city or multi-region AV strategies like those employed by Tesla, where vehicles must adapt to new environments, relying on broader generalization capabilities.

On each map, two long straight roads are selected, and cameras are placed at one end of each road to ensure the target vehicle has a long and unobstructed line of sight in front of the camera. This setup facilitates the accurate quantification of the maximum detection distance.

As shown in Algorithm 2, each iteration, referring to the procedure conducted on each unique map, is conducted at a specified lighting and weather intensity, with a camera positioned at one end of the road. Subsequently, a background vehicle, specifically a red sedan, is generated sequentially at distances of 5 m, 10 m, 15 m, ... up to 120 m from the camera. The red sedan was chosen due to its higher contrast in natural scenes, as well as its association with critical indicators in traffic, such as red lights

and warnings. After taking a photo, the vehicle is destroyed to ensure that each shot contains only one vehicle at a specific distance. This process iterates through all weather intensity steps (5 to 100, increasing by 5 each time) before switching to the following weather or lighting scenario. Once all the lighting, weather and distance combinations are recorded, the iteration transitions to the following map, where the process repeats.

Each image obtained during this phase contains information at a unique distance and scene metadata (map, lighting, weather type and intensity). Subsequently, these images will be used to evaluate whether the detection models can successfully identify targets under corresponding conditions and determine the maximum feasible detection distance.

4.3.2. Testing result

This study compares the performance of two models: the pre-trained COCO Model, which is fully trained on the public COCO dataset and the Extreme Weather Model, based on CARLA extreme weather data. The Extreme Weather Model is tested on specific and general regions to simulate the AVs operating within a single city (named the Specialization Model) and across multiple cities (named the Generalization Model). Quantitative tests of vehicle detection distances are conducted at different lighting (cloud, daytime and night), weather (foggy, rain and wet) and varying intensities (adjustable intensity parameter in CARLA, from 5 to 100). Each model was compared under two confidence thresholds of 0.25 and 0.50, meaning that a warning is issued when the computer vision model has a 25% or 50% confidence that "another vehicle is present" in the tested image. The average detection distance and variance are shown in appendix Table C.1, and the false positive rate is shown in appendix Table C.2.

The detection distance comparison chart, as shown in Figure 4.1, illustrates the average detection distances of all models under different scenarios. The Specialization Model has the best detection distances, with an average of 65 m under the 0.25 threshold and 60 m under the 0.50 threshold, which is higher than the Generalization Model with 54 m and 51 m, respectively. The COCO Model performs poorly under extreme weather conditions, with maximum detection distances of only 42 m and 36 m. This indicates that computer vision models not explicitly trained for extreme weather are more adversely affected by weather factors. Additionally, the ratios of the 0.25 threshold to the 0.50 in the Specialization and Generalization Models are 1.08 and 1.05, lower than the COCO Model's 1.16. This suggests that AVs trained on extreme weather data have more stable performance when confidence thresholds change and can more confidently use the 0.50 threshold to reduce false alarms and interference with the perception.

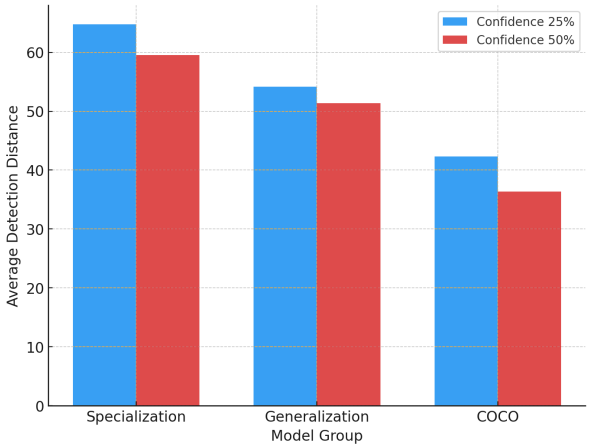

Figure 4.1: Average detection distance by model and confidence thresholds

The detection distance variance comparison chart, as shown in Figure 4.2, demonstrates that the variance of detection distances of the Generalization Model is significantly higher than that of the Specialization Model. The model in the source domain exhibits higher consistency under different weather conditions. In contrast, as a result of domain adaptation, the Generalization Model fluctuates wildly

across various scenarios, indicating that environmental changes still significantly impact AVs' generalization ability across regions. The variance at the 0.25 threshold is higher, which suggests that the model's detection distance fluctuates more at lower confidence thresholds. At the 0.50 threshold, the variance of all models decreases, but the variance of the Generalization Model remains relatively large, indicating insufficient consistency in cross-region operations.

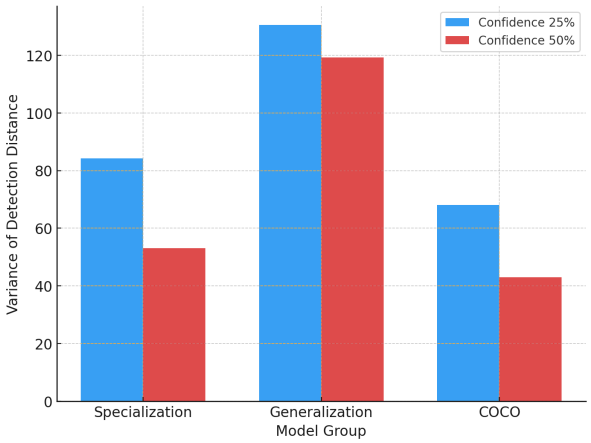

Figure 4.2: Variance of detection distance by model and confidence thresholds

From the false positive rate bar chart, as shown in Figure 4.3, it can be seen that the false positive rate in the Specification Model is significantly lower than that in the Generalization Model, indicating that AVs operating in specified regions perform more stably. Among them, the false positive rate is lower when the confidence threshold is 0.50, reflecting an advantage in reducing false alarms. The false positive rate in the Generalization Model is higher than that in the Specialization Model under both thresholds, especially at the lower confidence threshold (0.25), where the false alarm rate reaches 3.8%, further validating the challenge of model generalization in cross-city environments. The COCO Model has extremely low false positive rates under both threshold conditions, especially at the 0.50 threshold where it is 0. However, the model's overall detection distance performance under extreme weather conditions is inferior, possibly due to too much weather interference, which makes it unable to discern.

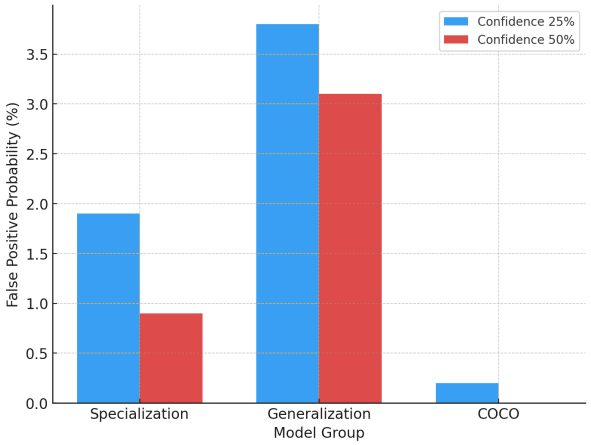

Figure 4.3: False positive rate by model and confidence threshold

The maximum detection distances under different times, weather, intensities and detection models are shown in Figure 4.4. The x-axis represents the intensity, the y-axis represents the detection distance and the different graphs illustrate various detection models with varying confidence thresholds.

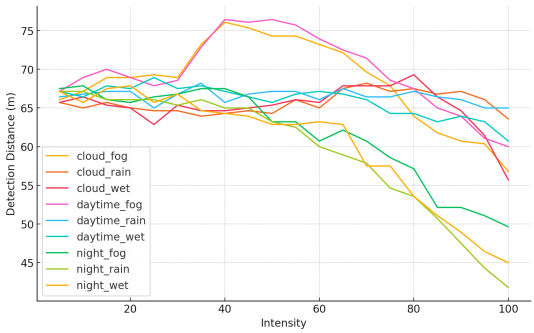

(a) Specialization Model detection distance at 0.25 confidence threshold

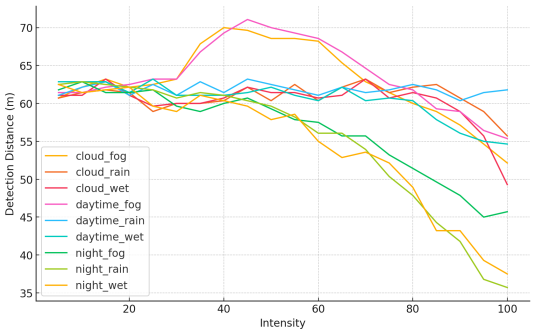

(b) Specialization Model detection distance at 0.50 confidence threshold

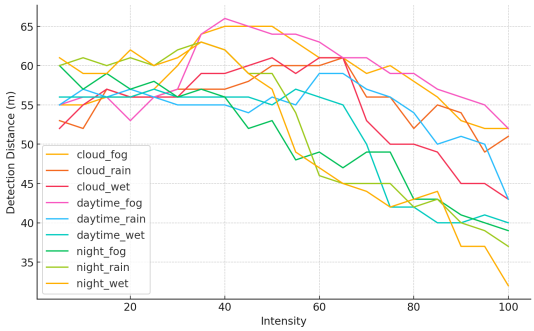

(c) Generalization Model detection distance at 0.25 confidence threshold

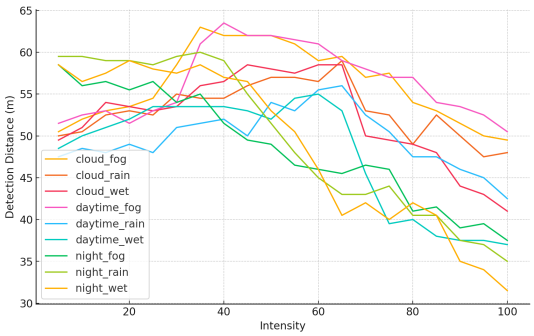

(d) Generalization Model detection distance at 0.50 confidence threshold

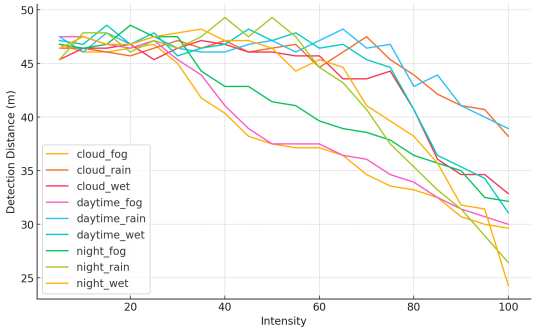

(e) COCO Model detection distance at 0.25 confidence threshold

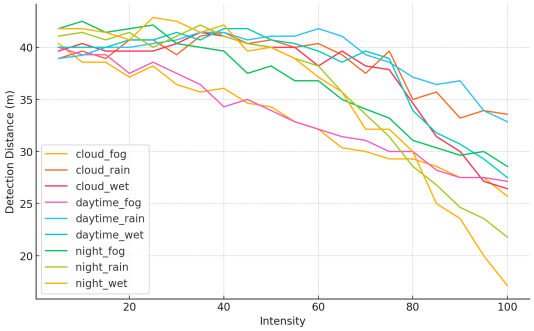

(f) COCO Model detection distance at 0.50 confidence threshold

Figure 4.4: Detection distance by weather, model and confidence

From the perspective of weather intensity, there is an overall trend of decreasing detection distance as intensity increases. This trend can be further divided into three intervals: low intensity (5-30), medium intensity (30-70) and high intensity (> 70). In the low-intensity range, overall performance remains relatively stable, with no significant differences in observing at nighttime and complex weather compared to the daytime. There may even be a slight improvement in some weather (such as foggy). As intensity increases to medium levels, detection performance gradually declines and the differences between weather conditions are widened. Foggy and daytime still perform relatively well, while performance degradation at night becomes more pronounced. Rainy days and daytime wet conditions also exhibit certain degrees of fluctuation within this interval. At high-intensity levels, detection performance significantly decreases across most weather conditions, with combinations of nighttime and complex weather, such as the wet night and the rainy night, performing particularly poorly. Detection distances in these conditions may fall below 20 m, reaching the lowest levels among all conditions.

Different models and confidence levels show significant differences in maximum detection distances, with lower confidence thresholds allowing longer detection distances. In the Specialization model, detection distances range from approximately 60 to 70 meters under low weather intensity, whereas in the Generalization Model, they decrease to from 45 to 60. Both distance and robustness under varying con-

ditions are lower in the Generalization Model than in the Specialization Model. In contrast, the COCO Model, which does not account for extreme weather conditions, only provides detection distances of 40 to 50 meters. Regarding the highest and lowest detection distance, the Specialization Model's foggy cloud and foggy daytime conditions show an increase in detection distance at medium intensity levels, significantly surpassing other weather and model conditions with distances exceeding 70 meters. These two weathers also show an increasing trend in the Generalization Model. However, their low-intensity performance is worse than that of other weather. Although the results are slightly better than others in the generalization model, the improvement is minimal, approximately 65 meters. In the COCO Model, the opposite result is observed: foggy in the COCO Model exhibits a clear negative impact on detection distance. Similarly, under medium intensity, foggy cloud and foggy daytime perform worse in the COCO Model compared to all other weather conditions, even worse than night, wet and rainy, which are regarded as unfavourable in other models. Regarding the lowest values, all models are from night_rainy or night_wet conditions; however, the numerical values still reflect the Specialization Model (≈ 40 m) $>$ the Generalization Model (≈ 35 m) $>$ the COCO Model(≈ 20-25 m).

From the perspective of weather types, foggy conditions perform the best. The performance is stable under low intensity (5-30) and can even show slight improvements. At high intensity (> 70), the performance degradation in foggy conditions is relatively slow. During training, all weather conditions are equally likely to appear. Therefore, rather than the dataset's bias, a more probable cause may be the "moderate enhancement effect": the scattering effect of low-intensity fog increases the contrast between the target and the background, thereby enhancing distance measurement performance. Rainy and wet conditions significantly decline performance at high intensity. The rainy and wet nights, affected by weather and lighting, perform the worst, especially at a high intensity (> 70). The distance measurement performance of wet night may drop to the lowest among all weathers. Daytime conditions generally perform better in distance measurement than nighttime conditions. Even within the intensity range of 20-50, distance measurement performance across various daytime weather conditions usually fluctuates minimally, demonstrating good intensity resilience. Complex weather has a more significant impact at night. Nighttime conditions show a noticeable acceleration in performance degradation when intensity exceeds 70; the wet night and the rainy night deteriorate the fastest when intensity exceeds 70. Rainy conditions remain relatively stable at medium intensity (40-60) regardless of the time and typically exhibit relatively stable performance or only slight fluctuations.

In terms of detection distance variance, as shown in Figure 4.5, differences in model, confidence, intensity and weather type are also reflected. Regarding weather intensity, most weather types are minimally affected by intensity, except the rainy and wet nights increase rapidly when intensity reaches around 60, similar to when detection distance decreases. Another condition with a changing trend, but not as pronounced as the first two, is wet cloud, which similarly affects detection distance. Road surface water often causes instability in detection distance, especially at night when street lights and car lights exacerbate this effect. However, this phenomenon may decrease at high weather intensity due to stabilization caused by reduced detection distance. Regarding model types, higher confidence provides more stable discrimination, reducing variance by approximately half. The COCO Model becomes the most stable model (with variance mostly below 100 under confidence 25 conditions), followed by the Specialization Model (≈ 100) and the Generalization Model (≈ 200). This may be because the COCO Model generally has poorer detection distance performance.

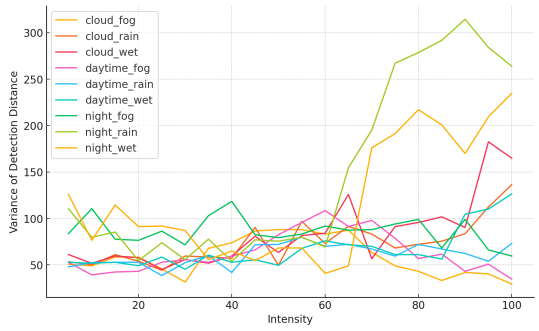

(a) Specialization Model variance at 0.25 confidence threshold

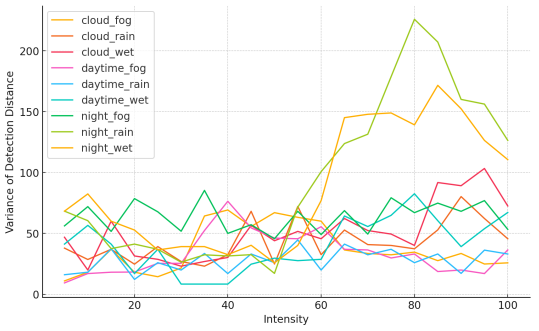

(b) Specialization Model variance at 0.50 confidence threshold

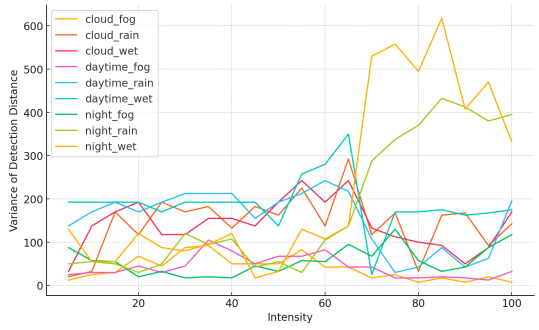

(c) Generalization Model variance at 0.25 confidence threshold

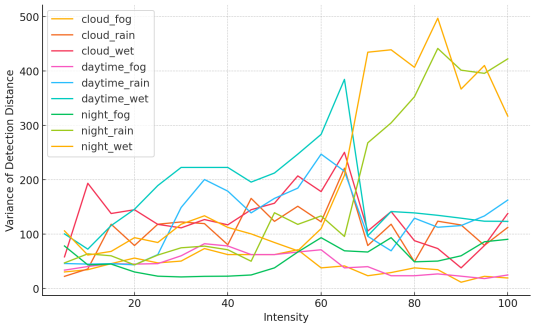

(d) Generalization Model variance at 0.50 confidence threshold

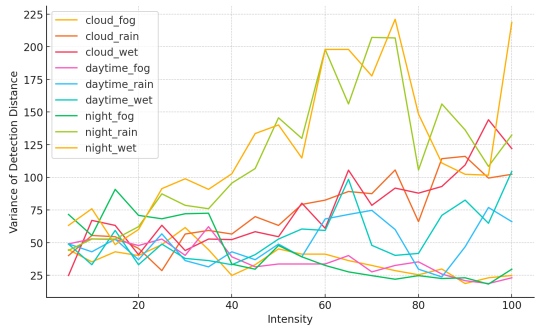

(e) COCO Model variance at 0.25 confidence threshold

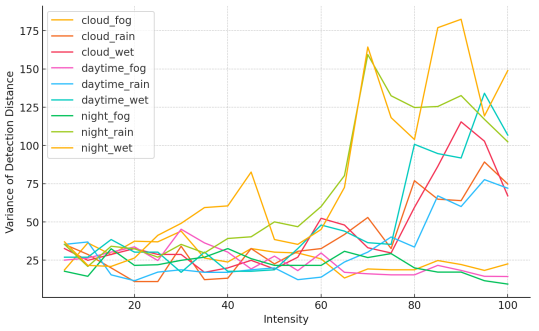

(f) COCO Model variance at 0.50 confidence threshold

Figure 4.5: Detection distance variance by weather, model and confidence

4.4. Braking distance simulation

This section utilizes the high-precision physics engine PyChrono to systematically simulate the braking distance of vehicles under different road conditions. By selecting representative road friction coefficients (dry, rainy, snowy, and icy surfaces), various slopes, and initial speeds, this study comprehensively evaluated the impact of these factors on braking performance. For each combination of parameters, experiments were repeated multiple times, ultimately constructing a three-dimensional braking distance data table, which provides a quantitative basis for subsequent comparative analyses with detection distances and the delineation of safe driving zones for AVs.

4.4.1. Simulation parameter design

Road surface friction coefficient μ is critical for simulating vehicle-road interactions. To quantify the effects of weather conditions, this study selects the following four representative friction coefficients, as shown in Table 4.5, to simulate various weather conditions, according to the literature [44].

Table 4.5: Friction coefficients for different surface conditions [44]

Coefficient of Friction	Surface Condition
0.60	Dry
0.40	Rainy
0.28	Snowy
0.18	Icy

The values chosen do not correspond precisely to all real roads but are sufficient to cover road conditions ranging from highly slippery to relatively dry. It is also important to note that in actual road environments, the friction coefficient may vary with temperature, dirt and other impurities. However, this approach intentionally prioritizes controlled comparisons over exhaustive environmental variability.

Slope also significantly affects the actual braking distance of a vehicle through gravitational effects:

- When going downhill, the gravitational component parallel to the road surface reinforces the vehicle's motion, thereby increasing braking distances;
- When going uphill, generate gravity-induced deceleration, effectively shortening required braking distances.

To systematically study this effect, this research varies the slope θ from -5° to $+5^\circ$ in increments of 0.5°. This range encompasses typical mild inclines and declines while covering specific, more extensive slopes.

As a critical determinant in braking systems, the initial velocity v is systematically simulated from $1km/h$ to $120km/h$ in increments of $1km/h$. Compared to testing only high-speed or low-speed scenarios, this discrete coverage approach captures the braking distance variation curve of the vehicle across a wide speed range.

This study selects sedans as the reference vehicle type in simulations. This model is relatively mainstream vehicle size, mass distribution and dynamic characteristics. Sedans are also highly prevalent on actual roads. Therefore, sedans can reasonably represent the braking performance of typical passenger vehicles.

Algorithm 4 outlines the process of braking distance testing. The main steps are as follows.

- Setting up the environment: Choose the road friction coefficient μ_i, the slope θ_j and then load the sedan model in PyChrono;
- Initialize speed: Accelerate the sedan to the desired initial speed v_k and keep this speed into the braking section at the beginning of the simulation;
- Apply full force braking: Apply maximum braking force to the vehicle and observe the vehicle position over time;
- End condition: The simulations stop when the vehicle speed drops below $0.5km/h$. Which is chosen to avoid infinite braking time caused by numerical jitter in the simulation;
- Record Braking Distance: Count the distance moved by the vehicle from the start of braking to the time when the speed is below the threshold;
- Repeat the test: For each (μ_i, θ_j, v_k) combination, simulation is repeated 5 times and averaged to reduce randomness or transient noise.

After completing the simulation, a three-dimensional table is obtained, representing the average braking distance under specific friction coefficients (representing different weather scenarios), slopes and initial speeds. This study processes and analyzes the results as follows.

4.4.2. Simulation result

The simulated braking distance data under different speeds, slopes and friction coefficients are shown in the Figure 4.6a. The friction coefficients used are 0.18 for icy, 0.28 for snowy, 0.4 for wet surfaces and 0.6 for dry surfaces, as referenced in the literature [44]. Because under low friction and high-speed conditions, the braking distance greatly exceeds the detection distance, making such scenarios overly dangerous and very rare, the figure only displays braking distances within 120 meters. From the figure, it can be seen that longer braking distances generally occur under high-speed and low-friction conditions. Additionally, all slopes exhibit long and short braking distances, indicating that slope also affects braking distance, though its impact is relatively minor compared to speed and friction.

The effects of speed, slope and friction on braking distance are illustrated in Figure 4.6. The statistical method selects the 25%, 50% and 75% values of each factor as representatives for low, medium and high categories respectively, as shown in Table 4.6. When investigating a particular factor, all its values were selected along the x-axis with three representative values of the other two factors, distinguished using different colors and markers to plot the braking distance as the y-axis.

Table 4.6: Representative values for friction, slope and speed at low, medium and high levels

Levels	Friction	Slope	Speed
Low	0.18	$-2.5°$	$30km/h$
Medium	0.40	$0°$	$60km/h$
High	0.60	$2.5°$	$90km/h$

From the figures, it can be observed that all three factors exhibit non-linear relationships. Specifically, speed demonstrates a clear quadratic relationship, as shown in Figure 4.6b, which aligns with most literature and empirical data. However, some studies present slope as having a linear relationship. This discrepancy may be because icy roads and high speeds are rarely tested in field experiments, causing the smoother portions of the quadratic function to be fitted and mistakenly interpreted as linear, as shown in Figure 4.6c. The impact of friction on braking distance, as shown in Figure 4.6d, illustrates characteristics similar to an inversely proportional function combined with different constants. Some research has simplified the relationship between friction and braking distance to a pure inverse proportional function, which can streamline calculations in scenarios with fixed friction. However, the numerical jumps between different friction levels may lead to inaccuracies in general scenarios, considering various weather conditions.

Additionally, the non-linear nature of all three factors and the wide range under different friction coefficients suggest that entirely fitting the data, rather than referencing discrete values from a table, could result in cumulative errors that affect accuracy.

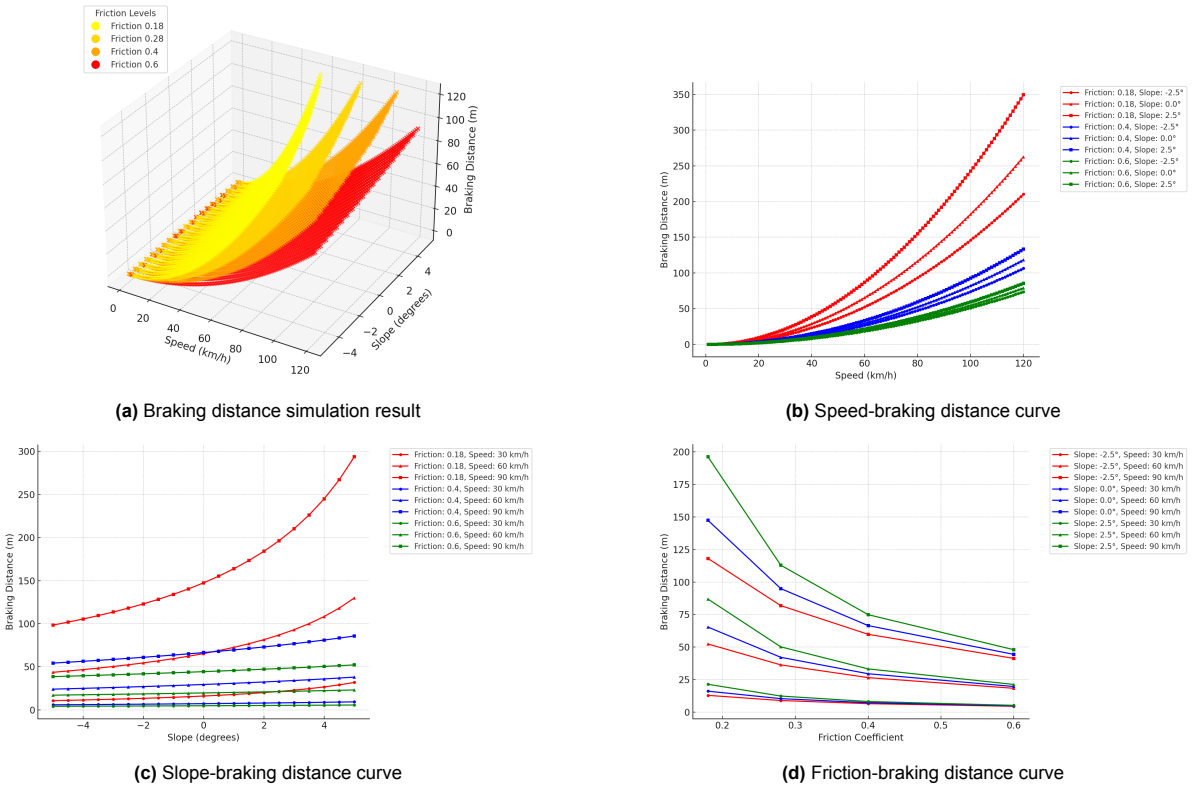

(a) Braking distance simulation result

(b) Speed-braking distance curve

(c) Slope-braking distance curve

(d) Friction-braking distance curve

Figure 4.6: Braking distance simulation results

4.4.3. Comparison of detection and braking distance

During the scenario simulation process, to investigate the highest theoretical speed at which braking can be achieved within the detection distance under different weather conditions, detection distances corresponding to low (25), medium (50) and high (85) weather intensities were selected for various friction coefficients. The theoretical maximum speed under the current friction, slope and detection distance was obtained by consulting a reference table. Since the CARLA simulator cannot provide experimental environments for snow and ice, their detection distances are based on those for rainy and wet conditions.

The foggy detection distance parameters are selected as:

- Low intensity: Specialization Model 69 m and Generalization Model 57 m;
- Medium intensity: Specialization Model 62 m and Generalization Model 49 m;
- High intensity: Specialization Model 54 m and Generalization Model 37 m.

The rainy and wet detection distance parameters are selected as:

- Low intensity: Specialization Model 65 m and Generalization Model 53 m;
- Medium intensity: Specialization Model 55 m and Generalization Model 46 m;
- High intensity: Specialization Model 45 m and Generalization Model 34 m.

To further study the theoretical maximum safe speed that AVs can achieve, according to the simulated braking distances and detection distance under the Specialization Model and the Generalization Model, this research compares the maximum speeds under various slopes and weather intensities, as shown in Figure 4.7 and Figure 4.8, respectively. All the figures use the same braking distance data and are classified by detection distance models. It was found that the Specialization Model generally allows for higher speeds than the Generalization Model by 5 – $15km/h$, especially in complex scenarios such as snowy and icy. At the same time, both perform well in dry environments. Regarding weather intensity, the theoretical speed decreases as intensity increases. Under high intensity, the Specialization Model

have a significant advantage, whereas the Generalization Model rapidly reduces to lower speeds. In contrast, the slope has a relatively consistent impact on both models, with slope changes affecting speeds by 20 – $25km/h$ across different models and weather conditions.

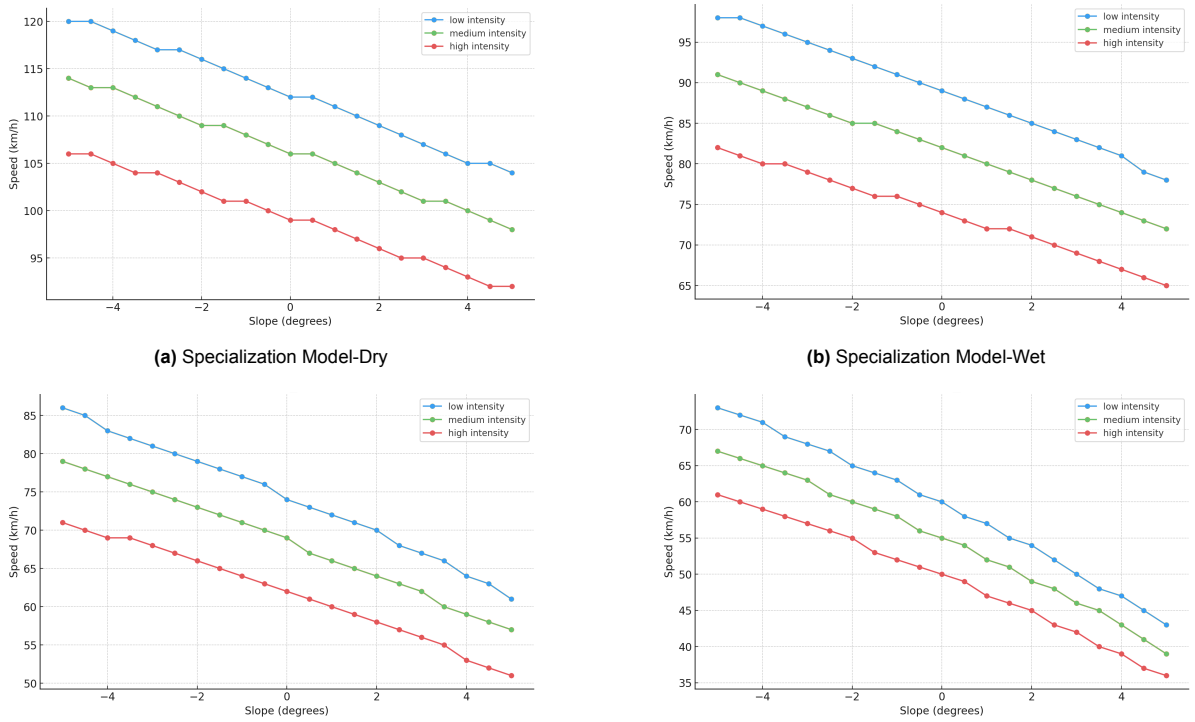

(a) Specialization Model-Dry

(b) Specialization Model-Wet

(c) Specialization Model-Snowy

(d) Specialization Model-Icy

Figure 4.7: Expected speed under different weather conditions with the Specialization Model

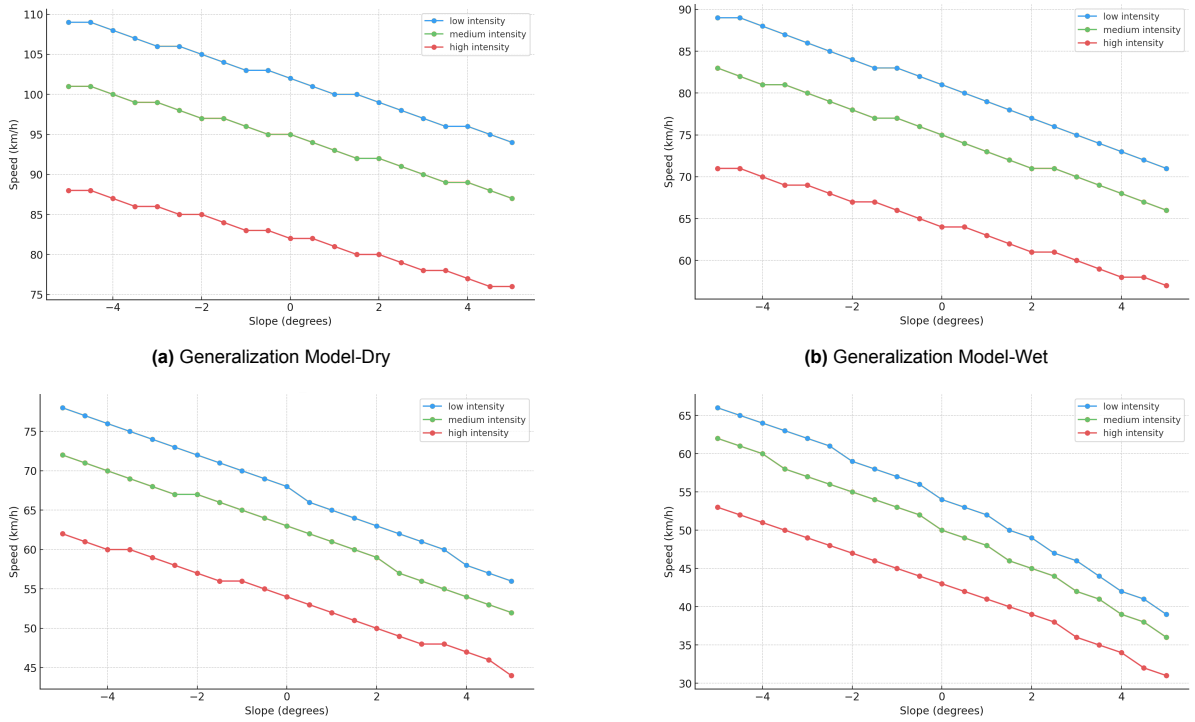

(a) Generalization Model-Dry

(b) Generalization Model-Wet

(c) Generalization Model-Snowy

(d) Generalization Model-Icy

Figure 4.8: Expected speed under different weather conditions with the Generalization Model

4.5. Reinforcement learning speed control

This section details the RL approach for adaptive vehicle speed control, which leverages real-time estimates of braking and detection distances. The RL agent learns to balance safety and efficiency under varying weather and road conditions by integrating key environmental factors such as road slope, friction and current speed into the state representation. Training in the CARLA simulation environment with the SAC algorithm enables the agent to optimize throttle and braking actions, ensuring that the vehicle maintains speeds that allow timely braking within the detectable range.

4.5.1. Training scenario and environment setup

This study selects Town 04 from CARLA, as shown in Figure 4.9, as the primary training environment for RL.

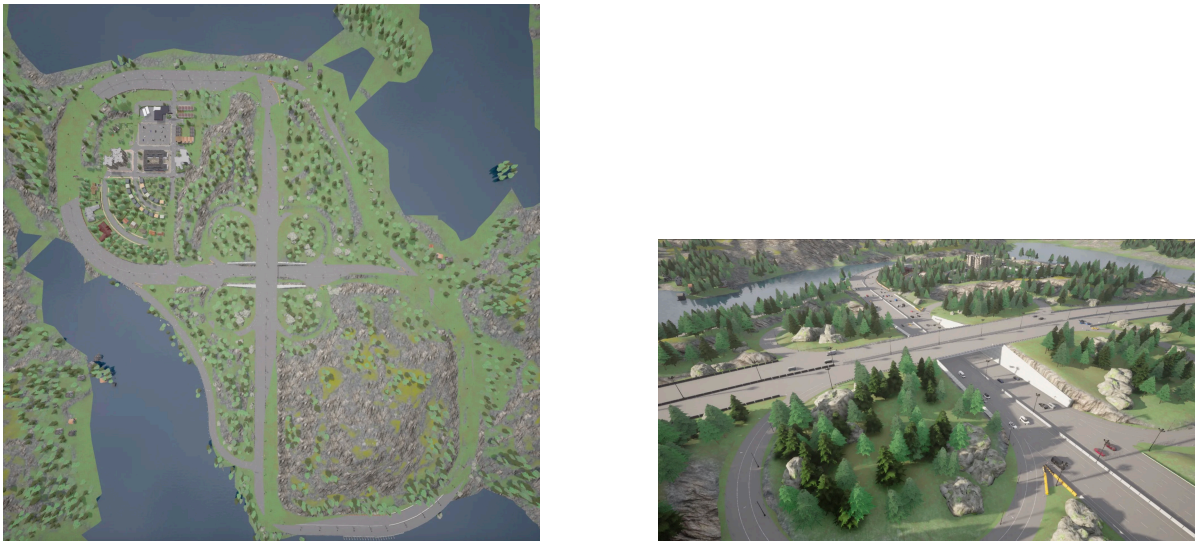

(a) Aerial of the town 04

(b) Overpass of the town 04

Figure 4.9: Aerial and overpass of the town 04

This map simulates a mountainous scenario with the following characteristics:

- Presence of a peaked-center bridge and flat roads, realistically reflecting the impact of slope on vehicle speed control;
- The bridge and roads have sufficient length to support the vehicle's acceleration and deceleration.

Such a map can cover slope variations within a single environment, providing the agent with relatively comprehensive training scenarios and ensuring the completion of the entire braking process under various slope and speed conditions.

Modeling the AV speed control problem as an RL task hinges on properly defining State, Action and Reward. This enables the agent to achieve adaptive speed control under complex and variable weather and road conditions. The following part details the RL system built within the CARLA environment, including its state, action and reward configurations.

At each simulation step, the agent receives the following information from the CARLA environment as the State:

- Current Speed v: The current speed of the ego vehicle, obtained through the simulator's speed sensor, measured in km/h.
- Slope θ: The current slope of the road, obtained through the simulator's vehicle attitude sensor, measured in $^\circ$.
- Road Friction μ: At the initialization of each episode, selected based on weather from the set $\{0.18, 0.28, 0.4, 0.6\}$.
- Braking Distance $d_{brake}(v, \theta, \mu)$: Retrieved from the lookup table based on vehicle speed, slope and friction. After fixing the friction, interpolation is performed based on speed and slope to obtain the braking distance.
- Detectable Distance d_{detect}: Obtained by referencing the lookup table based on the current weather and lighting.
- Front Vehicle Distance d_{front}: If the actual distance $d_{actual} \geq d_{detect}$, then d_{detect} is returned; otherwise, d_{actual} is returned.

Combined, the state vector is represented as:

$$s = \{v, \theta, \mu, d_{brake}, d_{detect}, d_{front}\}$$

The action output by the agent is the throttle/brake control, ranging from $[-1, +1]$:

- $a > 0$ indicates throttle, with larger values corresponding to greater acceleration.
- $a < 0$ indicates braking, with more negative values corresponding to stronger braking force.
- $a = 0$ indicates neither throttle nor additional braking, maintaining the current state.

The design of the reward function is crucial in RL. This study incorporates the alignment between detection and braking distance to encourage the agent to maintain a safe and controllable speed.

- Speed Objective: The desired vehicle speed $\hat{v}$ should remain within a reasonable range. If the vehicle speed is too low, traffic efficiency decreases; meanwhile, there are safety risks if it is too high. A negative penalty can be defined based on the deviation between the theoretical speed, calculated by braking distance and detection distance in section 4.4.3, and the actual speed:

$$r_v = -\alpha(v - \hat{v})^2$$

- Safety Constraint: If the current estimated braking distance $d_{brake} > d_{detect}$, indicating that the braking distance exceeds the detection distance, a significant negative reward is imposed:

$$r_{safe} = \begin{cases} 0 & \text{, if } d_{brake} \leq d_{detect} \\ -\beta & \text{, if } d_{brake} > d_{detect} \end{cases}$$

  where β is a large penalty coefficient.

- Collision Penalty: If the vehicle collides with the NPC vehicle, a large negative reward is given, and the episode is terminated.

$$r_{collision} = -\gamma_{collision}$$

- Smooth Driving: To encourage smooth operations, a minor penalty is imposed on the magnitude of action changes, preventing the agent from frequently switching between throttle and brake:

$$r_{soomth} = -\delta(a_t - a_{t-1})^2$$

The overall reward can be expressed as:

$$r = r_v + r_{safe} + r_{collision} + r_{smooth}$$

The coefficients for the terms can be determined through hyperparameter tuning.

4.5.2. Training process and implementation details

The training process and implementation details are structured to facilitate learning this continuous control policy using the SAC algorithm. At the beginning of each episode, the environment is reset: a weather type and intensity are randomly selected to determine the detection distance (using a Gaussian distribution for variability), the friction coefficient μ is specified based on the weather (reflecting conditions such as rainy, snowy or dry), and the ego vehicle is positioned at the start of a long slope in Town 04 with an initial speed of 40 km/h, while an NPC vehicle is placed randomly along the slope. The agent then constructs the initial state s_0 by reading the vehicle slope θ, friction coefficient μ, detection distance d_{detect} and front vehicle distance d_{front}, and by calculating d_{brake}.

The SAC algorithm is used during training to learn the continuous action policy. At each time step, the agent samples an action a_t from the current policy $\pi_\theta(a_t|s_t)$, which is the probability of selecting action a_t given state s_t, based on the observed state s_t, and then executes the corresponding throttle or brake control in CARLA. The simulation updates the environment over a short time step ($0.002s$), resulting in a new state that includes updated speed, slope and vehicle position. The reward for the action is calculated according to the reward function, and the experience tuple (s_t, a_t, r_t, s_{t+1})is stored in the replay buffer. Periodically, batches of experiences are sampled from the replay buffer to update the policy network using gradient descent—minimizing the error between the dual Q-networks and the target function, while also maximizing the expected return with a maintained entropy level. An episode

terminates either when a collision occurs or when a predefined time step limit is exceeded, after which the environment resets for the next episode.

After training for millions of steps, the SAC policy is expected to converge to an adaptive speed control strategy: that is, under different slopes, friction coefficients, and detection distances, it can make relatively safe speed decisions. The specific details are shown in Algorithm 5.

4.5.3. Speed control result

During the RL training process, higher penalty coefficients were set for collisions to ensure safety; as a result, no collisions occurred in any of the test results. However, this also led the system to adopt a more conservative speed control strategy. Additionally, the average speed for both acceleration and braking phases of low-speed driving was lower than the theoretical maximum speeds under different weather conditions obtained in the simulations above. Nevertheless, as shown in Figure 4.10, the RL strategy that provides current situation predictions of braking distance exhibited higher average speeds in all cases. The solid black line in the figure represents the median, and the dashed black line represents the mean.

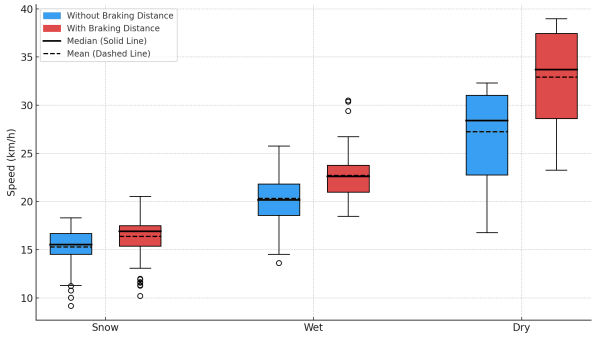

Figure 4.10: Average speed under different weather

Since weather conditions during training were randomly distributed, the test data combined all weather scenarios to simplify the comparative analysis. The impact of high-intensity weather is reflected in the outliers in the figure. Under ”ice” conditions, although the two strategies exhibit proportional differences, the overall values are relatively small, making the gap inconspicuous. Comparisons under the three weather conditions — ”snow”, ”wet” and ”dry” — show that the RL strategy providing the expected braking distance adopts higher average driving speeds in all cases, especially under ”dry” conditions. This result aligns with the braking distance simulations, where different friction coefficients have a nonlinear effect on braking distance. Models trained under low friction conditions cannot recognize the nonlinear increase in braking distance under high friction conditions, leading to a more conservative driving strategy during testing.

Additionally, the figure illustrates that as friction increases, the length of the box in the box plot (Interquartile Range) gradually increases while the number of outliers decreases. This indicates that speed control becomes more stable under high friction conditions. Under ”snow” and ”wet” conditions, the median of the speed control strategy that provides the expected braking distance is positioned higher within the box plot than the strategy that does not. In extreme weather conditions, the strategy providing the expected braking distance is more likely to select higher speeds, but insufficient detection distance still lowers the minimum speed control level.

Notably, for both strategies, the growth of the lower whisker is not significant as friction increases, indicating that insufficient detection distance imposes more significant constraints on the system’s minimum speed control strategy under extreme weather conditions. Under ”snow” and ”dry” conditions, the average speed control is lower than the median, further verifying this phenomenon. In contrast, under ”wet” conditions, the strategy providing the expected braking distance shows instances of selecting high speeds, resulting in the mean and median being close and the presence of high-value outliers.

In addition, a test comparing the maximum speed with the theoretical speed was conducted to demon-

strate that the results of the RL speed control are not simply achieved by reducing speed to avoid collisions. To avoid the impact of slopes on the maximum speed, the experiment was carried out on the long flat road of Town 04, and the detection condition was chosen as the mid-intensity Generalization Model. The experiment was repeated 10 times, and the average of the maximum speeds was taken. The theoretical speed was directly set to the speed at which the braking distance equals the detection distance, which can be the expected result of optimal control (MPC). However, it may also pose risks when the slope decreases. The results of the speed control, as shown in Figure 4.11, indicate that the RL control with simulated braking distance achieves higher speeds compared to the RL control using formula $d = \frac{v^2}{2\mu g}$ to calculate braking distance, especially performing better in dry conditions. This may be because the braking distance simulation better captures the characteristics of friction. As mentioned earlier, there exists a jump among different friction-braking distance relationships, and the collision penalty causes the RL control to be cautious about collisions caused by low friction; thus, when there is sufficient friction, it may not accurately increase the vehicle speed.

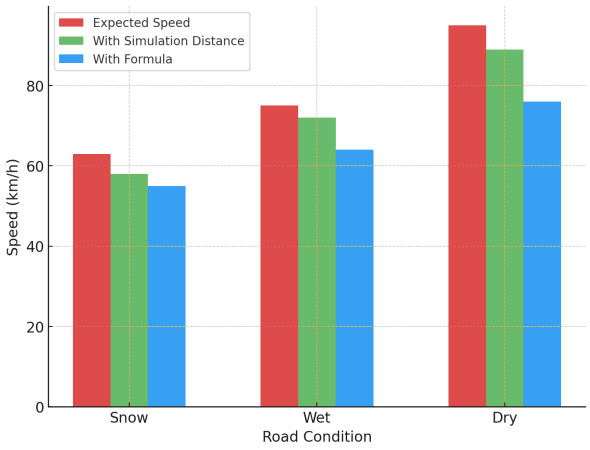

Figure 4.11: Max speed test under mid-intensity and flat road

4.6. Conclusion

This chapter provides a detailed account of the experimental process of testing AV under extreme weather conditions, including dataset generation, target detection distance testing, braking distance simulation and a speed control strategy based on RL. The experimental results reveal the impact of adverse weather on vehicle perception and dynamic performance, and offer theoretical and practical guidance for enhancing safety in complex driving scenarios.

5 Discussion

5.1. Introduction

This study conducts a comprehensive and quantitative experiment and analysis of AVs' visual perception and speed control under extreme weather conditions. Several representative conclusions and insights were obtained by comparing vehicle detection performance under different models (the Specialization Model, the Generalization Model and the COCO Model) and evaluating speed control performance when combined with braking distance constraints. This chapter will delve deeper into the following aspects: (1) the relationship between vehicle detection performance and weather intensity, as well as temporal factors; (2) the non-linear increases in braking distance arising from friction, slope and speed, and compound effects of detection distance and braking distance on speed control strategies; (3) comparisons and connections with existing research; and (4) limitations of the study.

5.2. Discussion of result

Based on the experimental results, the specialization model performs best under extreme weather conditions, significantly outperforming models generally pre-trained solely on the COCO dataset in average detection distance and variance stability. In contrast, the untrained regional model ranks intermediate but surpasses the COCO model. This conclusion underscores the importance of "training under extreme weather conditions specific to particular cities or environmental scenarios." Specifically, improvements in recognition accuracy and detection distance in local settings indicate that the model can better learn these localized features when the training data includes more samples—such as diverse target appearances, background scenes and lighting variations. However, when tested across different cities (the Generalization Model), the model cannot adapt to new environmental elements like city roads, architectural styles, and traffic signs, leading to reduced generalization. The disadvantage of the COCO model lies in its insufficient proportion of extreme weather samples. The general model does not address image quality issues caused by meteorological differences (raindrops, fog accumulation, and dim lighting), significantly reducing vehicle detection distance and accuracy. This phenomenon aligns with findings by researchers who observed performance improvements after locally retraining object detection models in extreme environments [85]. Additionally, it corroborates the widespread occurrence of performance collapse in universal datasets under extreme scenarios [61]. Moreover, based on previous conclusions, adapting a model trained on extreme weather conditions to clear weather is relatively easy, whereas adapting from clear weather to extreme conditions is much more difficult. Therefore, in future datasets, collecting data on clear weather may not be necessary and the focus should be on gathering data from extreme weather conditions. This approach aims to improve the model's adaptability and generalization in complex environments.

At low intensities (5 – 30), fog does not significantly reduce, and may even slightly enhance, detection performance. One possible explanation is the "moderate scattering enhancing contrast" effect [88]. However, this phenomenon still needs to be compared with other studies because it cannot be directly inferred from common sense, and insufficient research data supports it. Firstly, it might be due to the

simulator; this characteristic cannot be guaranteed in the real world. It is necessary to compare models trained exclusively on images generated from the real world with models trained on a combination of simulators and real-world datasets. At the same time, it could also be caused by unnoticed experimental errors. The combination of night and rain/wet conditions causes the most substantial interference to visual perception, significantly when the intensity exceeds 70, rapidly shortening the detection distance to approximately 20 – 30 meters. This indicates that multiple issues—such as raindrops forming noise on the lens, reflections from the ground and streetlights, and insufficient ambient light—compound together, making model recognition more challenging. Variance analysis shows that the trained region exhibits higher robustness to different weather conditions, while the untrained region experiences increased fluctuations under extreme weather. In some cases (e.g., night + heavy rain), the detection distance error fluctuations are pronounced, indicating that the model still requires more adaptation to new scene distributions.

Testing 25% and 50% confidence thresholds revealed that lower thresholds extend the theoretical detection range but also increase false positives and variability. The model trained with localized extreme weather maintains stable performance at high confidence levels, with a significantly reduced false positive rate. Although the COCO model has nearly zero false positives at the _50 threshold, the fundamental reason is that it fails to detect vehicles under extreme weather, resulting in ”empty detections.” However, from the value, the key factor affecting the detection range is the type of model rather than the confidence threshold. For vehicles with fixed-region designs, even when using a higher threshold, there is still sufficient braking distance, allowing them to consistently maintain a higher threshold to avoid deceleration caused by false alarms.

Simulation results indicate that speed, slope and friction are the key factors determining braking distance. As speed increases, braking distance grows quadratically; as friction decreases, braking distance significantly lengthens, with rapid escalation observed in scenarios such as ice and snow. The impact of the slope is relatively moderate but not negligible; in downhill scenarios under high speed or low friction conditions, braking distance can still increase substantially. This pattern aligns with the empirical formulas found in most traffic engineering literature and safe driving manuals. However, it should be noted that some literature considers the impact of slope to be a linear function, likely because they did not account for the quadratic behavior in low friction and high-speed situations, so the data resides in the flatter region of the quadratic curve. Additionally, the effect of different friction coefficients involves constant jumps. If a purely linear relationship is fitted, it is prone to errors under high-intensity weather or low friction conditions [60, 38, 15].

Both detection distance and braking distance impose constraints on vehicle speed. Under combinations of low friction and extreme weather, scenarios where ”safe braking distance > detection distance” frequently occur, forcing vehicles to limit their speed to ensure safety. The derived ”maximum safe speed” can typically be increased by 5–$15km/$h with the trained model; however, due to insufficient detection range, the untrained model must reduce speed further. In conditions such as night or heavy rain/fog, detection distance is significantly compressed, making it easy for vehicles to be unable to brake in time if they maintain high speeds. This thoroughly verifies the coupling relationship between perception performance (detection distance) and vehicle dynamics (braking capability): high perception ability ensures higher speeds. In contrast, low perception ability leads to conservative driving, sacrificing efficiency to guarantee safety.

The study employed RL for speed control to address extreme scenarios and incorporated ”estimated braking distance” information. The results show that when the agent knows the braking distance under current weather, slope, and road conditions, it can accelerate more boldly while ensuring zero collisions. Compared to strategies not providing braking distance information, the information-provided group achieved higher average speeds and maintained sufficient safety margins even in rain, wetland, and snow environments. In highly harsh conditions like ice, speeds were generally lower. Although there were still differences between strategies, they did not widen significantly—because, in these scenarios, the collision penalty coefficient is high, and the system as a whole tends to be conservative. This conclusion is consistent with RL studies focused on AVs on highways: the more comprehensive the perception dimensions of RL (including both road traffic conditions and the vehicle’s braking performance), the better the learned strategies can balance safety and efficiency [23, 82, 7].

This study addresses the shortcomings of traditional geofenced ODDs by proposing a technical frame-

work oriented towards dynamic ODDs. The aim is to enable AVs to autonomously adjust their speed and assess risks based on real-time environmental factors such as weather, slope, and road surface friction. To tackle the two major issues in current ODD research—lack of quantified boundaries and separate consideration of elements and the absence of comprehensive speed control—this study employs the calculation of detection distance and braking distance, supplemented by RL algorithms, to achieve adaptive speed regulation of vehicles in complex scenarios. The following summarizes the research from two aspects: the innovation/significance of the study and the significance/impact of the research findings.

The core focus of this study is to move away from the traditional approach of ”predefined geofencing” and adopt a dynamic ODD model that ”monitors the environment in real-time and adjusts vehicle behavior accordingly.” By quantitatively presenting environmental factors and integrating RL for adaptive speed control, vehicles can more flexibly respond to unexpected situations, reducing reliance on human takeover or emergency braking. This lays the technical foundation for the widespread application of future advanced AVs.

Shifting from ”linguistic descriptions” to ”quantitative metrics” for ODD boundaries, this study systematically generates scenario data under various weather, terrain, and traffic conditions using multi-platform collaborative simulations (CARLA + SUMO). It quantifies sensor detection capabilities and vehicle braking distances to establish more objective and measurable ODD boundaries. This approach fills the gap in previous academic and industrial ODD research, which relied heavily on experience without sufficient quantitative basis.

Another significant feature of this study is the cross-platform, multi-factor integrated system approach. The study deeply couples sensor performance with braking characteristics by utilizing CARLA and SUMO to generate highly diverse virtual traffic scenarios and employing PyChrono for detailed vehicle dynamics simulation. This forms an overall ”detection—braking—speed control solution.” This multi-factor, multi-platform integrated system offers a more systematic and cutting-edge methodological approach than traditional research focusing on a single module (such as only perception or control).

This study expands dynamic ODDs by incorporating the quantified ”detection distance” and ”braking distance” into RL (especially SAC) training. This enables vehicles to perform real-time speed adjustments under varying road conditions, slopes, and weather conditions, achieving a better balance between safety and efficiency. This fully demonstrates dynamic ODD expansion’s feasibility and practical value in high-level automation (L4/L5) applications.

This study offers a clear technical path for dynamic ODD by distinctly identifying scenarios where the ”detection distance is less than the braking distance.” It integrates actual safety constraints into vehicle speed decision-making, enhancing control over ODD boundaries in complex environments. Unlike traditional geofenced restrictions, vehicles can maintain automation across a broader area, reducing the need for human intervention and improving travel efficiency.

The research findings indicate that when vehicles can dynamically compare detection distance with braking distance and adjust their speed accordingly, they can effectively reduce collision risks even under adverse weather conditions or on complex slopes. Additionally, vehicles can autonomously increase their speed when environmental conditions permit to maintain traffic efficiency. This speed control model, which balances safety and efficiency, is expected to boost public trust in AV significantly.

This study combines sensor detection performance with vehicle braking characteristics and employs RL to optimize speed strategies, thereby verifying the mutual reinforcement between perception and control processes. Compared to merely enhancing perception accuracy or upgrading vehicle hardware, this research approach better adapts to the ever-changing real-world environments. It also lays a solid foundation for subsequent in-depth studies on multi-sensor fusion, multi-vehicle adaptation, and V2X communication technologies.

Regulatory bodies and the industry urgently need quantifiable and empirically-based safety assessment methods with the increasing demand for automation across various regions and weather conditions. The ”detection distance–braking distance–real-time control” process proposed in this study can directly inform the development of industry standards and the execution of real-world road tests and guide corporate research and development. This accelerates the refinement of automation regulations and

technical specifications, providing a practical and feasible technical pathway for deploying advanced AVs in more diverse environments.

5.3. Discussion of methodology

5.3.1. Discussion of extreme weather dataset generation

A uniform distribution was used to generate weather parameters, ensuring that conditions (sunny, night, cloudy, rainy and foggy) are approximately equally represented in the dataset. This approach ensures that the model has sufficient training samples under extreme conditions, allowing the early research phase to examine the model's generalization capability and robustness across diverse scenarios without being limited by the high or low frequency of specific weather conditions. Although weather patterns in the real world are not uniformly distributed-with most regions experiencing far more sunny days than extreme weather events-detection models trained on extreme weather data still maintain strong detection performance during sunny conditions, assuming that low-intensity conditions approximate sunny. In this study, the dataset is generated from simulators, but real-world data will be needed for training in the future. However, obtaining sufficient weather data in the real world is challenging, making it necessary to integrate both real-world and simulator data for training.

Various weather and lighting conditions were systematically designed in the detection distance tests, and the model's generalization capability was validated through multi-map experiments. However, several limitations remain that require further exploration. First, the experimental environment primarily focused on long straight roads, lacking dynamic traffic scenarios such as intersections, ramps, and complex curves. Obstructions, irregular road surfaces, and dynamic traffic participants (such as pedestrians and bicycles) in real driving environments can significantly impact detection distances, and the current testing methods do not fully cover these complex situations. Moreover, the test targets were mainly static vehicles, containing only one target in each experiment. While this facilitates quantifying the maximum detection distance, it differs from the complex scenarios of multi-target dynamic interactions in actual driving. The model's ability to handle multiple and long-distance dynamic targets has not been comprehensively evaluated.

5.3.2. Discussion of model performance test

This experiment focuses on quantifying the model's performance on different datasets rather than directly comparing the test results. So this study conducts tests on the source dataset Town 01 - 06, where the training data is consistent, and on adaptation datasets such as Town 07, Town 10, and Town 13. This is intended to quantify the model's performance fluctuations in familiar versus unknown environments and assess its domain adaptation capabilities. However, inherent differences among the datasets in scene layout, lighting conditions, target density and background complexity may introduce additional errors, which limits the direct comparison of test results. Therefore, while paying attention to changes in quantitative metrics, the potential biases arising from the differences in dataset characteristics must be considered to understand the model's actual performance better.

From the perspectives of analytical and research methods, the methodological choice of this study involved controlling the environment and weather intensity in the CARLA simulator, arranging vehicles at intervals ranging from 5 meters to 100 meters, and conducting a series of image captures and model detections. This experimental design ensures a quantitative analysis of weather variations and distance changes, making the results highly comparable. Additionally, by testing different confidence thresholds, the research findings provide a basis for parameter tuning: when higher detection distances are required (such as overtaking scenarios on highways), the threshold can be appropriately lowered to increase recall rates; when higher reliability is needed (such as in complex urban environments), the threshold can be raised to reduce false positives and improve detection stability.

Regarding target diversity, this study primarily used background vehicles for testing without considering different sizes and types of vehicles (such as trucks, motorcycles or pedestrians). Detection models may exhibit higher miss rates when facing smaller or uniquely shaped targets, especially under long-distance or low-light conditions, where such differences can be further amplified. Additionally, since all detection results were manually verified, false positives do not directly affect the maximum detection distance. However, in practical applications, even a small probability of false positives can cause

system decision confusion and reduce user trust. This indicates that despite setting different confidence thresholds, the model still struggles to avoid misclassifying background objects (such as traffic signs or barriers) as vehicles altogether.

Another significant limitation is that the experiments did not cover dynamic lighting changes and sudden weather conditions. For example, rapid lighting transitions at tunnel entrances or sudden heavy rain can significantly interfere with detection models. However, the current experimental scenarios mainly involve fixed time and weather settings, lacking simulations of dynamic lighting and meteorological condition changes. Furthermore, although CARLA and SUMO can provide high-fidelity simulation environments, the simulators still differ from real environments in extreme weather conditions such as fog and rain reflections, which may lead to discrepancies in experimental results when applied in real-world scenarios.

To enhance the comprehensiveness and adaptability of the experiments, it is recommended to introduce more complex dynamic scenario tests in future work, including intersections, multi-target scenarios, and complex road environments with ramps and sharp curves. Additionally, incorporating different sizes and types of vehicles into the tests can provide a comprehensive assessment of the model's detection capabilities across various traffic participants. Simulating dynamic lighting and sudden weather changes is also a key area for improvement. More realistic extreme driving conditions can be simulated by gradually adjusting weather parameters or introducing lighting transition modules. Moreover, considering multi-sensor fusion (such as combining LiDAR and millimeter-wave radar) to complement the limitations of a single RGB camera will help enhance the model's detection stability in low-light or complex environments.

To further reduce the impact of false positives, a time series filtering mechanism can be introduced into the detection results, using continuous detection or semantic segmentation-assisted classification methods to lower the false detection rate. Additionally, comparing and analyzing simulated data with real driving datasets and adapting and calibrating for simulation biases will help improve the model's robustness and generalization ability in real driving environments. Through these improvements, the detection distance testing method will become more comprehensive, providing more reliable and diverse experimental evidence for the performance evaluation of automation perception systems in complex environments.

5.3.3. Discussion of braking distance simulation

High-precision simulations of vehicle braking distances were conducted using PyChrono, covering various slopes, friction coefficients, and speed conditions. However, this method still has limitations in certain aspects that require further investigation and improvement.

Firstly, the setting of road surface friction coefficients is idealized. The study selected fixed values (0.18, 0.28, 0.4 and 0.6) from relevant literature to represent different weather conditions, enabling the simulation of vehicle braking performance under various environments. However, the friction coefficient changes dynamically in actual driving conditions, influenced by temperature, snow depth, and mud and sand factors. Especially under extreme weather conditions, this simplified setting may either underestimate or overestimate the actual braking distance of vehicles, failing to adequately reflect the interaction characteristics between the vehicle and the road surface in complex road conditions. Additionally, the dynamic characteristics of tires were not fully considered. In real-world driving, tire wear, insufficient pressure, or aging significantly affect friction and braking performance. This study assumed the tires were in good condition, which might lead to overly optimistic simulation results and thereby underestimate the potential safety risks caused by tire aging or poor condition.

Regarding slope settings, although the study covered a slope range from -5° to $+5^\circ$, slopes in real driving environments typically have dynamic characteristics. For example, the hill may continuously fluctuate during mountain or curve driving. However, this study used fixed slopes for simulations, which may not comprehensively reflect the braking performance of vehicles on complex slopes. Moreover, the simulation model did not incorporate air resistance and vehicle load. Air resistance significantly impacts vehicle deceleration at high speeds, especially on long slopes or during high-speed driving conditions, where aerodynamic factors can notably affect braking distances. Similarly, changes in vehicle load (such as the number of passengers or the weight of cargo) are directly related to vehicle inertia and

influence braking effectiveness. However, this study used a fixed vehicle mass for simulations and did not consider braking differences under varying load conditions, which may limit the generalizability of the results.

It is noteworthy that the simulation assumes a braking method of ”applying maximum braking force immediately” without considering the response delay of the braking system. In actual driving, braking systems have hydraulic or electronic control delays, which may cause the simulation results to deviate from real-world conditions, leading to an underestimation of braking distances in real driving environments. Additionally, this study only selected a standard passenger car (Sedan) as the reference vehicle. While this can represent the performance of most vehicles under ordinary road conditions, trucks, SUVs, and electric vehicles differ in mass, ground clearance, and braking systems, which can significantly impact braking distances. Therefore, testing a single vehicle type cannot comprehensively cover the braking performance of various vehicle types under different environments, limiting the broad applicability of the simulation results.

A dynamic friction model should be introduced in future work to enhance the simulation method’s accuracy and applicability. This model should consider real-time adjustments of the friction coefficient under varying temperatures, humidity, and tire conditions to more realistically reflect braking performance under complex weather conditions. Additionally, incorporating tire wear and pressure modeling modules into the simulation can quantify the impact of tire conditions on braking distances by setting different levels of tire wear. Regarding slope simulation, it is advisable to implement a dynamic slope variation model that simulates continuously ascending or descending scenarios on actual roads, thereby providing a more realistic validation of vehicle braking performance in dynamic slope environments. Furthermore, adding factors such as air resistance and load changes to the simulation—especially in high-speed scenarios—will ensure that the influence of air resistance on the braking process is dynamically calculated, making the simulation results more aligned with actual driving conditions.

5.3.4. Discussion of reinforcement learning speed control

This study effectively integrated detection and braking distance through RL methods in AV speed control, achieving an adaptive speed control strategy in dynamic environments. However, the model’s generalization capability has certain limitations. The training in this study was primarily based on a single map (Town 04) in CARLA. Although this map encompasses diverse scenarios, such as slopes and flat roads, the model’s robustness and adaptability may be insufficient in other untrained environments, such as complex urban intersections or mountain roads.

The inadequacy of handling complex traffic environments is also a significant limitation. The study focused on controlling the following distance for single-lane traffic, lacking strategies to address multi-lane dynamic traffic flows. Vehicles frequently need to change lanes, avoid obstacles, and interact with multiple targets in real driving scenarios. However, the existing model only performs speed control for following a single vehicle in simple scenarios, making it difficult to handle complex urban traffic conditions comprehensively. Additionally, the simulation environment did not include dynamic targets such as pedestrians, cyclists, and non-motorized vehicles, reducing the model’s applicability and safety under actual road conditions.

Furthermore, RL models’ training costs and exploration efficiency are limiting factors. High-fidelity simulation environments require substantial computational resources and time for training, especially when dealing with combinations of various weather conditions, slopes, and friction coefficients. The exploration process is time-consuming, and the model may become overfitted to specific training environments, resulting in unstable performance in unseen environments.

6

Conclusion

6.1. Introduction

This chapter synthesizes the contributions of this study in advancing ODD definitions for AV through quantitative analysis of sensor-brake system relationships under extreme weather and slope variations. Extreme weather data was collected via joint simulation for training an object detection model. The detection ranges of different models were quantified, and braking distances under various conditions were simulated. Finally, the detection and braking distances were combined to train an RL-based speed control system. The work establishes an adaptive framework to expand AV safety boundaries beyond static geofencing. The conclusions validate the methodology through simulations, addressing how perception limitations, braking dynamics and slope effects inform AV safety. Subsequently, future directions are outlined to enhance dynamic ODD adaptability across perception modeling, hierarchical control, simulation-real-world validation and regulatory alignment. Together, these insights bridge theoretical models with practical strategies, providing foundational steps toward scalable deployment of AV in complex and variable environments.

6.2. Conclusion

This study focuses on AVs' detection and braking distance under extreme weather conditions and varying slopes. It proposes a dynamic speed control strategy to define and expand the ODD for AV. The following conclusions, based on experimental results, address and summarize the research questions—with the first question primarily resolved through a literature review, while the focus was placed on the second and third questions.

The second research question — "How can these factors be quantitatively analyzed and considered to be applied in defining the ODD boundaries?" — this study quantifies the matching relationship between vehicle perception and braking capabilities by simulating various weather intensities in CARLA and testing different combinations of slopes, friction coefficients and speeds in PyChrono.

Regarding the third research question — "How can dynamic speed control strategies be designed so vehicles achieve safe and efficient driving through reasonable deceleration when facing environmental conditions beyond the defined ODD?" — the experimental results indicate that when the RL model incorporates real-time assessments of detection distance and braking distance into the decision-making process, the vehicle can flexibly adjust its speed according to conditions such as severe adverse weather, steep slopes or low-friction road surfaces. Compared to the theoretical speed (i.e., setting the vehicle's speed such that the current braking distance equals the detection distance—a speed that can be considered the expected outcome of optimal control methods like Model Predictive Control), the RL control reduces the maximum speed. This reduction helps mitigate collision risks caused by unpredictable changes in braking distance due to variations in downhill slope conditions. Additionally, compared to directly using parameters such as friction coefficient, slope and speed for control, the RL approach—utilizing simulated braking distances—can achieve higher driving speeds under high friction conditions. This suggests that the method effectively reduces the impact of the nonlinear relationship

between braking distance and other factors, which causes difficulties when using interpolation or calculation errors due to constants. Overall, from a conceptual standpoint, this adaptive control framework provides a practical approach for realizing truly ”environmentally adaptive” advanced AVs in the future.

In summary, this study establishes a quantitative relationship between sensor detection and braking systems under various intensities of extreme weather, slopes, and road friction conditions. It provides a practical and efficient solution for dynamic speed regulation by incorporating RL strategies. By thoroughly addressing the three aforementioned research questions, this paper not only lays a technical foundation for the systematic study of an integrated ”perception–braking–decision” framework but also holds positive implications for the large-scale deployment of AVs and the expansion of their ODDs in the future.

6.3. Future work

As ODD evolves from a static geofencing ODD to a dynamic ODD, future work must be continuously advanced on multiple levels to address the complexity and variability of real-world driving environments. The following outlines several directions worthy of in-depth research and practice, including perception modeling, speed control, simulation verification, regulatory integration, and system collaboration.

Firstly, in multi-source perception and environment modeling, further strengthening the comprehensive identification and quantification of road features, weather conditions, traffic flow, and the vehicle's health status is needed. Current geofencing ODDs typically operate only on fixed roads or under expected weather conditions, making adapting to frequent and uncontrollable external changes difficult. As the scope of AV applications expands, constructing a dynamic ODD boundary identification mechanism would allow the system to immediately adjust driving modes or downgrade operations upon sensing risk signals such as snow accumulation, heavy rain, or sudden accidents, thereby significantly reducing the risk of traffic accidents. Probability graph models or deep learning techniques can be combined to input environmental data, sensor performance, and vehicle dynamics into an online risk assessment module. Risk scoring allows The system to enable or restrict AV functions.

Secondly, regarding speed control strategies, it is essential to continue improving the hierarchical decision-making framework to enhance the adaptive capability of speed control in various complex scenarios. The high-level strategy can provide safety speed limits or acceleration restrictions based on the dynamic ODD's risk assessment results and trigger disengagement mechanisms in extreme cases (e.g., severe perception degradation and brake system malfunctions). The mid-level strategy should interactively assess the vehicle's surrounding traffic participants, especially in multi-lane, congested, or mixed traffic flow environments, by calculating optimal following distances and lane-changing speeds in real time. The low-level strategy implements acceleration and deceleration as well as steering execution. It can incorporate advanced vehicle dynamics models to estimate and compensate for tire wear, pressure changes, air resistance, and load in real time, thereby more accurately calculating braking distances and safe speeds.

Thirdly, expanding the existing simulation platforms' testing scenarios and functionalities is recommended in simulation and real-world data validation. On the one hand, more diverse virtual environments should be constructed on platforms like CARLA, SUMO, and PyChrono, including urban interchanges, mountainous bends, narrow rural roads, and tunnels, to evaluate the dynamic ODD applicability of AVs under more complex road conditions. On the other hand, continuous comparative analysis with accurate vehicle test data should be conducted through ”simulation-real vehicle” bidirectional calibration to correct simulation errors and improve the ability to simulate adverse weather, lighting changes, and extreme traffic events. This combination can cover high-risk or rare scenarios during the simulation phase, saving testing costs. At the same time, actual vehicle experiments provide genuine feedback, offering credible iterative bases for speed control strategies.

Finally, at the regulatory and industry standards level, it is necessary to closely collaborate with relevant departments and standardization organizations (such as SAE, ISO, etc.) to promote consensus on the definition, classification, and safety assessment of dynamic ODDs. Currently, most regulations only impose restrictions on geofencing or lower levels of automation, making it difficult to accommodate the evolving needs of dynamic ODDs. In the future, regulations should specify how vehicles should safely disengage automation modes when systems detect conditions beyond their capabilities (e.g.,

weather deterioration rendering radar ineffective, excessive gradients, or overloaded traffic). Additionally, quantitative metrics for multi-source sensor redundancy, cybersecurity protections, and vehicle-to-everything (V2X) collaboration can be explored to help automation companies better meet compliance requirements in product design.

Constructing and refining a dynamic ODD requires systematic upgrades and collaborations across perception layers, control layers, simulation verification, and regulatory standards. Through richer environmental perception and online risk assessment, AVs can flexibly adjust driving speeds and decision-making strategies in different scenarios. Integrating high-fidelity simulations with accurate vehicle test data for interactive calibration makes it possible to ensure safety while significantly reducing development costs and timelines. As multi-source perception, cloud platforms, and industry standards gradually mature and achieve compatibility, AVs can operate continuously, efficiently, and safely in broader and more complex environments. Conducting in-depth research and practice around these future work areas will provide the necessary technological accumulation and application support for developing dynamic ODD, ultimately driving the realization of AV's transition from geofencing to fully open-road scenarios.

References

[1] Angelos Amditis, Panagiotis Lytrivis, and Stamatis Manganiaris. “Infrastructure Supported Operational Design Domain: ISAD closing ODD gaps”. In: *Virtual ITS European congress*. 2020.

[2] Adina Aniculaesei et al. “A Method for ODD Specification and Verification with Application for Industrial Automated Driving Systems”. In: *2023 International Conference on Computational Science and Computational Intelligence (CSCI)*. IEEE. 2023, pp. 1519–1526.

[3] Muhammad Sajjad Ansar, Nael Alsaleh, and Bilal Farooq. “Behavioural modelling of automated to manual control transition in conditionally automated driving”. In: *Transportation research part F: traffic psychology and behaviour* 94 (2023), pp. 422–435.

[4] Sabrine Belmekki and Dominique Gruyer. “Advanced Road Safety: Collective Perception for Probability of Collision Estimation of Connected Vehicles”. In: *Computers* 13.1 (2024), p. 21.

[5] Johannes Betz, Melina Lutwitzi, and Steven Peters. “A new Taxonomy for Automated Driving: Structuring Applications based on their Operational Design Domain, Level of Automation and Automation Readiness”. In: *arXiv preprint arXiv:2404.17044* (2024).

[6] Faran Awais Butt et al. “On the integration of enabling wireless technologies and sensor fusion for next-generation connected and autonomous vehicles”. In: *IEEE Access* 10 (2022), pp. 14643–14668.

[7] Zhong Cao et al. “Driving-policy adaptive safeguard for autonomous vehicles using reinforcement learning”. In: *arXiv preprint arXiv:2012.01010* (2020).

[8] Thibault Charmet et al. “Overview of the Operational Design Domain Monitoring for Safe Intelligent Vehicle Navigation”. In: *2023 IEEE 26th International Conference on Intelligent Transportation Systems (ITSC)*. IEEE. 2023, pp. 5363–5370.

[9] Haolin Chen et al. “Study on the influence factors of takeover behavior in automated driving based on survival analysis”. In: *Transportation research part F: traffic psychology and behaviour* 95 (2023), pp. 281–296.

[10] Sikai Chen et al. “A taxonomy for autonomous vehicles considering ambient road infrastructure”. In: *Sustainability* 15.14 (2023), p. 11258.

[11] Wei Chen and Leila Kloul. “An ontology-based approach to generate the advanced driver assistance use cases of highway traffic”. In: *10th International Joint Conference on Knowledge Discovery, Knowledge Engineering and Knowledge Management.* 2018.

[12] Yiyang Chen et al. “Deep Reinforcement Learning in Autonomous Car Path Planning and Control: A Survey”. In: *arXiv preprint arXiv:2404.00340* (2024).

[13] HongSeok Cho. “Operational Design Domain (ODD) framework for driver-automation integrated systems”. PhD thesis. Massachusetts Institute of Technology, 2020.

[14] Ian Colwell et al. “An automated vehicle safety concept based on runtime restriction of the operational design domain”. In: *2018 IEEE Intelligent Vehicles Symposium (IV)*. IEEE. 2018, pp. 1910–1917.

[15] Andreea-catalina Cristescu et al. “A CORELATTION BETWEEN THE COEFFICIENT OF FRICTION AND BRAKING DISTANCE AND TIME”. In: *Annals of the Faculty of Engineering Hunedoara* 22.2 (2024), pp. 53–58.

[16] Youssef Damak et al. “Operational context-based design method of autonomous vehicles logical architectures”. In: *2020 IEEE 15th International Conference of System of Systems Engineering (SoSE)*. IEEE. 2020, pp. 439–444.

[17] Guimin Dong et al. “Deep Learning for Autonomous Vehicles and Systems”. In: *Autonomous Vehicles and Systems*. River Publishers, 2023, pp. 9–47.

[18] Frank Eichenseer, Shinjini Sarkar, and Ali Shakeri. “A Systematic Methodology for Specifying the Operational Design Domain of Automated Vehicles”. In: *2024 IEEE 35th International Symposium on Software Reliability Engineering Workshops (ISSREW)*. IEEE. 2024, pp. 13–18.

[19] Jacqueline Erhart et al. “Infrastructure support for automated driving: Further enhancements on the ISAD classes in Austria”. In: *Proceedings of 8th Transport Research Arena TRA* (2020), pp. 27–30.

[20] Emre Esenturk et al. “Analyzing real-world accidents for test scenario generation for automated vehicles”. In: *2021 IEEE Intelligent Vehicles Symposium (IV)*. IEEE. 2021, pp. 288–295.

[21] Francesca Favarò, Sky Eurich, and Nazanin Nader. “Autonomous vehicles’ disengagements: Trends, triggers, and regulatory limitations”. In: *Accident Analysis & Prevention* 110 (2018), pp. 136–148.

[22] Jamil Fayyad et al. “Deep learning sensor fusion for autonomous vehicle perception and localization: A review”. In: *Sensors* 20.15 (2020), p. 4220.

[23] Yuchuan Fu et al. “A decision-making strategy for vehicle autonomous braking in emergency via deep reinforcement learning”. In: *IEEE transactions on vehicular technology* 69.6 (2020), pp. 5876–5888.

[24] Hasitha Dilshani Gamage and Jinwoo Brian Lee. “Reinforcement learning based driving speed control for two vehicle scenario”. In: *Australasian transport research forum (ATRF), 39th*. Vol. 2017. 2017.

[25] Alfredo García, David Llopis-Castelló, and Francisco Javier Camacho-Torregrosa. “From the vehicle-based concept of operational design domain to the road-based concept of operational road section”. In: *Frontiers in Built Environment* 8 (2022), p. 901840.

[26] Magnus Gyllenhammar et al. “Towards an operational design domain that supports the safety argumentation of an automated driving system”. In: *10th European congress on embedded real time systems (ERTS 2020)*. 2020.

[27] Yu Han et al. “A new reinforcement learning-based variable speed limit control approach to improve traffic efficiency against freeway jam waves”. In: *Transportation research part C: emerging technologies* 144 (2022), p. 103900.

[28] Daniel Hillen and Jan Reich. “Model-based identification of operational design domains for dynamic risk assessment of autonomous vehicles”. In: *PhD thesis* (2020).

[29] Rasheed Hussain and Sherali Zeadally. “Autonomous cars: Research results, issues, and future challenges”. In: *IEEE Communications Surveys & Tutorials* 21.2 (2018), pp. 1275–1313.

[30] *ISO 23793-1:2024 Title of the Standard*. International Organization for Standardization. Part 1. 2024. URL: `https://www.iso.org/standard/XXXXXX`.

[31] Masao Ito. “Method of evaluating the influence factor of safety in the automated driving system: the chasm between SAE level 2 and level 3”. In: *Systems, Software and Services Process Improvement: 25th European Conference, EuroSPI 2018, Bilbao, Spain, September 5-7, 2018, Proceedings 25*. Springer. 2018, pp. 161–172.

[32] Masao Ito. “Supporting process design in the autonomous era with new standards and guidelines”. In: *Systems, Software and Services Process Improvement: 27th European Conference, EuroSPI 2020, Düsseldorf, Germany, September 9–11, 2020, Proceedings 27*. Springer. 2020, pp. 525–535.

[33] Masao Ito. “The uncertainty that the autonomous car faces and predictability analysis for evaluation”. In: *Systems, Software and Services Process Improvement: 26th European Conference, EuroSPI 2019, Edinburgh, UK, September 18–20, 2019, Proceedings 26*. Springer. 2019, pp. 83–95.

[34] Zhengmin Jiang et al. “Enhancing Autonomous Vehicle Safety Based on Operational Design Domain Definition, Monitoring, and Functional Degradation: A Case Study on Lane Keeping System”. In: *IEEE Transactions on Intelligent Vehicles* (2024).

[35] Duan Jianyu and Hongjun Zhang. “Model-based systemic hazard analysis approach for connected and autonomous vehicles and case study application in automatic emergency braking system”. In: *SAE International Journal of Connected and Automated Vehicles* 4.12-04-01-0003 (2021), pp. 23–34.

[36] Maria Jokela et al. “LiDAR performance review in arctic conditions”. In: *2019 IEEE 15th International Conference on Intelligent Computer Communication and Processing (ICCP)*. IEEE. 2019, pp. 27–31.

[37] Bernhard Kaiser et al. “Towards the definition of metrics for the assessment of operational design domains”. In: *Open Research Europe* 3 (2023).

[38] Ektor Karyotakis et al. “Minimizing stopping distance on split friction via steering and individual wheel braking optimization”. In: *The IAVSD International Symposium on Dynamics of Vehicles on Roads and Tracks*. Springer. 2023, pp. 380–389.

[39] Siddartha Khastgir. “Testing automated driving systems to calibrate drivers’ trust”. PhD thesis. University of Warwick, 2019.

[40] Vladislav Kibalov and Oleg Shipitko. “Safe speed control and collision probability estimation under ego-pose uncertainty for autonomous vehicle”. In: *2020 IEEE 23rd International Conference on Intelligent Transportation Systems (ITSC)*. IEEE. 2020, pp. 1–6.

[41] Hoseon Kim et al. “Evaluation of Autonomous Driving Safety by Operational Design Domains (ODD) in Mixed Traffic”. In: *Sustainability* 16.22 (2024), p. 9672.

[42] B Ravi Kiran et al. “Deep reinforcement learning for autonomous driving: A survey”. In: *IEEE Transactions on Intelligent Transportation Systems* 23.6 (2021), pp. 4909–4926.

[43] Philip Koopman. *How safe is safe enough?: Measuring and predicting Autonomous Vehicle Safety*. Carnegie Mellon University, 2022.

[44] A Abdi Kordani et al. “Effect of adverse weather conditions on vehicle braking distance of highways”. In: *Civil Engineering Journal* 4.1 (2018), pp. 46–57.

[45] Guofa Li et al. “Deep reinforcement learning enabled decision-making for autonomous driving at intersections”. In: *Automotive Innovation* 3 (2020), pp. 374–385.

[46] Yueyuan Li et al. “Choose your simulator wisely: A review on open-source simulators for autonomous driving”. In: *IEEE Transactions on Intelligent Vehicles* (2024).

[47] Xiaobo Liu et al. “Optimizing the safety-efficiency balancing of automated vehicle car-following”. In: *Accident Analysis & Prevention* 136 (2020), p. 105435.

[48] Zhaoyong Liu et al. *Research on Collision Avoidance and Vehicle Stability Control of Intelligent Driving Vehicles in Harsh Environments*. Tech. rep. SAE Technical Paper, 2022.

[49] Marcel Aguirre Mehlhorn, Andreas Richter, and Yuri AW Shardt. “Ruling the operational boundaries: A survey on operational design domains of autonomous driving systems”. In: *IFAC-PapersOnLine* 56.2 (2023), pp. 2202–2213.

[50] Leo Mendiboure et al. “Operational design domain for automated driving systems: Taxonomy definition and application”. In: *2023 IEEE Intelligent Vehicles Symposium (IV)*. IEEE. 2023, pp. 1–6.

[51] Predrag Milenkovic et al. “The influence of brake pads thermal conductivity on passanger car brake system efficiency”. In: (2010).

[52] Valentina Musat et al. “Multi-weather city: Adverse weather stacking for autonomous driving”. In: *Proceedings of the IEEE/CVF International Conference on Computer Vision*. 2021, pp. 2906–2915.

[53] Anum Mushtaq et al. “Multi-agent reinforcement learning for traffic flow management of autonomous vehicles”. In: *Sensors* 23.5 (2023), p. 2373.

[54] Demin Nalic et al. “Scenario based testing of automated driving systems: A literature survey”. In: *FISITA web Congress*. Vol. 10. 2020, p. 1.

[55] Matteo Oldoni and Siddartha Khastgir. “Introducing ODD-SAF: An Operational Design Domain Safety Assurance Framework for Automated Driving Systems”. In: *Automated Road Transportation Symposium*. Springer. 2022, pp. 133–151.

[56] Kareem Othman. “Public acceptance and perception of autonomous vehicles: a comprehensive review”. In: *AI and Ethics* 1.3 (2021), pp. 355–387.

[57] Budi Padmaja et al. “Exploration of issues, challenges and latest developments in autonomous cars”. In: *Journal of Big Data* 10.1 (2023), p. 61.

[58] Zhaowen Pang et al. “A Survey of Decision-Making Safety Assessment Methods for Autonomous Vehicles”. In: *IEEE Intelligent Transportation Systems Magazine* (2023).

[59] Giuseppina Pappalardo et al. “Assessing the operational design domain of lane support system for automated vehicles in different weather and road conditions”. In: *Journal of traffic and transportation engineering (English edition)* 9.4 (2022), pp. 631–644.

[60] Omid Rahmani et al. “A nonlinear analytical approach for estimating vehicle braking distance based on multi-body dynamic simulation”. In: *Sādhanā* 49.1 (2024), p. 20.

[61] Sudarshan Rajagopalan et al. “GenDeg: Diffusion-Based Degradation Synthesis for Generalizable All-in-One Image Restoration”. In: *arXiv preprint arXiv:2411.17687* (2024).

[62] Nagarjun Reddy et al. “Operational design domain requirements for improved performance of lane assistance systems: A field test study in The Netherlands”. In: *IEEE Open Journal of Intelligent Transportation Systems* 1 (2020), pp. 237–252.

[63] Andreas Reschka and Markus Maurer. “Conditions for a safe state of automated road vehicles”. In: *it-Information Technology* 57.4 (2015), pp. 215–222.

[64] Hanan Rizk, Ahmed Chaibet, and Ali Kribèche. “Model-based control and model-free control techniques for autonomous vehicles: A technical survey”. In: *Applied Sciences* 13.11 (2023), p. 6700.

[65] On-Road Automated Driving (ORAD) Committee. *Taxonomy and Definitions for Terms Related to Driving Automation Systems for On-Road Motor Vehicles*. Apr. 2021. DOI: `https://doi.org/10.4271/J3016_202104`. URL: `https://doi.org/10.4271/J3016_202104`.

[66] Daniel Rohne, Andreas Richter, and Edward Schwalb. “Implementing ODD as single point of knowledge to support the development of automated driving”. In: *2022 IEEE International Conference on Systems, Man, and Cybernetics (SMC)*. IEEE. 2022, pp. 1364–1370.

[67] Thomas Rothmeier, Werner Huber, and Alois C Knoll. “Time to Shine: Fine-Tuning Object Detection Models with Synthetic Adverse Weather Images”. In: *Proceedings of the IEEE/CVF Winter Conference on Applications of Computer Vision*. 2024, pp. 4447–4456.

[68] Ananya Roy, Moinul Hossain, and Yasunori Muromachi. “A deep reinforcement learning-based intelligent intervention framework for real-time proactive road safety management”. In: *Accident Analysis & Prevention* 165 (2022), p. 106512.

[69] Aniket Salvi, Gereon Weiss, and Mario Trapp. “Online Identification of Operational Design Domains of Automated Driving System Features”. In: *2024 IEEE Intelligent Vehicles Symposium (IV)*. IEEE. 2024, pp. 1743–1749.

[70] Aniket Salvi et al. “Fuzzy interpretation of operational design domains in autonomous driving”. In: *2022 IEEE Intelligent Vehicles Symposium (IV)*. IEEE. 2022, pp. 1261–1267.

[71] Fabian Schuldt. “Towards testing of automated driving functions in virtual driving environments”. In: *PhD thesis* (2017).

[72] Bobbie D Seppelt and John D Lee. “Modeling driver response to imperfect vehicle control automation”. In: *Procedia Manufacturing* 3 (2015), pp. 2621–2628.

[73] Shital Shah et al. “Airsim: High-fidelity visual and physical simulation for autonomous vehicles”. In: *Field and Service Robotics: Results of the 11th International Conference*. Springer. 2018, pp. 621–635.

[74] Yu Song, Madhav V Chitturi, and David A Noyce. “Intersection two-vehicle crash scenario specification for automated vehicle safety evaluation using sequence analysis and Bayesian networks”. In: *Accident Analysis & Prevention* 176 (2022), p. 106814.

[75] Chen Sun. “Operational Design Domain Monitoring and Augmentation for Autonomous Driving”. In: (2022).

[76] Qian Sun et al. “Hierarchical reinforcement learning for dynamic autonomous vehicle navigation at intelligent intersections”. In: *Proceedings of the 29th ACM SIGKDD Conference on Knowledge Discovery and Data Mining*. 2023, pp. 4852–4861.

[77] Oguz Tengilimoglu, Oliver Carsten, and Zia Wadud. “Implications of automated vehicles for physical road environment: A comprehensive review”. In: *Transportation research part E: logistics and transportation review* 169 (2023), p. 102989.

[78] Eric Thorn et al. *A framework for automated driving system testable cases and scenarios*. Tech. rep. United States. Department of Transportation. National Highway Traffic Safety …, 2018.

[79] United Nations Economic Commission for Europe. *UNECE Regulation No. 155 on Cybersecurity and Cybersecurity Management System for Vehicles (WP.29)*. Retrieved from `https://unece.org/transport/vehicle-regulations`. 2020.

[80] Jaap Vreeswijk, Anton Wijbenga, and Julian Schindler. “Cooperative automated driving for managing transition areas and the operational design domain (odd)”. In: *Proceedings of 8th Transport Research Arena TRA 2020* (2020).

[81] Walther Wachenfeld and Hermann Winner. “The release of autonomous vehicles”. In: *Autonomous Driving: Technical, Legal and Social Aspects* (2016), pp. 425–449.

[82] Xiao Wang and Matthias Althoff. “Safe Reinforcement Learning for Automated Vehicles via Online Reachability Analysis”. In: *IEEE Transactions on Intelligent Vehicles* (2023).

[83] Xuesong Wang et al. “Operational design domain of autonomous vehicles at skewed intersection”. In: *Accident Analysis & Prevention* 159 (2021), p. 106241.

[84] Patrick Weissensteiner et al. “Operational design domain-driven coverage for the safety argumentation of automated vehicles”. In: *IEEE Access* 11 (2023), pp. 12263–12284.

[85] Jian Yang, Qiuxiang Yang, and Qiang Li. “Method for Enhancing Unmanned Aerial Vehicle Target Detection in Challenging Environments Using Improved YOLOv8 Network”. In: *2024 6th Asia Symposium on Image Processing (ASIP)*. IEEE. 2024, pp. 7–13.

[86] Jingwen Yang, Ping Wang, and Yongfeng Ju. “Variable Speed Limit Intelligent Decision-Making Control Strategy Based on Deep Reinforcement Learning under Emergencies”. In: *Sustainability* 16.3 (2024), p. 965.

[87] Wenhao Yu et al. “SOTIF risk mitigation based on unified ODD monitoring for autonomous vehicles”. In: *Journal of intelligent and connected vehicles* 5.3 (2022), pp. 157–166.

[88] Weidong Zhang et al. “Underwater image enhancement via minimal color loss and locally adaptive contrast enhancement”. In: *IEEE Transactions on Image Processing* 31 (2022), pp. 3997–4010.

[89] Xizhe Zhang et al. “ODD and Behaviour Based Scenario Generation for Automated Driving Systems”. In: *IEEE Access* (2024).

[90] Yuhang Zhang et al. “Cooperative multi-agent reinforcement learning for large scale variable speed limit control”. In: *2023 IEEE International Conference on Smart Computing (SMARTCOMP)*. IEEE. 2023, pp. 149–156.

[91] Shiyue Zhao et al. “Collision-free emergency planning and control methods for CAVs considering intentions of surrounding vehicles”. In: *ISA transactions* 136 (2023), pp. 535–547.

[92] Weixuan Zhou et al. “Developing an improved automatic preventive braking system based on safety-critical car-following events from naturalistic driving study data”. In: *Accident Analysis & Prevention* 178 (2022), p. 106834.

A

The detailed flow chart of methodology

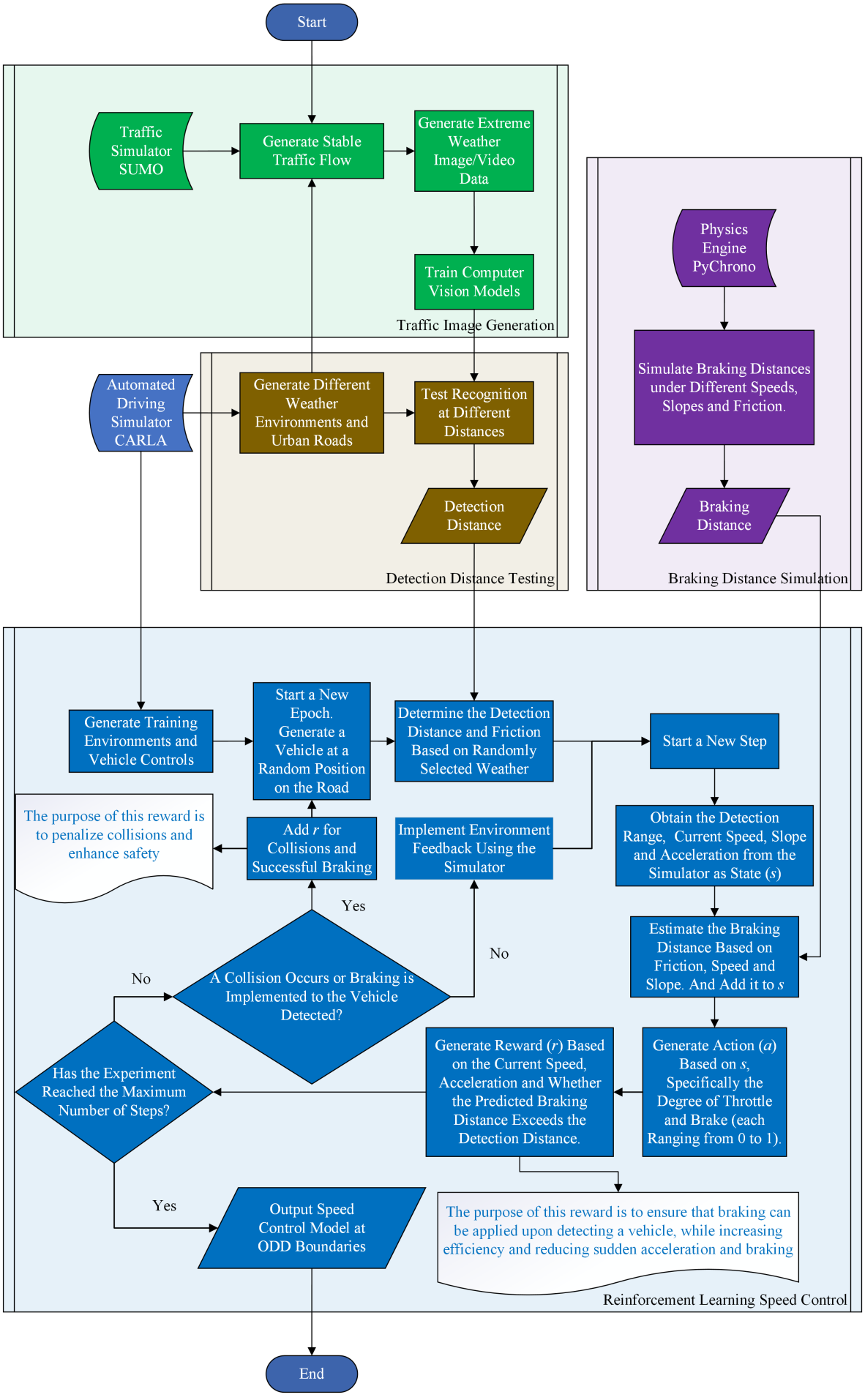

Figure A.1: The detailed flow chart of methodology

B

Pseudo-code for each research step

Algorithm 1 Dataset Generation Process

Input Parameters:
Map set $M = \{\text{Town01}, \text{Town02}, \ldots, \text{Town06}\}$
Weather parameters set $W_p = \{\text{Cloudiness}, \text{Precipitation}, \text{Precipitation Deposits}, \text{Fog Density}\}$
Weather intensity range $[0, 100]$
Number of vehicles range $[25, 100]$
Camera positions set CameraPositions
Number of images $N_{\text{images}} = 7,500$
Output: Image and video datasets
for each map map in Maps **do**
    for iteration $n = 1$ to N_{images} **do**
        Randomly generate weather parameter values weather, each parameter following a uniform distribution in $[0, 100]$
        Set the solar elevation angle, with a $3:1$ probability to determine daytime or nighttime
        Randomly generate the number of vehicles vehicle_num, following a uniform distribution in $[25, 100]$
        Randomly generate vehicle_num vehicles on the map, randomly selecting vehicle types
        Randomly select a camera position camera_pos in CameraPositions
        Place an RGB camera at position camera_pos
        Capture and save the image
        Use a bounding box tool to obtain annotation information
        Determine if there are any occlusions between the target vehicle and the camera
        Save annotation data
    end for
end for
Video Dataset Generation:
for each map map in Maps **do**
    Use SUMO to simulate traffic flow, setting vehicle types and speeds
    CARLA generates high-precision physical models based on SUMO's trajectories
    Record and save videos during the simulation process
    Use a bounding box tool to obtain annotation information from the videos
    Determine if there are any occlusions between the target vehicle and the camera
    Save annotation data
end for
Output: Generated images, videos, and corresponding annotation datasets

Algorithm 2 Detection Distance Testing Process - Data Collection

Input Parameters:
Town set $M = \{\text{Town01}, \text{Town02}, \ldots, \text{Town06}, \text{Town07}, \text{Town10}, \text{Town13}\}$
Location set $L_m, \forall m \in M$
Weather conditions set $W = \{\text{Rainy}, \text{Ground Water}, \text{Foggy}\}$
Time conditions set $T = \{\text{Daytime}, \text{Night}, \text{Cloudy}\}$
Weather intensity set $I = \{5, 10, \ldots, 120\}$
Distance set $D = \{5\,\text{m}, 10\,\text{m}, \ldots, 120\,\text{m}\}$
Output: Image dataset under all conditions
for each map m in M **do**
    Select two different long straight road locations for testing
    for each test location $l \in L_m$ **do**
        for each time condition $t \in T$ **do**
            for each weather condition $w \in W$ **do**
                for each weather intensity $i \in I$ **do**
                    Set environment: map m, location l, time t, weather w, intensity i
                    Place a camera at one end of the road
                    for each distance d in D **do**
                        Generate a background vehicle at a distance d
                        Capture and save the image
                        Destroy the background vehicle
                    end for
                end for
            end for
        end for
    end for
end for
Output: All collected image data

Algorithm 3 Detection Distance Testing Process - Model Testing

Input Parameters:
Image dataset (from data collection step)
Detection models set $E = \{\text{COCO yolo}, \text{CARLA model}\}$
Confidence threshold set $C = \{25\%, 50\%\}$
Output: Farthest detection distance under different conditions
for each detection model $e \in E$ **do**
    for each confidence threshold $c \in C$ **do**
        for each image i in the image dataset **do**
            Use model e to detect image i with confidence threshold c
            Record whether the target was successfully detected
        end for
        Calculate the farthest distance at which the target was successfully detected under the current model and confidence threshold
    end for
end for
Output: Statistical results of the farthest detection distance under different models and confidence thresholds

Algorithm 4 Braking Distance Test

Inputs:
Friction coefficient set $\mu = \{0.18, 0.28, 0.4, 0.6\}$
Slope set $\theta = \{-5°, -4.5°, \ldots, 5°\}$
Initial speed set $v = \{1\,\text{km/h}, 2\,\text{km/h}, \ldots, 120\,\text{km/h}\}$
Number of repetitions $N = 5$
for each friction coefficient $\mu_i \in \mu$ **do**
  for each slope $\theta_j \in \theta$ **do**
    for each initial speed $v_k \in v$ **do**
      for trial number $n = 1$ to N **do**
        Vehicle drives at speed v_k on slope θ_j
        Apply full brake until the speed is less than $0.5\,\text{km/h}$
        Record brake distance $d_{\mu_i,\theta_j,v_k,n}$
      end for
      Calculate average brake distance:
      $\bar{d}_{\mu_i,\theta_j,v_k} = \frac{1}{N} \sum_{n=1}^{N} d_{\mu_i,\theta_j,v_k,n}$
    end for
  end for
end for
Output: Average brake distance $\bar{d}_{\mu,v,\theta}$

Algorithm 5 Soft Actor-Critic (SAC) for Speed Control in CARLA

Inputs:
Replay Buffer Capacity N, Batch Size B, Learning Rate η, Discount Factor γ, Soft Update Rate τ, Entropy Coefficient α
Maximum episodes $max\_episodes$, maximum time steps per episode max_steps
Initialize policy network π_θ, critic networks Q_{ϕ_1}, Q_{ϕ_2}, and target networks $Q_{\phi'_1}$, $Q_{\phi'_2}$
Initialize replay buffer D
for each episode $e = 1$ to $max\_episodes$ **do**
  Reset environment, randomize weather, friction μ, slope θ, NPC position
  Observe initial state $s_0 = (v_{ego}, \theta, \mu, d_{detect}, d_{front})$
  for each time step $t = 1$ to max_steps **do**
    Sample action $a_t \sim \pi_\theta(a_t|s_t)$ from policy
    Apply action a_t in CARLA, observe next state s_{t+1}, reward r_t, done flag
    Store transition (s_t, a_t, r_t, s_{t+1}) in replay buffer D
    if size of $D \geq B$ **then**
      Sample mini-batch (s_i, a_i, r_i, s_{i+1}) from D
      Compute target Q-value:
      $y_i = r_i + \gamma \cdot \min(Q_{\phi'_1}(s_{i+1}, a_{i+1}), Q_{\phi'_2}(s_{i+1}, a_{i+1})) - \alpha \log(\pi_\theta(a_{i+1}|s_{i+1}))$
      Compute critic loss:
      $L_Q = (Q_{\phi_1}(s_i, a_i) - y_i)^2 + (Q_{\phi_2}(s_i, a_i) - y_i)^2$
      Update critic networks ϕ_1, ϕ_2 using gradient ∇L_Q
      Compute policy loss:
      $L_\pi = \mathbb{E}[\alpha \log(\pi_\theta(a_i|s_i)) - \min(Q_{\phi_1}(s_i, a_i), Q_{\phi_2}(s_i, a_i))]$
      Update policy network θ using gradient ∇L_π
      if adaptive entropy coefficient **then**
        Compute entropy loss:
        $L_\alpha = -\mathbb{E}[\alpha \cdot (\log(\pi_\theta(a_i|s_i)) + H_{target})]$
        Update α using gradient ∇L_α
      end if
      Update target networks:
      $\phi'_1 \leftarrow \tau\phi_1 + (1 - \tau)\phi'_1$
      $\phi'_2 \leftarrow \tau\phi_2 + (1 - \tau)\phi'_2$
    end if
    if collision or time step limit reached **then**
      Break
    end if
  end for
  Evaluate policy after each episode
end for
Output: Trained policy π_θ

C

The impact of weather and intensity on detection distance

Table C.1: Average detection distance and variance under various conditions

intensity	cloud_fog	cloud_rain	cloud_wet	daytime_fog	daytime_rain	daytime_wet	light_fog	light_rain	light_wet
Average detection distance under the Specialization Model at 25% confidence threshold									
5.00	66.07	65.71	65.71	67.14	66.43	67.14	67.50	67.14	67.14
10.00	67.14	65.00	66.43	68.93	66.79	66.43	67.86	67.14	65.71
15.00	68.93	65.71	65.36	70.00	67.14	67.86	66.07	66.07	67.50
20.00	68.93	65.00	65.00	68.93	67.14	67.50	65.71	66.07	67.86
25.00	69.29	64.64	62.86	67.86	65.00	68.93	66.43	66.07	65.71
30.00	68.93	64.64	65.36	68.57	66.79	67.50	66.79	65.36	66.79
35.00	73.21	63.93	64.64	72.86	68.21	67.86	67.50	66.07	64.64
40.00	76.07	64.29	64.64	76.43	65.71	67.14	67.50	65.00	64.29
45.00	75.36	64.64	65.00	76.07	66.79	66.43	66.43	65.00	63.93
50.00	74.29	64.29	65.36	76.43	67.14	65.71	63.21	63.21	62.86
55.00	74.29	66.07	66.07	75.71	67.14	66.79	63.21	62.50	62.86
60.00	73.21	65.00	65.71	73.93	66.07	67.14	60.71	60.00	63.21
65.00	72.14	67.50	67.86	72.50	67.50	66.79	62.14	58.93	62.86
70.00	69.64	68.21	67.86	71.43	66.43	66.07	60.71	57.86	57.50
75.00	67.86	67.14	67.86	68.57	66.43	64.29	58.57	54.64	57.50
80.00	63.93	67.50	69.29	67.50	67.14	64.29	57.14	53.57	53.57
85.00	61.79	66.79	66.43	65.00	66.43	63.21	52.14	50.71	51.07
90.00	60.71	67.14	64.64	63.93	66.07	63.93	52.14	47.50	48.93
95.00	60.36	66.07	61.43	61.07	65.00	63.21	51.07	44.29	46.43
100.00	56.79	63.57	55.71	60.00	65.00	60.71	49.64	41.79	45.00
Variance of detection distance under the Specialization Model at 25% confidence threshold									
5.00	50.69	53.30	60.99	52.75	47.80	52.75	83.65	110.44	125.82
10.00	48.90	50.00	51.65	39.15	52.34	51.65	110.44	79.67	76.37
15.00	58.38	60.99	59.48	42.31	52.75	52.75	77.61	85.30	114.42
20.00	58.38	53.85	57.69	42.99	52.75	49.04	76.37	54.53	91.21
25.00	45.60	44.09	45.05	52.75	38.46	58.38	86.26	73.76	91.76
30.00	31.46	59.48	55.63	55.49	52.34	45.19	71.57	55.63	86.95
35.00	67.72	58.38	51.79	52.75	60.03	60.44	102.88	77.61	55.63
40.00	73.76	57.14	59.48	59.34	41.76	52.75	118.27	53.85	64.84
45.00	86.40	90.25	80.77	66.07	71.57	55.49	82.42	76.92	54.53
50.00	87.91	49.45	63.32	82.42	71.98	49.45	79.26	75.41	68.13

(Continued on next page)

(Continued from previous page)

intensity	cloud_fog	cloud_rain	cloud_wet	daytime_fog	daytime_rain	daytime_wet	light_fog	light_rain	light_wet
55.00	87.91	96.84	81.46	95.60	79.67	67.72	83.10	79.81	68.13
60.00	83.10	73.08	84.07	108.38	69.92	75.82	91.76	69.23	40.80
65.00	87.36	91.35	125.82	91.35	72.12	71.57	87.36	154.53	48.90
70.00	63.32	83.10	56.59	97.80	67.03	69.92	87.91	195.05	175.96
75.00	48.90	68.13	91.21	78.57	59.34	60.99	93.96	267.17	191.35
80.00	42.99	72.12	95.60	56.73	71.98	60.99	98.90	278.57	217.03
85.00	33.10	75.41	101.65	61.54	67.03	56.18	68.13	291.76	200.69
90.00	41.76	83.52	90.25	42.99	62.23	104.53	98.90	314.42	169.92
95.00	40.25	112.23	182.42	50.69	53.85	110.03	66.07	284.07	209.34
100.00	29.26	136.26	164.84	34.62	73.08	126.37	59.48	263.87	234.62
Average detection distance under the Specialization Model at 50% confidence threshold									
5.00	60.71	60.71	61.07	61.43	61.07	62.86	61.79	62.50	62.50
10.00	62.14	61.43	61.07	61.43	62.14	62.86	62.86	62.86	61.43
15.00	63.21	61.79	63.21	62.14	62.86	62.86	61.43	62.50	61.79
20.00	62.14	61.43	61.07	62.50	61.07	61.43	61.43	62.14	62.14
25.00	62.50	58.93	59.64	63.21	62.50	63.21	61.79	61.79	59.64
30.00	63.21	60.00	60.00	63.21	61.07	61.07	59.64	60.71	58.93
35.00	67.86	60.00	60.00	66.79	62.86	61.07	58.93	61.43	61.07
40.00	70.00	60.36	60.71	69.29	61.43	61.07	60.00	61.07	60.36
45.00	69.64	62.14	62.14	71.07	63.21	61.43	60.71	60.36	59.64
50.00	68.57	60.36	61.43	70.00	62.50	62.14	59.29	59.64	57.86
55.00	68.57	62.50	61.43	69.29	61.79	61.07	57.86	58.21	58.57
60.00	68.21	60.36	60.71	68.57	61.07	60.36	57.50	56.07	55.00
65.00	65.36	62.14	61.07	66.79	62.14	62.14	55.71	56.07	52.86
70.00	62.86	63.21	63.21	64.64	61.43	60.36	55.71	53.93	53.57
75.00	61.43	61.43	60.71	62.50	61.79	60.71	53.21	50.36	52.14
80.00	60.00	62.14	61.43	61.79	62.50	60.36	51.43	47.86	48.93
85.00	58.93	62.50	60.71	59.29	61.79	57.86	49.64	44.29	43.21
90.00	57.14	60.71	58.93	58.93	60.36	56.07	47.86	41.79	43.21
95.00	54.64	58.93	55.71	56.43	61.43	55.00	45.00	36.79	39.29
100.00	52.14	55.71	49.29	55.36	61.79	54.64	45.71	35.71	37.50
Variance of detection distance under the Specialization Model at 50% confidence threshold									
5.00	10.99	37.91	46.84	9.34	16.07	41.21	56.18	68.27	68.27

(Continued on next page)

(Continued from previous page)

intensity	cloud_fog	cloud_rain	cloud_wet	daytime_fog	daytime_rain	daytime_wet	light_fog	light_rain	light_wet
10.00	18.13	28.57	19.92	17.03	18.13	56.59	71.98	60.44	82.42
15.00	36.95	36.95	60.03	18.13	37.36	41.21	51.65	37.50	60.03
20.00	18.13	24.73	31.46	18.27	12.23	17.03	78.57	41.21	52.75
25.00	14.42	39.15	28.71	25.41	25.96	36.95	67.72	36.95	36.40
30.00	21.57	26.92	23.08	25.41	19.92	8.38	51.79	26.37	39.15
35.00	64.29	23.08	26.92	52.34	33.52	8.38	85.30	32.42	39.15
40.00	69.23	32.55	30.22	76.37	17.03	8.38	50.00	31.46	32.55
45.00	55.63	68.13	56.59	54.53	33.10	24.73	57.14	32.55	40.25
50.00	67.03	24.86	43.96	46.15	25.96	29.67	45.60	17.17	25.82
55.00	63.19	72.12	51.65	45.60	44.64	27.61	68.13	71.57	40.11
60.00	60.03	32.55	45.60	55.49	19.92	28.71	49.04	100.69	76.92
65.00	36.40	52.75	62.23	36.95	41.21	64.29	68.68	123.76	145.05
70.00	33.52	40.80	52.34	36.40	32.42	55.63	49.45	131.46	147.80
75.00	32.42	40.11	49.45	29.81	36.95	64.84	79.26	178.71	148.90
80.00	34.62	37.36	40.11	33.10	25.96	82.55	67.03	225.82	139.15
85.00	27.61	52.88	91.76	18.68	33.10	60.44	74.86	207.14	171.57
90.00	33.52	80.22	89.15	19.92	17.17	39.15	68.13	160.03	152.34
95.00	24.86	62.23	103.30	17.03	36.26	53.85	76.92	156.18	126.37
100.00	25.82	45.60	72.53	36.40	33.10	67.17	53.30	126.37	110.58
Average detection distance under the Generalization Model at 25% confidence threshold									
5.00	55.00	53.00	52.00	55.00	55.00	56.00	60.00	60.00	61.00
10.00	55.00	52.00	55.00	56.00	57.00	56.00	57.00	61.00	59.00
15.00	56.00	57.00	57.00	56.00	56.00	56.00	59.00	60.00	59.00
20.00	56.00	56.00	56.00	53.00	57.00	56.00	57.00	61.00	62.00
25.00	57.00	56.00	56.00	56.00	56.00	57.00	58.00	60.00	60.00
30.00	60.00	57.00	56.00	57.00	55.00	56.00	56.00	62.00	61.00
35.00	64.00	57.00	59.00	64.00	55.00	56.00	57.00	63.00	63.00
40.00	65.00	57.00	59.00	66.00	55.00	56.00	56.00	62.00	62.00
45.00	65.00	58.00	60.00	65.00	54.00	56.00	52.00	59.00	59.00
50.00	65.00	60.00	61.00	64.00	56.00	55.00	53.00	59.00	57.00
55.00	63.00	60.00	59.00	64.00	55.00	57.00	48.00	54.00	49.00
60.00	61.00	60.00	61.00	63.00	59.00	56.00	49.00	46.00	47.00
65.00	61.00	61.00	61.00	61.00	59.00	55.00	47.00	45.00	45.00

(Continued on next page)

(Continued from previous page)

intensity	cloud_fog	cloud_rain	cloud_wet	daytime_fog	daytime_rain	daytime_wet	light_fog	light_rain	light_wet
70.00	59.00	56.00	53.00	61.00	57.00	50.00	49.00	45.00	44.00
75.00	60.00	56.00	50.00	59.00	56.00	42.00	49.00	45.00	42.00
80.00	58.00	52.00	50.00	59.00	54.00	42.00	43.00	42.00	43.00
85.00	56.00	55.00	49.00	57.00	50.00	40.00	43.00	43.00	44.00
90.00	53.00	54.00	45.00	56.00	51.00	40.00	41.00	40.00	37.00
95.00	52.00	49.00	45.00	55.00	50.00	41.00	40.00	39.00	37.00
100.00	52.00	51.00	43.00	52.00	43.00	40.00	39.00	37.00	32.00
Variance of detection distance under the Generalization Model at 25% confidence threshold									
5.00	12.50	20.00	32.50	25.00	137.50	192.50	87.50	50.00	130.00
10.00	25.00	32.50	137.50	30.00	170.00	192.50	57.50	55.00	55.00
15.00	30.00	170.00	170.00	30.00	192.50	192.50	55.00	50.00	55.00
20.00	67.50	117.50	192.50	45.00	170.00	192.50	20.00	30.00	120.00
25.00	45.00	192.50	117.50	30.00	192.50	170.00	32.50	50.00	87.50
30.00	87.50	170.00	117.50	45.00	212.50	192.50	17.50	120.00	80.00
35.00	92.50	182.50	155.00	105.00	212.50	192.50	20.00	95.00	95.00
40.00	50.00	132.50	155.00	80.00	212.50	192.50	17.50	107.50	120.00
45.00	50.00	182.50	137.50	50.00	155.00	192.50	45.00	42.50	17.50
50.00	50.00	162.50	192.50	67.50	192.50	137.50	32.50	55.00	32.50
55.00	82.50	225.00	242.50	67.50	212.50	257.50	57.50	30.00	130.00
60.00	42.50	137.50	192.50	82.50	242.50	280.00	55.00	105.00	107.50
65.00	42.50	292.50	242.50	42.50	217.50	350.00	95.00	137.50	137.50
70.00	17.50	117.50	132.50	42.50	107.50	25.00	67.50	287.50	530.00
75.00	25.00	167.50	112.50	17.50	30.00	170.00	130.00	337.50	557.50
80.00	7.50	32.50	100.00	17.50	42.50	170.00	57.50	370.00	495.00
85.00	17.50	162.50	92.50	20.00	87.50	175.00	32.50	432.50	617.50
90.00	7.50	167.50	50.00	17.50	42.50	162.50	42.50	412.50	407.50
95.00	20.00	92.50	87.50	12.50	62.50	167.50	87.50	380.00	470.00
100.00	7.50	142.50	170.00	32.50	195.00	175.00	117.50	395.00	332.50
Average detection distance under the Generalization Model at 50% confidence threshold									
5.00	50.50	50.00	49.50	51.50	47.50	48.50	58.50	59.50	58.50
10.00	52.00	50.50	51.00	52.50	48.50	50.00	56.00	59.50	56.50
15.00	53.00	52.50	54.00	53.00	48.00	51.00	56.50	59.00	57.50
20.00	53.50	53.00	53.50	51.50	49.00	52.00	55.50	59.00	59.00

(Continued on next page)

(Continued from previous page)

intensity	cloud_fog	cloud_rain	cloud_wet	daytime_fog	daytime_rain	daytime_wet	light_fog	light_rain	light_wet
25.00	54.50	52.50	53.00	53.00	48.00	53.50	56.50	58.50	58.00
30.00	58.50	55.00	53.50	54.00	51.00	53.50	54.00	59.50	57.50
35.00	63.00	54.50	56.00	61.00	51.50	53.50	55.00	60.00	58.50
40.00	62.00	54.50	56.50	63.50	52.00	53.50	51.50	59.00	57.00
45.00	62.00	56.00	58.50	62.00	50.00	53.00	49.50	55.00	56.50
50.00	62.00	57.00	58.00	62.00	54.00	52.00	49.00	51.50	53.00
55.00	61.00	57.00	57.50	61.50	53.00	54.50	46.50	48.00	50.50
60.00	59.00	56.50	58.50	61.00	55.50	55.00	46.00	45.00	46.00
65.00	59.50	59.00	58.50	59.00	56.00	53.00	45.50	43.00	40.50
70.00	57.00	53.00	50.00	58.00	52.50	45.50	46.50	43.00	42.00
75.00	57.50	52.50	49.50	57.00	50.50	39.50	46.00	44.00	40.00
80.00	54.00	49.00	49.00	57.00	47.50	40.00	41.00	40.50	42.00
85.00	53.00	52.50	48.00	54.00	47.50	38.00	41.50	40.50	40.50
90.00	51.50	50.00	44.00	53.50	46.00	37.50	39.00	37.50	35.00
95.00	50.00	47.50	43.00	52.50	45.00	37.50	39.50	37.00	34.00
100.00	49.50	48.00	41.00	50.50	42.50	37.00	37.50	35.00	31.50
Variance of detection distance under the Generalization Model at 50% confidence threshold									
5.00	30.28	22.22	58.06	33.61	45.83	100.28	78.06	46.94	105.83
10.00	34.44	35.83	193.33	40.28	44.72	72.22	43.33	63.61	61.39
15.00	45.56	118.06	137.78	45.56	45.56	115.56	44.72	60.00	68.06
20.00	55.83	78.89	144.72	44.72	43.33	145.56	30.28	43.33	93.33
25.00	46.94	118.06	117.78	45.56	62.22	189.17	22.50	61.39	84.44
30.00	50.28	122.22	111.39	60.00	148.89	222.50	21.11	74.72	118.06
35.00	73.33	119.17	126.67	82.22	200.28	222.50	22.22	77.78	133.61
40.00	62.22	80.28	116.94	78.06	178.89	222.50	22.50	71.11	112.22
45.00	62.22	165.56	144.72	62.22	138.89	195.56	24.72	50.00	100.28
50.00	62.22	123.33	156.67	62.22	165.56	212.22	37.78	139.17	84.44
55.00	71.11	151.11	206.94	66.94	184.44	246.94	66.94	117.78	69.17
60.00	37.78	122.50	178.06	71.11	246.94	283.33	93.33	133.33	110.00
65.00	41.39	221.11	250.28	37.78	215.56	384.44	69.17	95.56	208.06
70.00	23.33	78.89	105.56	40.00	95.83	96.94	66.94	267.78	434.44
75.00	29.17	118.06	141.39	23.33	69.17	141.39	93.33	304.44	438.89
80.00	37.78	48.89	87.78	23.33	129.17	138.89	48.89	352.50	406.67

(Continued on next page)

(Continued from previous page)

intensity	cloud_fog	cloud_rain	cloud_wet	daytime_fog	daytime_rain	daytime_wet	light_fog	light_rain	light_wet
85.00	34.44	123.61	73.33	26.67	112.50	134.44	50.28	441.39	496.94
90.00	11.39	116.67	37.78	22.50	115.56	129.17	60.00	401.39	366.67
95.00	22.22	79.17	78.89	18.06	133.33	123.61	85.83	395.56	410.00
100.00	19.17	112.22	137.78	24.72	162.50	123.33	90.28	422.22	316.94
Average detection distance under the COCO Model at 25% confidence threshold									
5.00	46.79	46.43	45.36	47.50	47.50	47.14	46.79	45.36	46.43
10.00	46.07	46.43	46.43	47.50	46.07	46.79	46.43	47.86	47.50
15.00	46.07	46.07	46.43	46.79	47.86	48.57	46.79	47.86	46.79
20.00	46.43	45.71	46.79	46.43	46.79	46.79	48.57	46.07	46.79
25.00	46.79	46.43	45.36	47.14	47.50	47.86	47.50	47.14	47.50
30.00	45.00	47.14	46.43	45.36	46.43	45.71	47.50	46.43	47.86
35.00	41.79	46.43	47.14	43.93	46.07	46.43	44.29	47.50	48.21
40.00	40.36	47.14	46.79	41.07	46.07	46.79	42.86	49.29	47.14
45.00	38.21	46.07	46.07	38.93	46.79	48.21	42.86	47.50	47.14
50.00	37.50	46.43	46.07	37.50	47.14	47.14	41.43	49.29	46.43
55.00	37.14	46.79	45.71	37.50	46.07	47.86	41.07	47.50	44.29
60.00	37.14	44.64	45.71	37.50	47.14	46.43	39.64	44.64	45.36
65.00	36.43	46.07	43.57	36.43	48.21	46.79	38.93	43.21	44.64
70.00	34.64	47.50	43.57	36.07	46.43	45.36	38.57	40.71	41.07
75.00	33.57	45.36	44.29	34.64	46.79	44.64	37.86	37.50	39.64
80.00	33.21	43.93	40.71	33.93	42.86	40.71	36.43	35.36	38.21
85.00	32.50	42.14	36.07	32.50	43.93	36.43	35.71	33.21	35.71
90.00	30.71	41.07	34.64	31.43	41.07	35.36	35.00	31.43	31.79
95.00	30.00	40.71	34.64	30.71	40.00	34.29	32.50	28.93	31.43
100.00	29.64	38.21	32.86	30.00	38.93	31.07	32.14	26.43	24.29
Variance of detection distance under the COCO Model at 25% confidence threshold									
5.00	44.64	40.11	24.86	49.04	49.04	48.90	71.57	44.09	63.19
10.00	35.30	55.49	67.03	52.88	42.99	33.10	55.49	52.75	75.96
15.00	42.99	54.53	63.19	52.34	52.75	59.34	90.80	52.75	48.49
20.00	40.11	45.60	40.80	47.80	36.95	33.10	70.88	62.23	60.03
25.00	48.49	28.57	63.32	52.75	56.73	48.90	68.27	87.36	91.35
30.00	61.54	56.59	43.96	40.25	36.26	37.91	72.12	78.57	98.90
35.00	44.64	59.34	52.75	62.23	31.46	36.26	72.53	75.96	90.80

(Continued on next page)

(Continued from previous page)

intensity	cloud_fog	cloud_rain	cloud_wet	daytime_fog	daytime_rain	daytime_wet	light_fog	light_rain	light_wet
40.00	24.86	56.59	52.34	39.15	42.99	33.10	33.52	95.60	102.75
45.00	33.10	69.92	58.38	31.46	36.95	40.80	29.67	106.73	133.52
50.00	45.19	63.19	54.53	33.65	48.90	52.75	47.80	145.60	140.11
55.00	41.21	79.26	80.22	33.65	39.15	60.44	39.15	129.81	114.84
60.00	41.21	82.55	60.99	33.65	68.13	59.34	32.55	197.94	197.94
65.00	36.26	89.15	105.49	40.11	71.57	98.49	27.61	156.18	197.94
70.00	32.55	87.50	78.57	27.61	74.73	47.94	24.73	207.14	177.61
75.00	28.57	105.63	91.76	32.55	60.03	40.25	21.98	206.73	221.02
80.00	25.41	66.07	87.91	35.30	29.67	41.76	24.73	105.63	148.49
85.00	29.81	114.29	92.99	25.96	23.76	70.88	22.53	156.18	110.99
90.00	18.68	116.07	109.48	20.88	46.84	82.55	23.08	136.26	102.34
95.00	23.08	99.45	144.09	18.68	76.92	64.84	18.27	108.38	101.65
100.00	24.86	102.34	121.98	23.08	66.07	104.53	29.67	132.42	218.68
Average detection distance under the COCO Model at 50% confidence threshold									
5.00	40.38	38.93	39.64	40.00	38.93	40.00	41.79	41.07	41.79
10.00	38.57	39.64	40.36	39.29	39.23	40.00	42.50	41.43	41.79
15.00	38.57	38.93	39.64	39.29	40.00	40.00	41.43	40.71	41.43
20.00	37.14	40.71	39.64	37.50	40.00	40.71	41.79	41.43	40.71
25.00	38.21	40.71	39.64	38.57	40.36	40.71	42.14	40.00	42.86
30.00	36.43	39.29	40.36	37.50	40.71	41.43	40.36	41.07	42.50
35.00	35.71	41.07	41.43	36.43	41.43	40.71	40.00	42.14	41.43
40.00	36.07	41.43	41.07	34.29	41.43	41.79	39.64	41.07	42.14
45.00	34.64	40.36	40.36	35.00	40.71	41.79	37.50	40.36	39.64
50.00	34.29	40.71	40.00	33.93	41.07	40.71	38.21	40.00	40.00
55.00	32.86	40.00	40.00	32.86	41.07	40.36	36.79	38.93	38.93
60.00	32.14	40.36	38.21	32.14	41.79	39.64	36.79	38.21	37.14
65.00	30.36	39.29	39.64	31.43	41.07	38.57	35.00	35.71	35.71
70.00	30.00	37.50	38.21	31.07	39.29	39.64	34.07	33.57	32.14
75.00	29.29	39.64	37.86	30.00	38.57	38.93	33.21	31.43	32.14
80.00	29.29	35.00	34.64	30.00	37.14	33.93	31.07	28.57	30.00
85.00	28.57	35.71	31.43	28.21	36.43	31.79	30.36	26.79	25.00
90.00	27.50	33.21	30.00	27.50	36.79	30.71	29.64	24.64	23.57
95.00	27.50	33.93	27.14	27.50	33.93	29.29	30.00	23.57	20.00

(Continued on next page)

(Continued from previous page)

intensity	cloud_fog	cloud_rain	cloud_wet	daytime_fog	daytime_rain	daytime_wet	light_fog	light_rain	light_wet
100.00	25.71	33.57	26.43	27.14	32.86	27.50	28.57	21.79	17.14
Variance of detection distance under the COCO Model at 50% confidence threshold									
5.00	18.59	35.30	32.55	25.00	35.30	26.92	17.72	35.30	36.95
10.00	36.26	28.71	24.86	26.37	36.86	26.92	14.42	20.88	21.57
15.00	28.57	19.92	28.71	30.22	15.38	38.46	32.42	34.07	20.88
20.00	37.36	10.99	32.55	33.65	11.54	30.22	21.57	32.42	26.37
25.00	36.95	10.99	28.71	24.73	17.17	30.22	21.98	26.92	41.21
30.00	43.96	34.07	28.71	45.19	18.68	17.03	24.86	35.30	49.04
35.00	26.37	12.23	17.03	36.26	17.03	30.22	26.92	29.67	59.34
40.00	23.76	13.19	19.92	30.22	17.03	17.72	32.55	39.15	60.44
45.00	32.55	32.55	24.86	19.23	18.68	17.72	25.96	40.25	82.55
50.00	30.22	22.53	19.23	27.61	19.92	18.68	21.57	50.00	38.46
55.00	29.67	30.77	26.92	18.13	12.23	32.55	21.57	46.84	35.30
60.00	25.82	32.55	52.34	29.67	13.87	47.94	21.57	60.03	45.05
65.00	13.32	41.76	47.94	17.03	23.76	43.96	30.77	80.22	72.53
70.00	19.23	52.88	33.10	16.07	30.22	36.40	26.69	159.34	164.29
75.00	18.68	32.55	29.67	15.38	40.11	35.30	29.26	132.42	118.13
80.00	18.68	76.92	59.48	15.38	33.52	100.69	19.92	124.73	103.85
85.00	24.73	64.84	86.26	21.57	67.03	94.64	17.17	125.41	176.92
90.00	22.12	63.87	115.38	18.27	60.03	91.76	17.17	132.55	182.42
95.00	18.27	89.15	102.75	14.42	77.61	134.07	11.54	117.03	119.23
100.00	22.53	74.73	67.03	14.29	71.98	106.73	9.34	102.34	148.90

Table C.2: False positive rate under various conditions

cloud_fog	cloud_rain	cloud_wet	daytime_fog	daytime_rain	daytime_wet	light_fog	light_rain	light_wet
the Specialization Model at 25% confidence threshold								
3.3	3.4	3.2	3.4	3.7	3.6	0.4	0.0	0.0
3.4	2.4	2.3	3.4	3.6	3.5	0.3	0.0	0.0
3.2	3.0	2.6	3.4	3.6	3.4	0.6	0.0	0.0
2.3	2.1	1.5	2.5	3.6	3.4	1.5	0.1	0.0
2.1	0.2	0.0	2.1	3.5	3.5	2.4	0.3	0.0
0.9	0.4	0.4	1.9	3.4	4.6	1.5	0.0	0.0
0.3	0.0	0.0	1.8	3.5	5.0	0.0	0.0	0.0
1.4	0.0	0.0	0.8	3.6	5.1	0.1	0.0	0.0
2.5	0.1	0.2	3.1	4.3	5.1	0.3	0.0	0.0
2.3	1.1	0.7	2.4	4.9	5.6	0.5	0.1	0.0
2.1	1.5	1.6	2.4	5.1	6.8	0.1	0.4	0.0
2.4	1.5	1.5	2.6	5.2	6.8	0.4	0.4	0.0
2.4	1.7	1.7	2.4	5.4	7.0	0.4	0.4	0.0
2.4	1.7	1.7	2.4	5.5	6.9	0.9	0.4	0.0
2.6	2.0	1.9	2.4	5.6	6.1	1.1	0.3	0.4
2.7	3.1	1.2	2.5	5.2	2.8	0.3	0.0	0.0
2.7	1.8	1.6	2.6	3.4	1.8	1.1	0.2	0.0
2.9	2.0	1.2	2.8	3.0	1.8	1.0	0.1	0.0
3.1	2.0	1.2	3.0	3.7	1.9	0.7	0.4	1.7
3.1	1.7	0.7	3.0	3.1	2.0	1.1	0.6	0.9
the Specialization Model at 50% confidence threshold								
1.8	0.7	0.4	2.3	3.1	2.2	0.4	0.0	0.0
1.8	0.1	0.1	2.4	3.1	2.1	0.5	0.0	0.0
1.3	0.1	0.0	2.2	3.2	2.3	1.6	0.0	0.0
0.1	0.0	0.0	1.8	3.3	2.3	2.2	0.0	0.0
0.0	0.0	0.0	1.8	3.0	2.4	2.6	0.0	0.0
0.0	0.0	0.0	1.6	3.0	2.4	2.0	0.0	0.0
0.0	0.0	0.0	0.1	2.9	2.4	1.5	0.0	0.0
0.4	0.0	0.0	0.0	2.7	2.0	1.3	0.0	0.0
0.9	0.0	0.0	0.9	2.9	2.1	1.2	0.0	0.0
1.1	0.0	0.0	0.9	2.7	2.2	1.1	0.0	0.0

(Table continued on next page)

(Table continued from previous page)

cloud_fog	cloud_rain	cloud_wet	daytime_fog	daytime_rain	daytime_wet	light_fog	light_rain	light_wet
1.4	0.2	0.1	1.1	3.9	2.5	0.9	0.0	0.0
1.7	0.6	0.4	1.7	5.0	4.6	0.4	0.0	0.0
1.7	1.6	1.7	1.7	4.6	4.7	0.1	0.0	0.0
1.7	1.4	1.0	1.7	4.1	2.1	0.3	0.0	0.0
1.7	1.6	0.6	1.7	3.7	1.3	0.1	0.0	0.0
1.7	1.1	0.0	1.7	2.1	1.4	0.1	0.0	0.0
1.8	0.0	0.0	1.7	1.6	1.4	0.0	0.0	0.8
1.6	0.0	0.0	1.9	1.1	1.3	0.0	0.0	0.9
1.3	0.2	1.2	2.0	1.2	0.8	0.0	0.0	2.8
1.1	0.0	0.8	1.5	0.8	0.1	0.0	0.0	1.8
the Generalization Model at 25% confidence threshold								
9.6	9.6	9.6	9.6	9.6	9.2	0.0	0.0	0.0
8.2	9.6	9.6	6.8	9.6	9.2	0.0	0.0	0.0
4.8	9.6	9.6	4.8	9.6	9.2	0.0	0.0	0.0
4.8	9.6	9.6	4.8	9.6	9.2	0.0	0.0	0.0
4.8	9.6	9.6	4.4	9.6	9.2	0.0	0.0	0.0
4.8	9.6	9.6	3.2	9.6	9.2	0.0	0.0	0.0
4.8	9.0	9.6	4.8	9.6	9.2	0.0	0.0	0.0
4.8	8.4	9.6	5.0	9.4	9.2	0.0	0.0	0.0
7.2	9.2	10.0	8.2	9.0	9.2	0.0	0.0	0.0
7.2	8.8	9.8	6.0	9.2	9.2	0.0	0.0	0.0
6.2	7.8	9.2	7.8	9.0	8.8	0.0	0.0	0.0
5.4	7.8	8.4	6.4	8.0	7.8	0.2	0.0	0.0
5.2	8.0	9.6	5.4	8.0	8.8	0.2	0.0	0.0
4.8	8.0	7.4	4.6	6.0	6.0	0.2	0.0	0.0
4.8	8.2	7.0	4.8	6.2	6.8	0.0	0.4	0.0
4.8	8.4	5.0	4.8	7.6	10.0	0.2	0.8	0.0
4.8	8.6	4.8	4.8	8.8	10.8	0.2	2.2	0.0
4.8	8.8	4.8	4.8	10.0	11.2	0.2	1.0	0.0
4.8	8.2	2.6	4.8	9.6	10.2	0.0	1.6	0.0
4.8	4.6	0.0	4.8	10.6	8.8	0.2	2.0	0.0
the Generalization Model at 50% confidence threshold								
7.2	8.4	8.4	8.4	8.7	7.5	0.0	0.0	0.0

(Table continued on next page)

(Table continued from previous page)

cloud_fog	cloud_rain	cloud_wet	daytime_fog	daytime_rain	daytime_wet	light_fog	light_rain	light_wet
6.4	7.9	8.4	6.0	8.2	7.5	0.0	0.0	0.0
3.6	8.5	9.0	4.3	8.2	7.2	0.0	0.0	0.0
2.9	7.2	7.7	2.4	8.1	8.4	0.0	0.0	0.0
2.7	7.8	8.8	2.0	7.9	8.1	0.0	0.0	0.0
3.9	7.8	8.3	1.6	7.9	8.7	0.0	0.0	0.0
4.8	7.9	7.1	2.4	7.9	8.7	0.0	0.0	0.0
4.8	7.2	7.2	4.9	7.9	8.3	0.0	0.0	0.0
5.8	8.8	7.3	6.6	7.7	8.5	0.0	0.0	0.0
5.9	7.9	8.4	5.6	7.5	7.6	0.0	0.0	0.0
5.4	6.2	6.5	6.7	5.6	5.8	0.0	0.0	0.0
4.9	5.9	5.9	5.6	5.7	4.5	0.0	0.0	0.0
4.9	6.2	7.0	5.2	6.9	6.9	0.0	0.0	0.0
4.8	6.2	6.2	4.8	4.7	5.5	0.0	0.2	0.0
4.8	6.2	5.8	4.8	4.6	4.1	0.0	0.0	0.0
4.8	6.4	4.5	4.8	7.0	5.2	0.0	0.3	0.0
4.8	5.9	2.6	4.8	6.0	5.5	0.0	1.1	0.0
4.8	7.4	2.4	4.8	7.0	7.3	0.0	0.4	0.0
4.5	6.4	1.3	2.7	7.7	7.4	0.0	0.7	0.0
2.7	3.9	0.0	2.2	7.8	5.2	0.0	1.1	0.0
The COCO Model at 25% confidence threshold								
0.0	0.0	1.5	0.0	1.4	1.5	1.5	0.0	0.0
0.0	0.0	1.3	0.0	1.3	1.6	1.4	0.2	0.0
0.0	0.0	1.4	0.0	1.3	1.6	1.9	0.3	0.0
0.0	0.0	1.4	0.0	1.3	1.6	1.1	0.1	0.0
0.0	0.0	1.4	0.0	1.3	1.6	0.4	0.1	0.0
0.0	0.0	0.9	0.0	1.2	0.9	0.3	0.1	0.0
0.0	0.0	0.1	0.0	0.5	0.9	0.2	0.2	0.0
0.0	0.0	0.0	0.0	0.2	0.1	0.2	0.2	0.0
0.0	0.0	0.0	0.0	0.1	0.3	0.2	0.5	0.0
0.0	0.0	0.0	0.0	0.0	0.0	0.0	0.4	0.0
0.0	0.0	0.0	0.0	0.0	0.0	0.0	0.6	0.0
0.0	0.0	0.0	0.0	0.0	0.0	0.0	0.4	0.0
0.0	0.0	0.0	0.0	0.0	0.0	0.0	0.1	0.0

(Table continued on next page)

(Table continued from previous page)

cloud_fog	cloud_rain	cloud_wet	daytime_fog	daytime_rain	daytime_wet	light_fog	light_rain	light_wet
0.0	0.0	0.0	0.0	0.0	0.0	0.0	0.3	0.0
0.0	0.0	0.0	0.0	0.0	0.0	0.0	0.1	0.0
0.0	0.0	0.0	0.0	0.0	0.0	0.0	0.3	0.0
0.0	0.0	0.0	0.0	0.0	0.0	0.0	0.0	0.1
0.0	0.0	0.0	0.0	0.0	0.0	0.0	0.0	0.2
0.0	0.0	0.0	0.0	0.0	0.0	0.0	0.0	0.9
0.0	0.0	0.0	0.0	0.0	0.0	0.0	0.0	0.6
The COCO Model at 50% confidence threshold								
0.0	0.0	0.0	0.0	0.0	0.0	0.0	0.0	0.0
0.0	0.0	0.0	0.0	0.0	0.0	0.0	0.0	0.0
0.0	0.0	0.0	0.0	0.0	0.0	0.0	0.0	0.0
0.0	0.0	0.0	0.0	0.0	0.0	0.0	0.0	0.0
0.0	0.0	0.0	0.0	0.0	0.0	0.0	0.0	0.0
0.0	0.0	0.0	0.0	0.0	0.0	0.0	0.0	0.0
0.0	0.0	0.0	0.0	0.0	0.0	0.0	0.0	0.0
0.0	0.0	0.0	0.0	0.0	0.0	0.0	0.0	0.0
0.0	0.0	0.0	0.0	0.0	0.0	0.0	0.0	0.0
0.0	0.0	0.0	0.0	0.0	0.0	0.0	0.0	0.0
0.0	0.0	0.0	0.0	0.0	0.0	0.0	0.0	0.0
0.0	0.0	0.0	0.0	0.0	0.0	0.0	0.0	0.0
0.0	0.0	0.0	0.0	0.0	0.0	0.0	0.0	0.0
0.0	0.0	0.0	0.0	0.0	0.0	0.0	0.0	0.0
0.0	0.0	0.0	0.0	0.0	0.0	0.0	0.0	0.0
0.0	0.0	0.0	0.0	0.0	0.0	0.0	0.0	0.0
0.0	0.0	0.0	0.0	0.0	0.0	0.0	0.0	0.0
0.0	0.0	0.0	0.0	0.0	0.0	0.0	0.0	0.0
0.0	0.0	0.0	0.0	0.0	0.0	0.0	0.0	0.0
0.0	0.0	0.0	0.0	0.0	0.0	0.0	0.0	0.0
0.0	0.0	0.0	0.0	0.0	0.0	0.0	0.0	0.0
0.0	0.0	0.0	0.0	0.0	0.0	0.0	0.0	0.0

Speed Control Method for Autonomous Vehicles at the Boundaries of the Operational Design Domain

Hanzhang Guo

***Abstract*—This paper presents a comprehensive and quantitative framework for enhancing the safety of autonomous vehicles by integrating sensor detection performance with braking dynamics under extreme weather conditions and variable road slopes. Using high-fidelity simulations in CARLA and PyChrono, extreme weather datasets are generated, sensor detection distances are evaluated and braking distances are simulated under varying friction coefficients and slopes. This study quantifies the relationship between detection distance and safe braking performance, establishing objective metrics for the dynamic Operational Design Domain of AVs. Furthermore, an adaptive speed control strategy based on reinforcement learning — implemented via the Soft Actor-Critic algorithm — is proposed, which continuously adjusts vehicle speed to ensure that braking distances remain within sensor detection limits. Experimental results demonstrate that models trained with extreme weather data significantly outperform general-purpose detectors and that integrating real-time braking distance predictions into the control strategy improves safety margins and operational efficiency across diverse driving scenarios.**

***Index Terms*—Autonomous Vehicles, Operational Design Domain, Extreme Weather, Reinforcement Learning**

I. Introduction

THE rapid development of autonomous vehicles (AVs) is transforming the landscape of transportation. Relying on advanced sensors (e.g., LiDAR, millimetre-wave radar, and cameras) along with perception and decision-making algorithms, AVs can perform tasks such as acceleration, steering and obstacle avoidance [31]. The key to this technology is the operational design domain (ODD), which delineates the environment where AVs can operate safely and efficiently. According to SAE J3016 [25], while Level 5 automation can imply full functionality across unlimited areas in the future, current research primarily focuses on Level 4 systems, which are restricted to well-defined ODDs. However, the uncertainties inherent in real-world environments — such as adverse weather, complex road geometries and unpredictable traffic behaviours — pose significant challenges for AVs.

Environmental factors are critical in defining the ODD boundaries of AVs, as they simultaneously affect both sensor performance and vehicle dynamics. Under optimal conditions, sensors reach their maximum detection range; however, adverse weather—such as heavy rain, dense fog or snowfall—significantly diminishes this capability [4, 31]. Concurrently, challenging road conditions, including steep gradients and slippery surfaces, degrade vehicle braking performance [11, 32]. The combined impact of these factors ultimately establishes the safe operational boundary for AVs. Moreover, studies indicate that approximately 52% of AV fallback events are due to perception errors, highlighting the critical need for robust risk assessments that address environmental sensor limitations and vehicle dynamics challenges [9].

Common responses, such as human takeover, pulling over or deceleration, each have significant drawbacks. Untrained passengers cannot guarantee a successful takeover [3, 1], and if extreme weather conditions prevent an AV from perceiving its surroundings, humans may also fail to do so [24]. Moreover, pulling over requires complete information on the map, or it will be challenging to find a safe place; stopping can disrupt traffic flow and increase the likelihood of rear-end collisions. While deceleration, although conceptually aligned with automation, relies on precise analyses of environmental impacts. This gap underscores the necessity for an integrated framework that quantifies how weather conditions, road gradients and other environmental factors affect sensor performance and vehicle dynamics. Given these challenges, data-driven approaches, such as reinforcement learning (RL), are particularly well-suited to this task, as they can leverage real-time data to continuously learn, adapt and optimize speed control strategies amid dynamic environmental uncertainties.

This paper proposes a comprehensive approach to quantify environmental factors' impacts on AV detection and braking performance, and optimize dynamic speed control strategies at the ODD boundaries. This study seeks to answer the following questions:

- How do adverse weather conditions quantitatively degrade sensor detection performance?
- What is the relationship between road gradients, surface friction and braking distances?
- Can RL effectively optimize speed control strategies in real-time when operating at the boundaries of the ODD?

The remainder of the paper is organized as follows. Section II reviews related work on AV sensor performance, risk assessment and speed control strategies. Section III details the methodology used to collect data, quantify key parameters and develop the speed control model. Section IV presents the experimental results and evaluates the performance of the proposed speed control strategy. Section V discusses the implications of the findings and compares them with existing approaches, and Section VI concludes with final remarks and potential directions for future research.

II. Related Works

The concept of the ODD for AVs has evolved significantly over the past decades. Early research in the mid-20th century primarily focused on isolated experiments in controlled environments, with military and aerospace applications pioneering unmanned driving [16, 29]. Initial AV deployments relied

heavily on geofencing and closed-road testing, which allowed for rapid prototyping under limited environmental conditions but failed to capture the full complexity of real-world driving [21, 14].

A significant turning point occurred with the DARPA Grand and Urban Challenges in the early 2000s, which shifted attention towards developing key AV technologies such as visual perception, path planning and sensor fusion [30, 19]. As these technologies matured, industry standards (e.g., SAE J3016) began emphasizing the need to delineate precise functional boundaries for different levels of automation, thereby formalizing the concept of ODD [25].

Recent studies have highlighted that traditional ODD definitions, primarily based on geographical restrictions, are insufficient for handling dynamic factors encountered in complex driving environments. For instance, geo-fencing approaches, while effective in constrained scenarios such as specific urban districts or highway segments, often neglect variables such as adverse weather conditions, dynamic traffic flows and road surface irregularities [22, 27]. This limitation has spurred research into dynamic ODD frameworks, which integrate real-time data from multiple sources[28, 6], including LiDAR, radar, cameras and Vehicle-to-Everything (V2X) communications for state changes[10, 17, 2].

Several studies have proposed adaptive operational strategies to address the challenges posed by dynamic environments. Hierarchical degradation models, for example, allow AV systems to transition through multiple control modes — from normal operation to degraded states and finally to a Minimal Risk Manoeuvre (MRM) when conditions deteriorate beyond safe limits [15, 7, 26]. Complementary approaches include variable speed limit systems and scenario-based testing frameworks, which aim to enhance safety by dynamically adjusting vehicle behaviour based on environmental inputs [13, 33, 30].

Despite these advances, several critical challenges persist. Many existing studies provide only qualitative descriptions of how heavy precipitation, low visibility, steep slopes or mixed traffic conditions affect vehicle performance [27, 12]. There is a notable gap in the literature regarding the quantitative assessment of sensor detection and braking distances under varying environmental and road conditions. Such quantitative methods are essential for integrating dynamic ODD evaluation into advanced decision-making frameworks, such as those based on RL [20, 5].

In summary, while considerable progress has been made in advancing dynamic ODD frameworks through multimodal sensor fusion, hierarchical degradation strategies and scenario-driven validation, a unified and quantitative approach remains challenging. Addressing this gap is critical for enhancing the safety and reliability of AVs in complex, real-world environments, and it forms the primary focus of this work.

III. Methodology

Ensuring the safety of AVs in extreme weather and complex terrain requires a comprehensive approach that incorporates perception capabilities and vehicle dynamics. To address this challenge, an integrated methodology is proposed that combines high-fidelity simulation for generating extreme weather vehicle detection datasets, systematic testing of sensor detection distances, braking distance simulations and adaptive speed control via RL. The following sections detail each module of the approach and explain how they collectively ensure that braking distances remain within sensor detection limits under a wide range of operational conditions.

A. Extreme Weather Data Generation

The research's foundation is the creation of a rich and diverse dataset that captures the visual complexities encountered by AVs in extreme weather. The CARLA simulator is employed for this purpose due to its comprehensive capabilities in rendering various weather conditions, including rainy, foggy, nighttime and cloudy scenarios. CARLA's integration with the SUMO traffic flow simulator mimics realistic traffic scenarios, providing different traffic capacity data generation environments.

Within CARLA, datasets are generated using six built-in maps (Town 01 – 06) that cover urban, rural and highway areas. Moreover, weather parameters such as cloudiness, precipitation, precipitation deposits, fog density and the sun azimuth angle are uniformly adjusted to ensure diversity. The approach maintains a day-to-night ratio of approximately $3:1$. Furthermore, the simulation generates between 25 and 100 NPCs of various types—such as sedans, SUVs, trucks and motors—on each map to simulate dynamic traffic scenarios. The generated data comprises both static images and dynamic videos. For instance, $45,000$ static photos are captured using RGB cameras—with a resolution of 1920×1080 and a $90°$ field of view—at randomly chosen vehicle positions, while 60 minutes of dynamic traffic video are recorded through co-simulation with SUMO. Finally, automated bounding box annotations, derived from CARLA's positional data, ensure consistent labelling even under extreme weather conditions and minimize human error.

B. Detection Distance Testing

To integrate perception with vehicle dynamics, it is first necessary to understand the limits of the sensor systems. In this experiment, a red sedan—selected for its high visual contrast—is placed at discrete distances ranging from 5 m to 120 m (in increments of 5 m) from a fixed camera along long, unobstructed roads on different maps, including both the trained maps (Town 01 - 06) and untrained maps (Town 07, 10 and 13). The tests are conducted under a variety of conditions, including combined weather scenarios (fog, rain or wet) with intensity levels set by CARLA from 5 to 100 (in increments of 5), as well as under different lighting conditions (cloudy, daytime or nighttime).

Based on this defined testing environment, sensor performance was evaluated using three detection models, as shown in table I. The first is the COCO Model, a public general-purpose YOLO model developed on the COCO dataset. The second, named the Specialization Model, was trained on the Extreme Weather Dataset and tested on trained maps that simulate

fixed-city AVs. The third, the Generalization Model, was also trained on the Extreme Weather Dataset but tested on the untrained maps to simulate inter-city AVs. Model performance was quantified by recording the maximum distance at which the vehicle was detected at two confidence thresholds (25% and 50%). Additionally, the false positive rates were analyzed to compare results across the three models. This rigorous assessment provides sensor detection distances, which will be compared with braking distances to determine whether the system can ensure safe stopping.

TABLE I: Details of the three tested models

	the Specialization Model	**the Generalization Model**	**the COCO Model**
Model	Extreme Weather Model	Extreme Weather Model	COCO YOLO Model
Test Map	Fixed-city Maps	Inter-city Maps	Fixed-city Maps

C. Braking Distance Simulation

The next module of the methodology focuses on simulating vehicle dynamics to evaluate braking performance under various conditions. The braking process is simulated using the physics engine PyChrono to estimate braking distances. The simulation parameters include road surface friction, slope and initial speed, factors that directly influence braking performance.

Four distinct friction coefficients are considered: 0.60 for dry conditions, 0.40 for rainy weather, 0.28 for snowy conditions and 0.18 for icy roads. Road slopes are varied from $-5°$ (downhill) to $+5°$ (uphill) in increments of $0.5°$. And the vehicle is tested across a speed range from 1 km/h to 120 km/h in 1 km/h increments. A sedan model is accelerated to a predetermined speed in each simulation run and subjected to maximum braking. The simulation concludes when the vehicle's speed falls below 0.5 km/h. To ensure statistical reliability, the braking distances are averaged over 5 runs for each friction, slope and initial speed combination. This results in a three-dimensional lookup table, $d_{brake}(\mu, \theta, v)$. This lookup table serves as a reference to assess whether the braking distance remains within the limits defined by the sensor detection distance under weather and slope conditions.

D. Reinforcement Learning Speed Control

With measures of both detection and braking distances, the final module focuses on ensuring safe operational speeds through adaptive control. The speed control problem is formulated as an RL task, employing the Soft Actor-Critic (SAC) algorithm to learn an optimal policy. The primary objective is to maintain the safety constraint—ensuring that the braking distance (d_{brake}, simulated in section III-C) does not exceed the detection distance (d_{detect}, from section III-B). The value of d_{brake} is based on the lookup table above, using the actual friction while interpolating both slope and speed. The value of d_{detect} is determined under various weather conditions, with these values modelled as a normal distribution based on their mean and variance. To simplify the learning process, the system assumes that the detection distance depends solely on weather conditions, thereby ensuring reliable recognition within that range. So the system incorporates a parameter d_{front} to represent the distance to the vehicle immediately ahead. When the preceding vehicle is outside the detection distance, d_{front} is set equal to d_{detect}; meanwhile, if the vehicle is within the detection distance, d_{front} is updated with the actual distance measured by the simulator.

The RL state vector is defined as $s = \{v, \theta, \mu, d_{brake}, d_{detect}, d_{front}\}$, where v is the current vehicle speed, θ is the road slope, μ is the friction coefficient (determined by the weather condition), d_{brake} is the braking distance, d_{detect} is the maximum sensor detection distance (accounting for measurement variance), and d_{front} is the distance to the vehicle ahead. d_{detect} is updated at the beginning of each episode, while the other state variables are updated after each action step. The action space is continuous, with actions $a \in [-1, +1]$ representing throttle (for positive values) and braking (for negative values). The reward function is designed to balance multiple objectives: it penalizes deviations from an ideal speed, imposes a penalty when the safety criterion ($d_{brake} > d_{detect}$) is violated, applies a significance penalty upon collisions, and discourages abrupt control changes to promote smooth driving.

Training is conducted in the Town 04 map in CARLA, which features variable slopes and provides a challenging yet realistic environment. Each training episode begins with randomized weather conditions, ensuring the agent experiences diverse friction and detection distance scenarios, and the episode terminates (i.e., the next episode begins) immediately after a collision occurs or when the vehicle successfully comes to a complete stop. The agent's experiences are stored in a replay buffer, and policy updates are performed using SAC's gradient-based optimization methods. The performance of the RL agent is subsequently validated against a baseline approach that does not incorporate simulated braking distance information but only speed, slope and friction.

E. Summary

The integrated methodology leverages high-fidelity simulation environments to generate diverse extreme weather datasets, systematically quantify sensor detection capabilities and vehicle braking performance, and employ advanced RL for adaptive speed control. By ensuring that the braking distance consistently remains within the sensor detection distance, the approach provides a robust framework for enhancing the operational safety of AVs under challenging environmental conditions.

IV. RESULTS

AVs operate reliably in a variety of challenging weather and lighting conditions. This study evaluates the performance of three vehicle detection models—a pre-trained COCO model, a region-specific extreme weather model (the Specialization Model), and a cross-region adapted extreme weather model (the Generalization Model)—to understand their detection capabilities under fog, rain and wet conditions. This research also explores the impact of these perception systems on braking distance and speed control, integrating real-time braking

distance predictions into an RL-based strategy. The results presented below highlight how extreme weather training can enhance detection performance and, consequently, allow for safer and more efficient AV operation.

A. Detection Distance Evaluation

Vehicle detection performance was evaluated under varying weather (fog, rain and wet), lighting (cloudy, daytime and night) and intensities (with CARLA intensity values ranging from 5 to 100) using three models: (i) a pre-trained COCO model, (ii) an extreme weather model trained for a specific region, named as the Specialization Model, and (iii) an extreme weather model adapted for cross-region operation, named as the Generalization Model. For each model, two confidence thresholds (25% and 50%) were applied, where a detection is triggered when the model's confidence exceeds the respective threshold.

As shown in Figure 1, the Specialization Model achieved the best overall performance with average detection distances of 65 m (25% threshold) and 60 m (50% threshold), compared with 54 m and 51m for the Generalization Model. In contrast, under extreme weather conditions, the COCO model attained maximum detection distances of only 42 m and 36m, respectively. The ratio of distances between the 25% and 50% thresholds was lower for the extreme weather models (1.08 for the Specialization Model and 1.05 for the Generalization Model) than for the COCO model (1.16), indicating that models trained with extreme weather data are less sensitive to changes in confidence threshold and can more reliably operate at higher confidence levels.

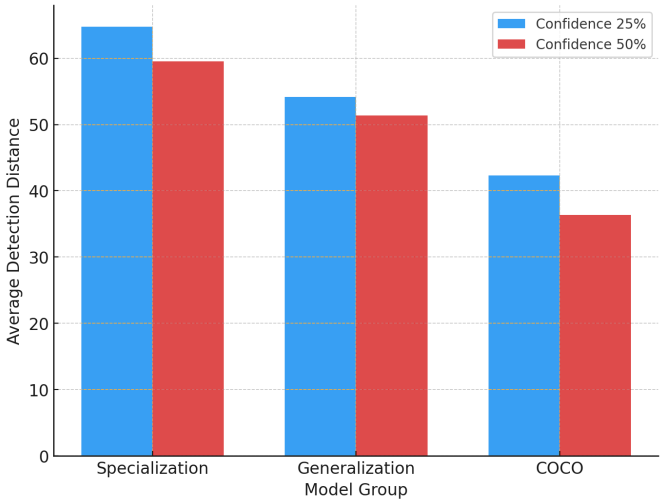

Fig. 1: Detection distance under different models and confidence threshold

Figure 2 illustrates that the detection distance variance for the Generalization Model is considerably higher than that of the Specialization Model, suggesting that domain adaptation challenges remain when extending performance across regions.

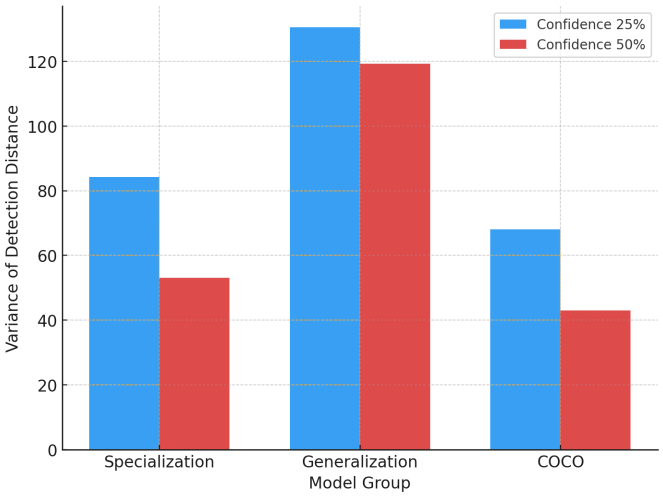

Fig. 2: Variance of detection distance under different models and confidence threshold

Furthermore, analysis across weather intensities revealed three regimes, as shown in Figure 3:

- **Low intensity** $(5 - 30)$**:** Detection distances remain relatively stable, with even slight improvements observed under some conditions (e.g., fog).
- **Medium intensity** $(30 - 70)$**:** A gradual decline in detection performance is observed; differences between weather types become more pronounced.
- **High intensity** (> 70)**:** A significant degradation occurs, particularly for nighttime and complex weather conditions, with detection distances dropping below 20 m.

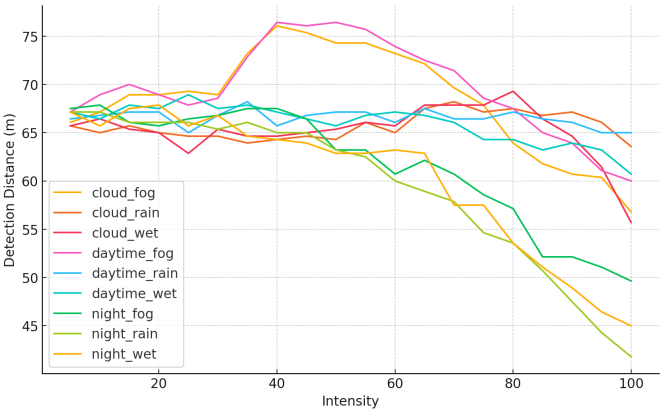

Fig. 3: Detection distance under different weather with the Specialization Model

The false positive ratio of different models and thresholds is shown in the Figure 4. It can be seen that the Specialization Model has a lower false positive ratio compared to the Generalization Model. The COCO Model exhibits the lowest false positive rate, but this might be due to insufficient detection capability. Even with a higher threshold, the Specialization Model can provide a sufficient detection range, so a higher threshold can be used to reduce unnecessary braking caused by false positives.

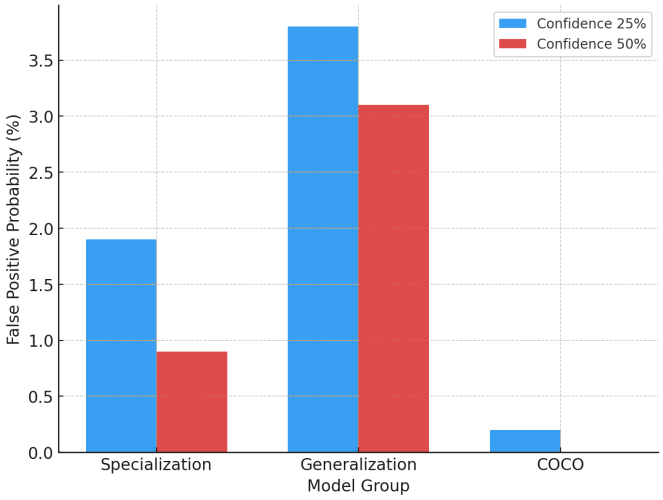

Fig. 4: False positive ratio under different models and confidence threshold

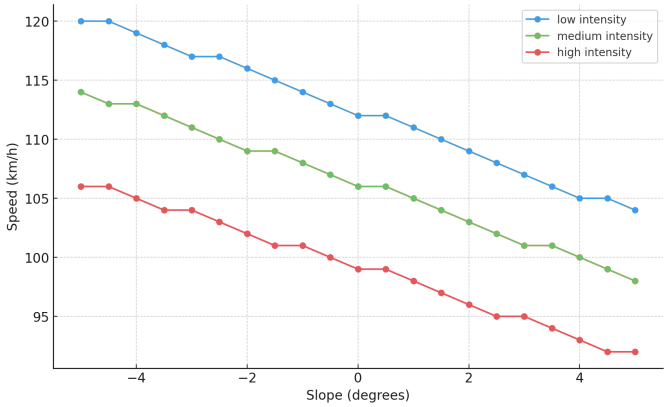

Fig. 6: Theoretical speed with the Specialization model under dry road condition

B. Braking Distance and Speed Control Analysis

Braking distance simulations were conducted over various speeds, slopes and friction coefficients. Figure 5 shows that braking distance increases sharply with speed and friction.

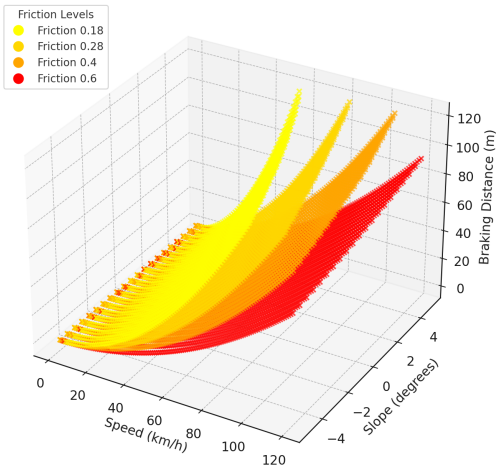

Fig. 5: Braking distance under different friction, slope and initial speed

To determine the maximum safe speed—i.e., the highest speed at which braking can be completed within the detection range—the simulated braking distances were compared with the detection distances obtained for foggy, rainy and wet conditions. For example, under foggy conditions, the Specialization Model provided detection distances of 69 m (low intensity), 62 m (medium), and 54 m (high). In comparison, the corresponding values for the Generalization Model were 57 m, 49 m, and 37 m, respectively. Figures 6 and 7 show that the Specialization Model allowed for safe speeds $5 - 15$ km/h higher than the Generalization Model across varying slopes and weather intensities.

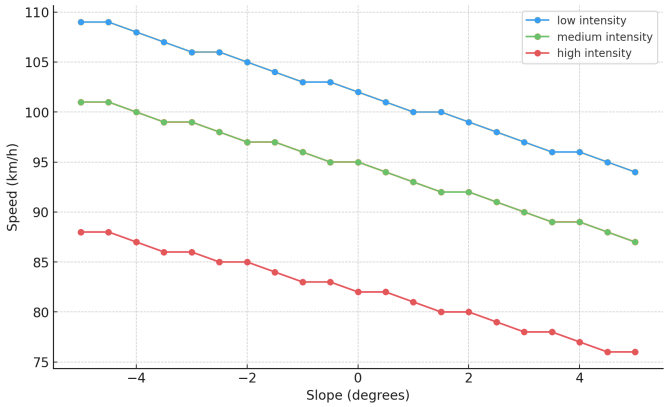

Fig. 7: Theoretical speed with the Generalization model under dry road condition

In addition, an RL-based speed control strategy that incorporated real-time braking distance predictions was implemented. Although high penalty coefficients during training led to conservative behaviour overall, the RL strategy using the expected braking distance (solid median line in Figure 8) resulted in higher average speeds than a strategy without such predictions. Under dry conditions, in particular, this approach enabled the AV to operate closer to the theoretical speed limits derived from the simulations. However, under extreme weather (notably snowy or wet conditions), insufficient detection distances constrained the system's lower speed limits, leading to a broader variability in controlled speeds. In the box plot, it is represented as a shorter box with longer whiskers.

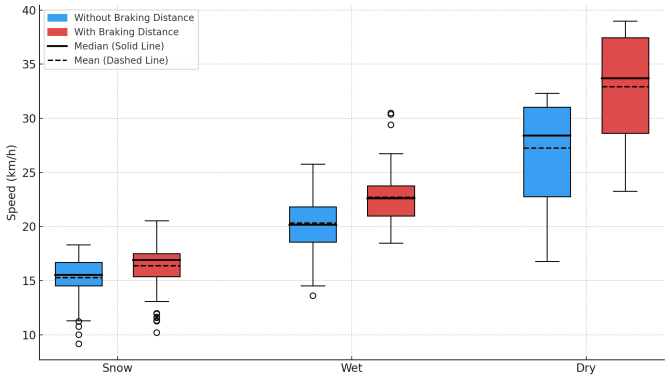

Fig. 8: Speed control result of RL compared

C. Summary of Key Findings

In summary, training perception models on extreme weather data notably improved detection distance and stability, mainly when operating with higher confidence thresholds. The Specialization Model outperformed the Generalization Model and the pre-trained COCO model across all tested weather scenarios. Moreover, simulation results confirmed that braking distances increase non-linearly with speed and are highly sensitive to friction conditions. Integrating braking distance predictions into an RL-based speed control strategy allowed for higher average speeds—especially under favourable friction conditions—while maintaining safety margins under adverse weather.

V. Discussion

This study conducted comprehensive and quantitative experiments and analyses on the visual perception and speed control of AVs under extreme weather conditions. The study evaluated speed control performance by comparing vehicle detection performance across different models (the Specialization Model, the Generalization Model and the COCO model) and incorporating braking distance constraints.

A. Key Findings and Their Implications

Experiments show that under extreme weather conditions, computer vision models trained on extreme weather data outperform models pre-trained on general datasets (e.g., COCO) in terms of detection range and stability—even in generalized test regions. Although the extreme weather dataset does not include ideal sunny conditions, it still demonstrated excellent detection performance at lower weather intensities during testing. This indicates that generalizing from extreme weather to ideal weather is easier than vice versa, suggesting that future computer vision training could focus on extreme weather conditions while reducing training on sunny conditions.

In terms of specific weather conditions, rainy weather and nighttime reduced detection capabilities as expected. However, the fog behaved unexpectedly. When using a general dataset for training, fog negatively affected detection range. In contrast, after training with the extreme weather dataset, fog at medium to low intensities positively affected detection range—especially in the Specialization Model, which outperformed other weather conditions, even those at low intensities. However, this might be a simulator error and requires further experimental verification.

Simulations of vehicle braking distance further demonstrate that speed, friction, and road slope all have nonlinear effects. Unlike previous studies that characterized the impact of road slope as linear, under low-friction and high-speed conditions the effect of road slope exhibits quadratic characteristics. This discrepancy may be because previous research focused on regions where the quadratic curve is relatively mild [23, 18, 8]. Additionally, the relationship between friction coefficients is not an ideal inverse function but includes an extra constant; therefore, directly applying linear fitting when estimating with different friction values can lead to significant errors.

Integrating the simulated braking distance results into a reinforcement learning (RL)-based speed control framework yielded promising outcomes compared to directly using uncalculated conditions (speed, friction, and road slope), especially in dry weather. This is likely due to the nonlinearity of braking distance, which means that uncalculated conditions cannot accurately capture its behaviour.

B. Limitations and Future Directions

Despite the achievements of this study, several limitations warrant further investigation. First, the experimental setup was primarily based on long, straight road segments and stationary target vehicles, which does not fully capture the complexity of dynamic urban environments. Future work should include multi-object scenarios, intersections, and dynamic lighting changes (such as entering and exiting tunnels) to more accurately simulate real-world conditions. Additionally, the simulation used idealized friction coefficients and fixed vehicle parameters, which may not fully represent the diversity encountered in practice. Incorporating dynamic models with different vehicle types and loads will be crucial for improving the accuracy of braking simulations.

Finally, although the RL-based speed control method proved effective in controlled environments, its generalization to complex multi-lane traffic conditions remains an open challenge. Expanding the framework to include interactions with dynamic obstacles such as pedestrians and cyclists, as well as integrating multi-sensor fusion technologies (e.g., LiDAR and radar), will be key to developing robust real-world applications.

VI. Conclusion

This study investigates the interplay between sensor detection distance and braking performance in AVs under extreme weather conditions and varying road slopes. Experimental results reveal that moderate fog can unexpectedly enhance detection distance compared to low-visibility conditions such as rain or nighttime, suggesting the presence of adaptive sensor behaviour or data processing mechanisms under foggy environments.

By quantifying the relationship between detection distance and safe braking distance through simulations in CARLA and PyChrono, objective metrics for defining the ODD of

AVs have been established. The findings demonstrate that safe vehicle operation is maintained only when the detection distance exceeds the braking distance. When this balance is disrupted, the system restricts its operational domain or initiates deceleration protocols.

A dynamic speed control strategy based on RL is proposed to address these challenges. This approach incorporates real-time assessments of detection and braking distances, enabling the vehicle to adjust its speed in response to adverse weather, steep slopes, or low-friction road surfaces. Compared to conventional methods, the strategy effectively reduces maximum speed under risky conditions and mitigates collision risks due to unpredictable variations in braking performance.

Overall, the work provides a practical framework for integrating perception, braking, and decision-making processes in autonomous driving systems, thereby contributing to the systematic expansion of dynamic ODDs. Future research will focus on enhancing multi-source environmental perception, refining adaptive speed control in complex traffic scenarios, and validating these methods through high-fidelity simulations and real-world experiments. Additionally, efforts to align these advancements with emerging regulatory standards and cloud-based cooperative frameworks will further promote safe and efficient autonomous driving.

References

[1] Muhammad Sajjad Ansar, Nael Alsaleh, and Bilal Farooq. "Behavioural modelling of automated to manual control transition in conditionally automated driving". In: *Transportation research part F: traffic psychology and behaviour* 94 (2023), pp. 422–435.

[2] Sabrine Belmekki and Dominique Gruyer. "Advanced Road Safety: Collective Perception for Probability of Collision Estimation of Connected Vehicles". In: *Computers* 13.1 (2024), p. 21.

[3] Haolin Chen et al. "Study on the influence factors of takeover behavior in automated driving based on survival analysis". In: *Transportation research part F: traffic psychology and behaviour* 95 (2023), pp. 281–296.

[4] Sikai Chen et al. "A taxonomy for autonomous vehicles considering ambient road infrastructure". In: *Sustainability* 15.14 (2023), p. 11258.

[5] Yiyang Chen et al. "Deep Reinforcement Learning in Autonomous Car Path Planning and Control: A Survey". In: *arXiv preprint arXiv:2404.00340* (2024).

[6] HongSeok Cho. "Operational Design Domain (ODD) framework for driver-automation integrated systems". PhD thesis. Massachusetts Institute of Technology, 2020.

[7] Ian Colwell et al. "An automated vehicle safety concept based on runtime restriction of the operational design domain". In: *2018 IEEE Intelligent Vehicles Symposium (IV)*. IEEE. 2018, pp. 1910–1917.

[8] Andreea-catalina Cristescu et al. "A CORELATTION BETWEEN THE COEFFICIENT OF FRICTION AND BRAKING DISTANCE AND TIME". In: *Annals of the Faculty of Engineering Hunedoara* 22.2 (2024), pp. 53–58.

[9] Francesca Favarò, Sky Eurich, and Nazanin Nader. "Autonomous vehicles' disengagements: Trends, triggers, and regulatory limitations". In: *Accident Analysis & Prevention* 110 (2018), pp. 136–148.

[10] Jamil Fayyad et al. "Deep learning sensor fusion for autonomous vehicle perception and localization: A review". In: *Sensors* 20.15 (2020), p. 4220.

[11] Alfredo García, David Llopis-Castelló, and Francisco Javier Camacho-Torregrosa. "From the vehicle-based concept of operational design domain to the road-based concept of operational road section". In: *Frontiers in Built Environment* 8 (2022), p. 901840.

[12] Magnus Gyllenhammar et al. "Towards an operational design domain that supports the safety argumentation of an automated driving system". In: *10th European congress on embedded real time systems (ERTS 2020)*. 2020.

[13] Yu Han et al. "A new reinforcement learning-based variable speed limit control approach to improve traffic efficiency against freeway jam waves". In: *Transportation research part C: emerging technologies* 144 (2022), p. 103900.

[14] Rasheed Hussain and Sherali Zeadally. "Autonomous cars: Research results, issues, and future challenges". In: *IEEE Communications Surveys & Tutorials* 21.2 (2018), pp. 1275–1313.

[15] Masao Ito. "Supporting process design in the autonomous era with new standards and guidelines". In: *Systems, Software and Services Process Improvement: 27th European Conference, EuroSPI 2020, Düsseldorf, Germany, September 9–11, 2020, Proceedings 27*. Springer. 2020, pp. 525–535.

[16] Masao Ito. "The uncertainty that the autonomous car faces and predictability analysis for evaluation". In: *Systems, Software and Services Process Improvement: 26th European Conference, EuroSPI 2019, Edinburgh, UK, September 18–20, 2019, Proceedings 26*. Springer. 2019, pp. 83–95.

[17] Maria Jokela et al. "LiDAR performance review in arctic conditions". In: *2019 IEEE 15th International Conference on Intelligent Computer Communication and Processing (ICCP)*. IEEE. 2019, pp. 27–31.

[18] Ektor Karyotakis et al. "Minimizing stopping distance on split friction via steering and individual wheel braking optimization". In: *The IAVSD International Symposium on Dynamics of Vehicles on Roads and Tracks*. Springer. 2023, pp. 380–389.

[19] Philip Koopman. *How safe is safe enough?: Measuring and predicting Autonomous Vehicle Safety*. Carnegie Mellon University, 2022.

[20] Zhaoyong Liu et al. *Research on Collision Avoidance and Vehicle Stability Control of Intelligent Driving Ve-*

hicles in Harsh Environments. Tech. rep. SAE Technical Paper, 2022.

[21] Marcel Aguirre Mehlhorn, Andreas Richter, and Yuri AW Shardt. "Ruling the operational boundaries: A survey on operational design domains of autonomous driving systems". In: *IFAC-PapersOnLine* 56.2 (2023), pp. 2202–2213.

[22] Giuseppina Pappalardo et al. "Assessing the operational design domain of lane support system for automated vehicles in different weather and road conditions". In: *Journal of traffic and transportation engineering (English edition)* 9.4 (2022), pp. 631–644.

[23] Omid Rahmani et al. "A nonlinear analytical approach for estimating vehicle braking distance based on multi-body dynamic simulation". In: *Sādhanā* 49.1 (2024), p. 20.

[24] Nagarjun Reddy et al. "Operational design domain requirements for improved performance of lane assistance systems: A field test study in The Netherlands". In: *IEEE Open Journal of Intelligent Transportation Systems* 1 (2020), pp. 237–252.

[25] On-Road Automated Driving (ORAD) Committee. *Taxonomy and Definitions for Terms Related to Driving Automation Systems for On-Road Motor Vehicles*. Apr. 2021. DOI: https://doi.org/10.4271/J3016_202104. URL: https://doi.org/10.4271/J3016_202104.

[26] Daniel Rohne, Andreas Richter, and Edward Schwalb. "Implementing ODD as single point of knowledge to support the development of automated driving". In: *2022 IEEE International Conference on Systems, Man, and Cybernetics (SMC)*. IEEE. 2022, pp. 1364–1370.

[27] Aniket Salvi et al. "Fuzzy interpretation of operational design domains in autonomous driving". In: *2022 IEEE Intelligent Vehicles Symposium (IV)*. IEEE. 2022, pp. 1261–1267.

[28] Bobbie D Seppelt and John D Lee. "Modeling driver response to imperfect vehicle control automation". In: *Procedia Manufacturing* 3 (2015), pp. 2621–2628.

[29] Chen Sun. "Operational Design Domain Monitoring and Augmentation for Autonomous Driving". In: (2022).

[30] Eric Thorn et al. *A framework for automated driving system testable cases and scenarios*. Tech. rep. United States. Department of Transportation. National Highway Traffic Safety …, 2018.

[31] Walther Wachenfeld and Hermann Winner. "The release of autonomous vehicles". In: *Autonomous Driving: Technical, Legal and Social Aspects* (2016), pp. 425–449.

[32] Wenhao Yu et al. "SOTIF risk mitigation based on unified ODD monitoring for autonomous vehicles". In: *Journal of intelligent and connected vehicles* 5.3 (2022), pp. 157–166.

[33] Yuhang Zhang et al. "Cooperative multi-agent reinforcement learning for large scale variable speed limit control". In: *2023 IEEE International Conference on Smart Computing (SMARTCOMP)*. IEEE. 2023, pp. 149–156.